



TECHNISCHE UNIVERSITÄT MÜNCHEN

Fakultät für Medizin

Frauenklinik und Poliklinik

Fachgebiet Experimentelle Gynäkologie

Expression, function and clinical relevance of CXCR3 in ovarian cancer

Claudia Alexandra Windmüller

Vollständiger Abdruck der von der Fakultät für Medizin der Technischen Universität München zur Erlangung des akademischen Grades eines

Doktors der Naturwissenschaften (Dr. rer. nat.)

genehmigten Dissertation

Vorsitzende: Prof. Dr. Gabriele Multhoff

Prüfer der Dissertation: 1. Prof. Dr. Manfred Schmitt

2. Prof. Dr. Michael Groll

3. Prof. Dr. Christian Ries

Die Dissertation wurde am 07.09.2016 bei der Technischen Universität München eingereicht und durch die Fakultät für Medizin am 14.06.2017 angenommen.

TABLE OF CONTENT

ABBREVIATIONS	VII
LIST OF FIGURES	XI
LIST OF TABLES	XIII
I. ABSTRACT	1
II. INTRODUCTION	2
1. Ovarian cancer	2
1.1. Epidemiology of ovarian cancer.....	2
1.2. Histological classification of tumors and prognostic factors.....	3
1.3. Hereditary ovarian cancer.....	5
1.4. Carcinogenesis of ovarian cancer.....	5
1.5. Treatment of ovarian cancer.....	7
2. Ovarian cancer as immunogenic tumors	7
3. Chemokines and chemokine receptors	10
3.1. CXC chemokines.....	10
3.2. CXCR3.....	11
3.3. CXCL9 and CXCL10 expression in cancer.....	15
3.4. CXCR3 expression in cancer.....	17
III. AIMS OF THE STUDY	20
IV. MATERIAL	21
1. Human tissue and ascites samples and patient cohort	21
1.1. Immunohistochemically used human tissue samples and patient cohort...21	
1.2. Human ascites samples for ELISA.....	22
1.3. Human ascites samples for migration assay.....	23
1.4. Human ascites samples for the generation of primary cells.....	24
2. Eukaryotic cell lines	24
2.1. Culture media for eukaryotic cell lines.....	25
2.2. Supplements in 500 ml culture medium.....	25
2.3. Culture media for primary epithelial ovarian cancer cells.....	25

2.4.	Cell culture solutions	25
3.	Proteins	26
4.	Antibodies	26
5.	Technical devices.....	27
6.	Consumables.....	28
7.	Laboratory chemicals and reagents	29
8.	Buffers and solutions	33
9.	Kits	34
10.	Plasmids	35
V.	METHODS	37
1.	Cell culture	37
1.1.	Cultivation of cells	37
1.2.	Freezing and thawing of cells	37
1.3.	Primary culture of ascites derived epithelial ovarian cancer cells	37
1.4.	Stable knockdown of a target gene in ID8 cells	38
2.	Migration assay	39
3.	Proliferation assay	39
4.	Flow cytometry	40
5.	Protease array	40
6.	Enzyme-linked immunosorbent assay (ELISA).....	40
7.	Western blot	41
7.1.	Cell lysis.....	41
7.2.	Determination of protein concentration	41
7.3.	Immunoblot analysis	41
8.	Immunohistochemistry	42
8.1.	Immunohistochemical staining	42
8.2.	Scoring of immunostaining.....	43
9.	Statistics	44

VI.	RESULTS	45
1.	Expression analyses of CXCR3 chemokines in ovarian cancer.....	45
1.1.	Expression of CXCL9 and CXCL10 and prognostic impact.....	45
1.1.1.	Discovery set.....	45
1.1.2.	Validation set	52
1.1.3.	Combined cohorts	58
1.2.	Expression of CXCR3 and correlation with survival data.....	63
1.2.1.	Discovery set.....	64
1.2.2.	Validation set	67
1.2.3.	Combined cohorts	70
1.2.4.	CXCR3 expression in lymph node metastases	72
1.3.	Combined expression of receptor and ligand.....	74
1.3.1.	Discovery set.....	74
1.3.2.	Validation set	76
1.3.3.	Combined cohorts	79
2.	Expression and function of CXCR3 in ovarian cancer cell lines.....	84
2.1.	CXCR3 expression in human ovarian cancer cell lines.....	84
2.2.	Proliferation of ovarian cancer cells upon chemokine stimulation.....	86
2.3.	Migration of ovarian cancer cells towards chemoattractants.....	87
2.4.	Protease expression upon chemokine stimulation	90
3.	Expression and function of CXCR3, CXCL9 and CXCL10 in ascites	91
3.1.	Chemokine ligand concentrations in ovarian cancer ascites.....	91
3.2.	Correlation of chemokine concentrations in ascites with residual tumor ..	93
3.3.	Migration of ovarian cancer cell lines towards ascites	94
3.4.	CXCR3 in primary epithelial ovarian cancer cells	97
4.	Stable knockdown of CXCR3 in murine ovarian cancer cells.....	99
4.1.	CXCR3 expression in ID8 cells.....	99
4.2.	Generation of stable mCXCR3 knockdown cells	101
4.3.	Migratory capacity of mCXCR3 knockdown cells.....	102
4.4.	Proliferation of mCXCR3 knockdown cells	103
VII.	DISCUSSION	105
1.	CXCL9 and CXCL10 are potent anti-tumor mediators	105

2.	CXCR3 as therapeutic target.....	107
3.	Conclusion	111
VIII.	REFERENCES.....	113
IX.	ACKNOWLEDGEMENTS	123

ABBREVIATIONS

α	anti (antibody related)
aa	amino acid
ADAM	a disintegrin and metalloproteinase
Akt	oncogene first identified in virus isolated from a murine thymoma
APC	antigen-presenting cell
APS	ammonium persulfate
ASA	acetylsalicylic acid
BRCA1	breast cancer 1
BRCA2	breast cancer 2
BSA	bovine serum albumin
BCA	bicinchoninic acid
CA 125	cancer antigen 125
Ca ²⁺	calcium
CaCl ₂	calcium chloride
cAMP	cyclic adenosine monophosphate
CCL5	chemokine (C-C motif) ligand 5
CD3	cluster of differentiation 3
CD4	cluster of differentiation 4
CD8	cluster of differentiation 8
C.I.	confidence interval
CMF	cyclophosphamide, methotrexate, 5-fluorouracile
ColVII	type VII collagen
C-terminus	carboxyl-terminus
CTL	cytotoxic T lymphocyte
CXCL9	chemokine (C-X-C motif) ligand 9
CXCL10	chemokine (C-X-C motif) ligand 10
CXCR3	chemokine (C-X-C motif) receptor 3
CX ₃ CL1	chemokine (C-X ₃ -C motif) ligand 1
CX ₃ CR1	chemokine (C-X ₃ -C motif) receptor 1
DAB	3,3'-diaminobenzidine
DAPI	4'-6-diamidino-2-phenylindole
DC	dendritic cell
DMEM	Dulbecco's modified eagle medium
DMSO	dimethyl sulfoxide
DNA	deoxyribonucleic acid
EBSS	Earle's balanced salt solution
ECL	enhanced chemiluminescence
EDTA	ethylenediaminetetraacetic acid
EGFR	epidermal growth factor receptor
ELISA	enzyme-linked immunosorbent assay
ELR	glutamic acid, leucine, arginine
EMT	epithelial-mesenchymal transition
EOC	epithelial ovarian cancer
ERK	extracellular-signal regulated kinase

FACS	fluorescence-activated cell sorting
FCS	fetal calf serum
FIGO	Fédération Internationale de Gynécologie et d'Obstétrique
FOXP3	forkhead box protein P3
g	gram (weight context)
g	gravitational constant (centrifugation context)
G2 phase	gap 2 phase (cell cycle)
G α (s, q, i)	guanine nucleotide-binding protein subunit α (s, q, i)
G β	guanine nucleotide-binding protein subunit β
G γ	guanine nucleotide-binding protein subunit γ
GAPDH	glyceraldehyde 3-phosphate dehydrogenase
h	hour
h[protein]	human
HBOC	hereditary breast ovarian cancer syndrome
HCl	hydrogen chloride
HEPES	4-(2-hydroxyethyl)-1-piperazineethanesulfonic acid
HER2(/neu)	human epidermal growth factor receptor 2
HGSC	high-grade serous ovarian cancer
HR	hazard ratio
HRP	horseradish peroxidase
H ₂ O ₂	hydrogen peroxide
IFN- α	Interferon-alpha
IFN- β	Interferon-beta
IFN- γ	interferon-gamma
IgG	immunoglobulin G
IgG (H+L)	immunoglobulin G heavy and light chain
IHC	immunohistochemistry
IL-2	interleukin 2
IP-10	interferon gamma-induced protein 10
I-TAC	interferon-inducible T cell alpha chemoattractant
KCl	potassium chloride
k.d.	knockdown
KH ₂ PO ₄	potassium dihydrogen phosphate
K-ras	Kirsten rat sarcoma viral oncogene homolog
LTR	long terminal repeat
M	molar
M[X/0/1]	metastasis status
m[protein]	murine
MAPK	mitogen-activated protein kinase
MCDB	medium for molecular, cellular and developmental biology
MET	mesenchymal-epithelial transition
Mg ²⁺	magnesium
MgCl ₂	magnesium chloride
MHCI	major histocompatibility complex I
MHCII	major histocompatibility complex II
Mig	monokine induced by gamma interferon
min	minute

miRNA	micro ribonucleic acid
mM	millimolar
MMLV	Moloney murine leukemia virus
MMP	matrix metalloproteinase
M phase	mitosis phase
mRNA	messenger ribonucleic acid
N	normality or equivalent concentration
N[X/0/1]	lymph node status
n.a.	not available
NaCl	sodium chloride
NaF	sodium fluoride
Na ₂ HPO ₄ 2H ₂ O	disodium hydrogen phosphate dihydrate
NaOH	sodium hydroxide
NK cell	natural killer cell
NKT cell	natural killer T cell
n.s.	not significant
nt	nucleotide
N-terminus	amino-terminus
OS	overall survival
PAGE	polyacrylamide gel electrophoresis
PBS	phosphate-buffered saline
PD-1	programmed cell death protein-1
PFS	progression-free survival
PGE ₂	prostaglandin E2
PI3K	phosphatidylinositol-3-kinase
PKA	protein kinase A
PLCβ	phospholipase Cβ
pN[0/1/2]	pathological lymph node classification
Pro	proline
PVDF	polyvinylidene fluoride
R[0/1/2]	residual tumor status
r[protein]	recombinant
Ras	rat sarcoma
RNA	ribonucleic acid
RPMI	medium from the Roswell Park Memorial Institute
scr	scrambled short hairpin ribonucleic acid
SDS	sodium dodecyl sulfate
SDS-PAGE	sodium dodecyl sulfate polyacrylamide gel electrophoresis
shRNA	short hairpin ribonucleic acid
siRNA	small interfering ribonucleic acid
src	sarcoma oncogene coding for a protein kinase
T[X/0/1/2/3]	tumor status
TBS	tris-buffered saline
TBST	tris-buffered saline and Tween-20
TBSTT	tris-buffered saline and Tween-20 and Triton X-100
TCR	T cell receptor
TEMED	N,N,N',N'-tetramethylethylenediamin

Abbreviations

Th1	T helper cell type 1
TILs	tumor infiltrating lymphocytes
TMB	3,3',5,5'-tetramethylbenzidine
TNM	tumor, lymph node, metastasis
UICC	Union for International Cancer Control
uPA	urokinase-type plasminogen activator
Val	valine
VEGF	vascular endothelial growth factor
v/v	volume per unit volume
w/v	weight per unit volume
XCL1	chemokine (X-C motif) ligand 1
XCR1	chemokine (X-C motif) receptor 1

LIST OF FIGURES

Figure 1: Cancer types according to estimated deaths, United States 2015.	2
Figure 2: The Cancer-Immunity Cycle.	9
Figure 3: Three-dimensional model of human CXCR3.	12
Figure 4: Variants of the CXCR3 receptor	14
Figure 5: CXCR3-A and CXCR3-B intracellular signaling	15
Figure 6: CXCR3 expression on lymphocytes and cancer cells	19
Figure 7: Map of shRNA cloning vector pRS	36
Figure 8: Immunohistochemical staining and scoring of CXCL9 in ovarian cancer tissue	45
Figure 9: Immunohistochemical staining and scoring of CXCL10 in ovarian cancer tissue	46
Figure 10: Prognostic significance of CXCL9 and CXCL10 expression in high-grade serous ovarian cancer (discovery set)	49
Figure 11: Prognostic significance of CXCL9 and CXCL10 expression in high-grade serous ovarian cancer (validation set)	55
Figure 12: Prognostic significance of CXCL9 and CXCL10 expression in high-grade serous ovarian cancer (combined cohorts)	60
Figure 13: Immunohistochemical staining and scoring of CXCR3 in tumor cells	63
Figure 14: Protein expression of CXCR3 in tumor lysates	64
Figure 15: Prognostic significance of CXCR3 expression in high-grade serous ovarian cancer (discovery set)	66
Figure 16: Prognostic significance of CXCR3 expression in high-grade serous ovarian cancer (validation set)	69
Figure 17: Prognostic significance of CXCR3 expression in high-grade serous ovarian cancer (combined cohorts)	71
Figure 18: CXCR3 expression in lymph nodes	73
Figure 19: Prognostic significance of combined CXCR3 and CXCL9 or CXCL10 expression in high-grade serous ovarian cancer (discovery set)	76
Figure 20: Prognostic significance of combined CXCR3 and CXCL9 or CXCL10 expression in high-grade serous ovarian cancer (validation set)	79
Figure 21: Prognostic significance of combined CXCR3 and CXCL9 or CXCL10	

expression in high-grade serous ovarian cancer (combined collectives).....	82
Figure 22: Protein expression of CXCR3 in SKOV-3 and OVCAR-3 cells	85
Figure 23: FACS analysis of wildtype OVCAR-3 and SKOV-3 cells	86
Figure 24: Proliferation of OVCAR-3 and SKOV-3 cells stimulated with chemokines...87	
Figure 25: Migration of OVCAR-3 and SKOV-3 cells towards CXCL9.....	88
Figure 26: Migration of OVCAR-3 and SKOV-3 cells towards FCS	89
Figure 27: Protease Array	90
Figure 28: Chemokine concentrations in ascites from human serous ovarian cancer patients	92
Figure 29: Microscopic evaluation of migration	95
Figure 30: Migration of OVCAR-3 cells towards human ascites.....	96
Figure 31: Migration of SKOV-3 cells towards human ascites.....	97
Figure 32: primary epithelial ovarian cancer cells.....	98
Figure 33: Migration of EOC cells towards ascites.....	99
Figure 34: Protein expression of mCXCR3 in ID8 cells	100
Figure 35: FACS analysis of wildtype ID8 cells	101
Figure 36: FACS analysis of transfected ID8 cells.....	102
Figure 37: Migration of mCXCR3 knockdown cells towards mCXCL10	103
Figure 38: Proliferation of mCXCR3 knockdown cells	104

LIST OF TABLES

Table 1: Ovarian cancer staging (modified from Wittekind et al., 2015).....	3
Table 2: Patient characteristics of the discovery and validation collectives for the immunohistochemical CXCL9 and CXCL10 staining.	21
Table 3: Patient characteristics of the discovery and validation collectives for the immunohistochemical CXCR3 staining.	22
Table 4: Ascites for migration assay: patient and tumor characteristics	23
Table 5: Ascites for isolation of primary epithelial ovarian cancer cells: patient and tumor characteristics.....	24
Table 6: CXCL9 and CXCL10 expression in ovarian cancer (discovery set).....	47
Table 7: Median progression-free and overall survival according to CXCL9 and/or CXCL10 expression (discovery set) – univariate analysis	48
Table 8: Cox multivariate analysis for the progression-free and overall survival (discovery set).....	50
Table 9: CXCL9 and CXCL10 expression in ovarian cancer (validation set)	53
Table 10: Median progression-free and overall survival according to CXCL9 and/or CXCL10 expression (validation set) – univariate analysis.....	54
Table 11: Cox multivariate analysis for the progression-free and overall survival (validation set)	56
Table 12: CXCL9 and CXCL10 expression in ovarian cancer (combined cohorts)	58
Table 13: Median progression-free and overall survival according to CXCL9 and/or CXCL10 expression (combined cohorts) – univariate analysis.....	59
Table 14: Cox multivariate analysis for the progression-free and overall survival (combined cohorts)	61
Table 15: CXCR3 expression in ovarian cancer (discovery set).....	64
Table 16: Median progression-free and overall survival according to CXCR3 expression (discovery set).....	65
Table 17: Cox multivariate analysis for the progression-free and overall survival (discovery set).....	66
Table 18: CXCR3 expression in ovarian cancer (validation set).....	67
Table 19: Median progression-free and overall survival in relation to CXCR3 expression (validation set)	68

Table 20: Cox multivariate analysis for the progression-free and overall survival (validation set)	69
Table 21: CXCR3 expression in ovarian cancer (combined cohorts)	70
Table 22: Median progression-free and overall survival in relation to CXCR3 expression (combined cohorts)	71
Table 23: Cox multivariate analysis for the progression-free and overall survival (combined cohorts)	72
Table 24: CXCR3 expression in lymph node metastases	73
Table 25: CXCL9, CXCL10 and CXCR3 in ovarian tumor (discovery set).....	74
Table 26: Median progression-free and overall survival in relation to CXCR3 and CXCL9 or CXCL10 (discovery set) – univariate analysis	75
Table 27: CXCL9, CXCL10 and CXCR3 in ovarian tumor (validation set)	77
Table 28: Median progression-free and overall survival in relation to CXCR3 and CXCL9 or CXCL10 (validation set) – univariate analysis.....	77
Table 29: CXCL9, CXCL10 and CXCR3 in ovarian tumor (combined cohorts)	80
Table 30: Median progression-free and overall survival in relation to CXCR3 and CXCL9 or CXCL10 (combined cohorts) – univariate analysis.....	81
Table 31: Cox multivariate analysis for the progression-free and overall survival (combined cohorts)	83
Table 32: Upregulation of proteases upon CXCL9 stimulation	91
Table 33: Correlations between CXCL9 and CXCL10 present in ascites.....	92
Table 34: Cox multivariate analysis for the progression-free and overall survival.....	93
Table 35: Ascites samples for migration assays	95

I. ABSTRACT

Expression of the chemokine receptor CXCR3 and its ligands CXCL9 and CXCL10 in tumors has divergent roles, either promoting or inhibiting tumor progression. The two chemokines CXCL9 and CXCL10 influence the tumor microenvironment by facilitating the chemotactic recruitment of CXCR3⁺ NK cells and T cells and can therefore impair tumor growth and metastasis formation. Expression of CXCR3 on tumor cells on the other hand is known to enhance tumor growth, tumor cell migration and metastasis resulting in a poor prognosis for cancer patients. This thesis is assessing the expression, function and clinical relevance of CXCR3 and its ligands in high-grade serous ovarian cancer (HGSC).

The expression of CXCR3, CXCL9 and CXCL10 was determined immunohistochemically in HGSC specimens. An overexpression of the chemokine ligands CXCL9 and CXCL10 was associated with a significantly prolonged overall and progression-free survival, whereas a CXCR3 overexpression on tumor cells predicted poor outcome. To analyze the effects of CXCR3 *in vitro*, two different ovarian cancer cell lines (OVCAR-3 and SKOV-3) were examined regarding CXCR3 expression, proliferation and protease expression upon chemokine stimulation and migration towards CXCR3 ligands. The ovarian cancer cells migrated towards CXCL9 and this migration could be suppressed by use of an anti-CXCR3 antibody. ELISA measurements demonstrated the CXCL9 and CXCL10 expression in 102 human ovarian cancer ascites samples. 10 different ascites samples were used as chemoattractants in migration assays. The ovarian cancer cell lines migrated towards the ascitic fluid in a CXCR3-dependent manner. Additionally, primary epithelial ovarian cancer cells isolated from patient derived ovarian cancer ascites were also CXCR3-dependently migratory active towards ascitic fluid. Moreover, a CXCR3 knockdown, that was generated in the murine ovarian cancer cell line ID8, was no longer able to migrate towards murine CXCL10.

These results demonstrate the ambivalent tumor supportive and inhibitory role of CXCR3 and its ligands in HGSC. CXCL9 and CXCL10 are potent anti-tumor effectors, but tumor CXCR3 exerts tumor-promoting functions by inducing ovarian cancer cell migration and peritoneal metastasis that result in a poor patient outcome.

II. INTRODUCTION

1. Ovarian cancer

1.1. Epidemiology of ovarian cancer

Ovarian cancer results from a malignant transformation of the ovarian tissue, mostly from the surface epithelium. Risk factors include age, dietary factors like adiposity and endocrinological factors (Rottman et al., 2014). It is a deadly disease as it is the fifth most common cause of cancer related deaths among women in the western world with an estimated five year survival rate of about 45% (Siegel et al., 2015). In Germany there have been 7380 new cases diagnosed in 2012 and 5646 patients died as a consequence of the disease. Although the total incidence of ovarian cancer is low compared to lung or breast cancer, the ratio of incidence and mortality is very high (*Krebs in Deutschland 2011/2012*, 2015).

Estimated deaths			
	Females		
	Lung & bronchus	71660	26%
	Breast	40290	15%
	Colon & rectum	23600	9%
	Pancreas	19850	7%
	Ovary	14180	5%
	Leukemia	10240	4%
	Uterine corpus	10170	4%
	Non-Hodgkin lymphoma	8310	3%
	Liver & intrahepatic bile duct	7520	3%
	Brain & other nervous system	6380	2%
	All sites	277280	100%

Figure 1: Cancer types according to estimated deaths, United States 2015.

Indicated are the most common cancer types that are expected to occur in women in the United States in 2015 in absolute numbers and in percent, highlighted is the ovary (modified from Siegel et al., 2015).

The high mortality rate is due to the absence of symptoms in the early stages, therefore the majority (75%) of the patients present at a late stage with symptoms like ascites formation and bowel obstruction where an already advanced metastasis into the

peritoneal cavity has occurred (Lengyel, 2010). Also the lack of screening methods accounts to this high mortality rate. Both the transvaginal sonography and the CA-125 tumor marker are no efficient tools in detecting early stage ovarian cancer (Schmalfeldt et al., 2014b).

1.2. Histological classification of tumors and prognostic factors

Based on their histological appearance, the ovarian tumors are classified into the following subtypes: tumors of epithelial origin (90%), germ band tumors (5-8%), germ cell tumors (3-5%) and rare others. The epithelial tumors comprise the serous carcinomas (70-80%) as the major subtype and the rarer types clear cell (3%), endometrioid (<5%) and mucinous cancers (<3%) (Mayr et al., 2014; Sundar et al., 2015).

The tumors are furthermore classified according to their histopathological grading and can be well (grade 1), moderately (grade 2) or poorly differentiated (grade 3) (Kosary, 1994). For ovarian serous carcinoma a 2-tier system comparing low-grade versus high-grade carcinomas is now in use, as a universal grading scheme is missing (Malpica et al., 2004; Vang et al., 2009).

Tumor staging is based on the TNM-system of the Union for International Cancer Control (UICC), which refers to the size and extent of the primary tumor (T), the involved regional lymph nodes (N) and the distant metastases (M) and which covers with the classification of the Fédération Internationale de Gynécologie et d’Obstétrique (FIGO) (Mayr et al., 2014; Wittekind et al., 2015).

Table 1: Ovarian cancer staging (modified from Wittekind et al., 2015)

TNM	FIGO	Definition
T - Tumor		
TX		Primary tumor cannot be evaluated
T0		No signs of tumor
T1	I	Limited to ovaries
T1a	IA	Limited to one ovary, capsule intact, no tumor on ovarian surface, no malignant cells in the ascites or in the peritoneum
T1b	IB	Limited to both ovaries, capsule intact, no tumor on ovarian surface, no malignant cells in the ascites or peritoneal washings
T1c	IC	Limited to one or both ovaries, capsule ruptured, tumor on ovarian surface or malignant cells in ascites or peritoneal washings

TNM	FIGO	Definition
T2	II	Pelvic extension
T2a	IIA	Extension to uterus and/or tubes, no malignant cells in the ascites or peritoneal washings
T2b	IIB	Extension to other pelvic tissues and/or tubes, no malignant cells in the ascites or peritoneal washings
T2c	IIC	Pelvic extension and malignant cells in the ascites or peritoneal washing
T3 and/or N1	III	Peritoneal metastasis beyond pelvis
T3a	IIIA	Microscopic peritoneal metastasis beyond pelvis
T3b	IIIB	Macroscopic peritoneal metastasis beyond pelvis ≤ 2 cm
T3c and/or N1	IIC	Peritoneal metastasis beyond pelvis >2 cm and/or regional lymph node metastasis
N - regional lymph nodes		
NX		Regional lymph nodes cannot be evaluated
N0		No regional lymph nodes metastasis
N1		Regional lymph nodes metastasis present
M - distant metastasis		
MX		Distant metastasis cannot be evaluated
M0		No distant metastasis
M1		Metastasis to distant organs (excluding peritoneal metastasis)

The 10-year survival rate is associated with the FIGO stage, as it is approximately 73% in FIGO I, 45% in FIGO II, 21% in FIGO III and below 5% in FIGO IV (Jelovac et al., 2011).

Epithelial ovarian cancers can be divided into two major groups. Group I is composed of low-grade and slowly developing tumors (low-grade serous, low-grade endometrioid, clear cell and mucinous carcinomas). They are presented at early stages when they are confined to the ovary. The type II tumors are high-grade serous ovarian carcinomas (HGSC), they are the most aggressive tumors and have a poorer survival compared to other subtypes. Moreover the high-grade serous ovarian carcinomas differ from low-grade serous carcinomas as they process and evolve more rapidly and they are associated with different mutations (Kurman et al., 2010; Levanon et al., 2008). This thesis is focused on the type II tumors, the high-grade serous ovarian carcinomas, as they represent the clinically most important and largest subgroup.

Taken together, the histological subtype, the tumor grade and the tumor stage are well-established clinical prognostic factors, together with age and general state of health of the patient and the residual tumor mass after debulking surgery. Especially the residual

tumor mass is the strongest independent prognostic factor (Mayr et al., 2014). The tumor status after surgery is described as R0 (no residual tumor), R1 (microscopic residual tumor) or R2 (macroscopic residual tumor) (Hermanek et al., 1994). Patients with residual tumor of 1 cm or greater (R2) after primary surgery had a higher risk of death compared with those who underwent optimal debulking surgery (Tingulstad et al., 2003).

1.3. Hereditary ovarian cancer

About 10% of the ovarian tumors are a result of a genetic predisposition. Clinical characteristics are young age at first diagnosis of the patients and a familiar history of breast and ovarian cancer. The median age of a patient with sporadic tumor is 69 years compared to only 50-55 years for patients with a hereditary ovarian cancer, depending on the mutations involved (Kiechle et al., 2014). The majority of hereditary ovarian cancers can be attributed to mutations in the genes BRCA1 (chromosome 17q21) or BRCA2 (chromosome 13q12) that are inherited dominantly. These mutations are strong risk factors for developing breast and ovarian cancer (“hereditary breast ovarian cancer syndrome”, HBOC). The cumulative risk to develop ovarian cancer by age of 70 with a BRCA1 mutation is 40%-60%, women with a BRCA2 mutation have a lower cancer risk of about 11% (Kiechle et al., 2014; Tinelli et al., 2010). The tumors developed by BRCA1/2 mutation carriers are predominantly high-grade serous ovarian cancers. The proteins BRCA1 and BRCA2 are required for DNA double strand break repair processes and are inactivated by different mutations. The mutation carriers are more sensible to a platinum-based chemotherapy because the therapy leads to an increased DNA damage, that cannot be efficiently repaired. For that reason the patients carrying a BRCA1/2 mutation show a favorable outcome and a longer survival compared to patients without mutations (Bolton et al., 2012; Despierre et al., 2010).

1.4. Carcinogenesis of ovarian cancer

The malignant transformation of cancer cells is a multistep process, that involves several genetic changes like mutations, copy number changes or DNA methylation that lead to tumor suppressor gene inactivation or oncogene dysregulations. For example the oncogene K-ras is often overexpressed in ovarian cancer, as well as the oncogenes HER2/neu or p53 which results in malfunctions in several biological processes like cell proliferation or apoptosis (Holschneider et al., 2000). The origin of

ovarian cancer is traditionally attributed to the ovarian surface epithelium and subsequent changes are supposed to promote the development of the different subtypes. Recently though it has been postulated that at least part of these cancers, especially the serous ovarian cancers, arise from the fallopian tube, endometrium or mesothelium of the peritoneal cavity and spread to the ovary secondarily (Kurman et al., 2010; Lengyel, 2010).

For metastasis at advanced stages, the cancer cells have to first detach from the primary tumor. Therefore, the cells undergo several morphological, molecular and functional changes to shift from an epithelial cell type to a mesenchymal phenotype, a transforming process called epithelial-mesenchymal transition (EMT). Hereby the cells lose their polarity and their cell-cell adhesion and become more invasive and migratory (Kalluri et al., 2009). After detachment from the primary tumor, ovarian cancer metastasis is thought to occur in a rather passive way, as the cancer cells are carried by peritoneal fluid or ascites to the mesothelium of peritoneum and omentum, where they can again actively attach and form secondary cancer sites by undergoing a reverse transformation, now from the mesenchymal cell type back to the epithelial cell type (mesenchymal-epithelial transition, MET) (Lengyel, 2010).

Besides hypoalbuminemia, dietary deficiency or cachexia, ascites within the peritoneal cavity can be formed due to obstruction of lymphatic channels by the tumor, so that the physiologically produced peritoneal fluid can no longer be absorbed, or due to tumor neoangiogenesis. Moreover, ovarian cancer cells secrete vascular endothelial growth factor (VEGF) which enhances the vascular permeability and promotes ascites formation (Lengyel, 2010; Tan et al., 2006).

Ovarian cancer initially spreads to adjacent organs by direct extension of cancer cells, e.g. to fallopian tubes, uterus, adnexa, rectum, bladder and pelvic wall. After this direct extension, metastasis most frequently occurs via the so called transcoelomic route, meaning the metastasis to peritoneum and omentum. The pelvic lymph nodes are furthermore often involved. Peritoneal or ascitic fluid carrying ovarian cancer cells passes the gate to the lymphatic and the circular system, leading to lymph node and haematogenous metastases, the latter ones though being very rare (Tan et al., 2006).

1.5. Treatment of ovarian cancer

The first line of treatment is a debulking surgery, with the aim to achieve a complete removal of the tumor, as the residual tumor mass is the strongest independent prognostic factor and critical for patient survival. Optimal tumor debulking is defined as residual tumor being less than 1 cm (Schmalfeldt et al., 2014a). The surgery is followed by an adjuvant chemotherapy. For low-grade cancers a monotherapy with carboplatin is recommended. For high-grade ovarian cancers (FIGO IIb-IV) a systemic treatment composed of carboplatin, paclitaxel and the antiangiogenic monoclonal antibody bevacizumab is used (Burges et al., 2014). Carboplatin exerts its cytotoxic effects through forming crosslinks between DNA molecules and induction of carboplatin-DNA adducts. Paclitaxel stabilizes the microtubule polymer so that it cannot get disassembled. This leads to cell cycle arrest in the G2/M phase irrespective of the p53 status so that mitosis cannot take place. Moreover, the paclitaxel induced cell cycle arrest hinders the repair of the carboplatin-DNA adducts, so that the combination of both chemotherapeutics is beneficial (Jiang et al., 2015). The vascular endothelial growth factor (VEGF) is present in 97% of all ovarian cancers and enhances tumor neoangiogenesis, ascites formation and malignant progression of the tumor. It can be pharmaceutically inhibited by the monoclonal antibody bevacizumab. Additional administration of bevacizumab to the carboplatin/paclitaxel therapy elongates progression-free survival, its effect on overall survival is not yet known (Burger et al., 2007; Burges et al., 2014). The median progression-free survival of advanced ovarian cancer is 18 months. Patients with a recurrence six or more months after the initial chemotherapy are called platinum-sensitive, progression in the first six months after completing platinum-based chemotherapy or even during ongoing therapy is defined as platinum-resistant disease. Therapy options for platinum-sensitive patients are secondary cytoreductive surgery and retreatment with platinum-based combinations. Platinum-resistant patients are not treated by combination therapeutics but rather by sequential single agents such as the cytostatic drugs topotecan, doxorubicin or taxane drugs like paclitaxel or docetaxel (Jayson et al., 2014; Jelovac et al., 2011).

2. Ovarian cancer as immunogenic tumors

Despite the improvements in surgery and chemotherapy over the past decade, ovarian cancer is still a highly deadly and often a chemoresistant disease. Therefore, new

therapeutic approaches like immunotherapies are necessary. The interaction of immune system components and tumors gained more and more attention as the tumor-suppressive lymphocytic infiltration was more and more investigated. Both the Cancer Genome Atlas project and Tothill et al. delineated four distinct subtypes of high-grade ovarian cancers by analyzing mRNA and miRNA expression levels, termed ‘immunoreactive’, ‘differentiated’, ‘proliferative’ and ‘mesenchymal’. The ‘immunoreactive’ subtype was defined by the chemokine receptor CXCR3 and its ligands CXCL9, CXCL10 and CXCL11 and it displayed an enhanced T cell infiltration and an improved clinical outcome compared to the other subtypes (Cancer Genome Atlas Research, 2011; Tothill et al., 2008). Regarding the T cell infiltration, Zhang et al. could correlate the presence of intratumoral CD3⁺ T cells with a better progression-free and overall survival in patients with advanced ovarian carcinoma. In this study, the five-year overall survival rate was enhanced approximately eightfold comparing patients whose tumors contained T cells versus patients whose tumors contained no T cells (Zhang et al., 2003). Another study could correlate the tumor-infiltration of CD8⁺ T lymphocytes with a prolonged overall survival in ovarian cancer patients (Sato et al., 2005).

For an anticancer immune response that results in effective killing of tumor cells, several steps have to occur, which is referred by Chen and Mellman to the so called “Cancer-Immunity Cycle” and shown in Figure 2. Cancer cell antigens are released by cancer cell death and then presented on major histocompatibility complex I and II (MHCI and MHCII) molecules by dendritic cells (DCs) and antigen-presenting cells (APCs) to T cells. That leads to priming and activation of effector T cell responses like effector T cells trafficking into tumors. The cytotoxic T lymphocytes (CTLs) infiltrate the tumors, recognize and bind cancer cells by interaction of the T cell receptor (TCR) with its antigen bound to MHCI and finally kill the target cancer cells. This releases additional cancer cell antigens so that the first step is repeated and the cycle starts anew. In numerous revolutions of the cycle the immune response is amplified and broadened (Chen et al., 2013).

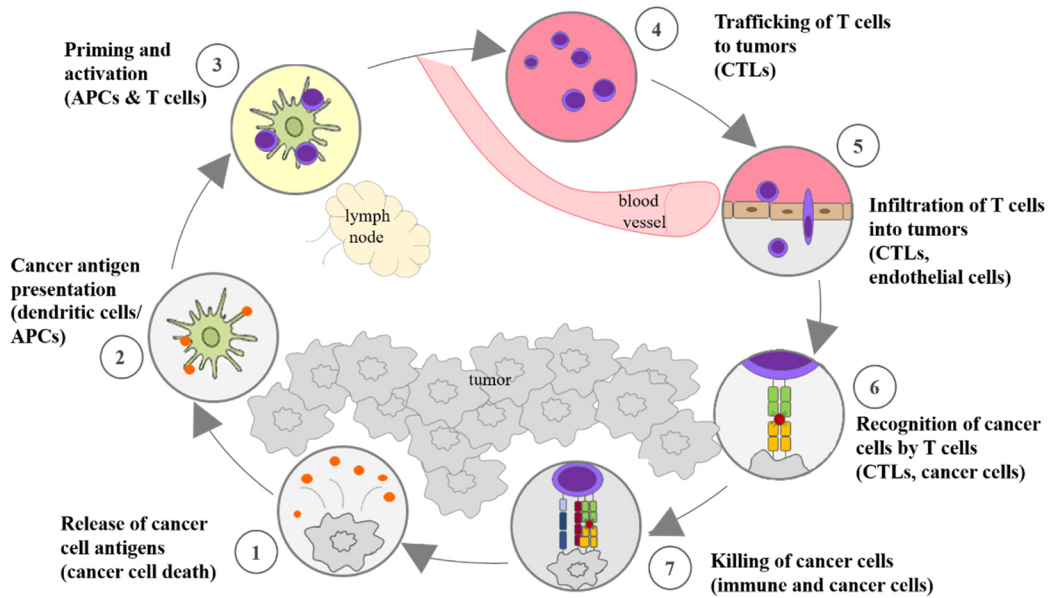


Figure 2: The Cancer-Immunity Cycle.

Effective immune response to cancer cells is a cyclic process, that can be divided into seven steps. Each step is described above, mentioning the activities, the involved cell types and the anatomic location of the events (modified from Chen & Mellman, 2013).

For the treatment of ovarian cancer several immunotherapies and anti-cancer vaccinations have been developed such as monoclonal antibody therapies directed against CA-125 or HER2, vaccines directed towards whole tumor antigens gained from tumor cells, lysates or RNA, treatments containing interleukin 2 (IL-2) and adoptive transfer of *ex vivo* expanded tumor infiltrating lymphocytes (TILs) (Kandalaf et al., 2011). But so far, the vaccines and the different immunotherapies are not very efficient. Despite the vaccination strategy the therapies induce tumor-specific T cells that are present in the blood, but are often deficient at the tumor sites. Hence, one of the key steps towards an effective anticancer immune response is the recruitment and infiltration of tumor suppressive lymphocytes into the tumor, referring to step number four in the “Cancer-Immunity Cycle” (Figure 2). This is besides others the major task of the chemokines (Abastado, 2012). Not only T lymphocytes, but also natural killer cells play an important role in an effective anticancer immune response, as they recognize transformed cancer cells that often have a reduced or absent MHC I expression and thereby evading cytotoxic T lymphocyte-mediated killing. Chemokine ligands CXCL9 and CXCL10 and their receptor CXCR3 are involved in the recruitment of NK cells to the tumor, which was shown to prolong survival in lymphoma-bearing mice (Wendel et al., 2008). The chemokines are therefore potent

key players in promoting tumor-suppressive immune infiltration in solid malignancies.

3. Chemokines and chemokine receptors

Chemokines are a superfamily of approximately 50 low molecular weight (8-12 kDa) chemotactic cytokines and their respective receptors. They are important mediators of leukocyte migration, angiogenesis, hematopoiesis, embryogenesis, tumor growth and metastasis (Allen et al., 2007; Vandercappellen et al., 2008). The chemokines are divided into four subgroups designated as CXC, C, CC or CX₃C, based on the presence or spacing of the first two conserved cysteine residues at the amino-terminal part of the protein (Rossi et al., 2000). Based on their function and expression pattern chemokines can be additionally classified into two main groups, the homeostatic/constitutive and the inflammatory/inducible chemokines. The homeostatic chemokines play a role in immune surveillance and in lymphocyte and dendritic cell trafficking during hematopoiesis and are constitutively expressed in certain cell types and tissues, whereas the inflammatory chemokines are not constitutively expressed but are induced and regulated by proinflammatory stimuli such as cytokines (Rotondi et al., 2007; Vandercappellen et al., 2008).

3.1. CXC chemokines

The CXC chemokines are inflammatory chemokines except for CXCL12 and CXCL13, which are homeostatic (Vandercappellen et al., 2008). CXC chemokines are characterized by a single non-conserved amino acid between the first two cysteine residues at the protein's amino-terminus, hence the designation CXC. The group of the CXC chemokines can be further subdivided according to the presence or absence of a three amino acid motif preceding the CXC domain, the glutamic acid-leucine-arginine- or ELR-motif and are referred to as ELR⁺ or ELR⁻. The lack of the ELR-motif is known to correlate with an angiostatic activity, thus ELR⁻ CXC chemokines like CXCL9 and CXCL10 are linked to antagonize angiogenesis with one exception for CXCL12 (Strieter et al., 2004; Strieter et al., 1995).

The angiostatic chemokines CXCL9, CXCL10 and CXCL11 are interferon-gamma (IFN- γ) inducible chemokines that bind exclusively to their receptor CXCR3, with CXCL11 having the highest binding affinity to the receptor followed by CXCL9 and CXCL10 (Murphy et al., 2000). Before the CXC nomenclature was initiated, CXCL9

was called Mig (monokine induced by gamma interferon), CXCL10 was known as IP-10 (interferon gamma-induced protein 10) and I-TAC (interferon-inducible T cell alpha chemoattractant) stood for CXCL11 (Vandercappellen et al., 2008).

In response to IFN- γ stimulation CXCL9 and CXCL10 are produced and secreted by a variety of cells including monocytes, macrophages, antigen-presenting cells, B cells, endothelial cells, fibroblasts and keratinocytes (Luster et al., 1987; Park et al., 2002). CXCL9 expression is stimulated solely by IFN- γ , whereas CXCL10 expression is stimulated by all three interferons, IFN- α , IFN- β and IFN- γ (Farber, 1990; Vanguri et al., 1990).

CXCL11 is known to exert different biological functions compared to CXCL9 and CXCL10. While CXCL11 is important for the polarization of CD4⁺ T cells into T regulatory cells and therefore plays a role in restraining and mediating of inflammatory autoimmunity, the chemokines CXCL9 and CXCL10 induce T cell polarization into effector T cells (Karin et al., 2015). Moreover, CXCL9 and CXCL10 attract different leukocytes including monocytes, natural killer cells or T lymphocytes to sites of inflammation. Several CXC chemokines have been shown to induce optimal lymphocytic chemotaxis at concentrations ranging between 3–30 μ M (Taub, 2000). This thesis is focused on CXCL9 and CXCL10 as they are the major key players in mediating the recruitment of tumor-suppressive CXCR3⁺ T and NK cells to solid tumors like ovarian tumors.

3.2. CXCR3

The chemokines CXCL9, CXCL10 and CXCL11 exert their biological effects by binding exclusively their common receptor CXCR3, which is expressed by activated T cells and circulating blood T cells, NK cells, B cells, dendritic cells and endothelial cells (Garcia-Lopez et al., 2001; Qin et al., 1998), but also by a variety of cancers including breast cancer (Datta et al., 2006), ovarian cancer (Furuya et al., 2011) and prostate cancer (Engl et al., 2006). Among the T lymphocytes, CXCR3 is expressed on CD4⁺ as on CD8⁺ T cells and it is mostly expressed on CD4⁺ Th1 lymphocytes with around 90% CXCR3⁺ cells in this subtype (C. H. Kim et al., 2003; Loetscher et al., 1996). Particularly the receptor expression on T lymphocytes and NK cells participates in the localization of these major key players of the immune defense at sites of inflammation.

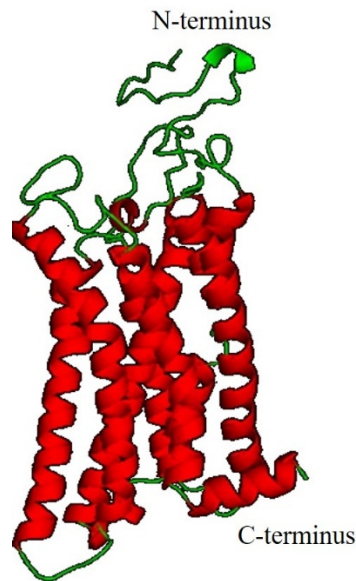


Figure 3: Three-dimensional model of human CXCR3.

The backbone ribbon is shown in green, the seven α -helices in red. N-terminus and C-terminus are labeled (modified from Trotta et al., 2009).

CXCR3 is coupled to a heterotrimeric G protein and is structurally composed of an extracellular amino-terminal part, six membrane-spanning loops separated by seven transmembrane domains and a cytoplasmic carboxyl-terminal part (Billottet et al., 2013; Thompson et al., 2007). The three loops of the extracellular amino-terminal domain are important for receptor activation and weak ligand binding, the three loops of the intracellular carboxyl-terminal domain are involved in signal transduction upon ligand binding through phosphorylation of serine and threonine residues. The aspartate-arginine-tyrosine sequence in the third transmembrane domain of CXCR3 is essential for induction of chemotaxis, calcium mobilization and extracellular-signal regulated kinase (ERK) phosphorylation. In general, chemokine ligand binding results in receptor activation and internalization, which leads to calcium influx and induction of several signaling pathways involving kinases such as mitogen-activated protein kinase/extracellular-signal regulated kinase (MAPK/ERK) and Akt/protein kinase B and eventually to cytoskeleton rearrangement and cell migration (Colvin et al., 2004; Lacotte et al., 2009). More recent studies have shown that different chemokine ligands bind to different receptor domains and induce different signals upon CXCR3 binding. It was investigated by Xanthou et al. that the N-terminus of CXCR3 and first extracellular loop is important for CXCL10- and CXCL11-mediated receptor activation, but not for CXCL9-induced signaling and that the third extracellular loop

is responsible only for CXCL9- and CXCL10-mediated chemotaxis (Xanthou et al., 2003). Moreover, it was noted that high affinity binding and receptor activation are distinct functions. The receptor N-terminus is not important for high-affinity binding, but for determination whether a chemokine binds to receptor and if it binds as agonist or antagonist. For maximal and high-affinity ligand binding the carboxyl terminus plays a key role. The interaction between CXCR3 and its ligands is proposed to be a multi-site model where multiple and distinct receptor domains are necessary for appropriate ligand binding and receptor activity (Colvin et al., 2004; Murphy et al., 2000; Xanthou et al., 2003).

For receptor desensitization and hence regulation of the receptor responsiveness, the receptor is either uncoupled from the heterotrimeric G-protein or internalized, meaning the receptor is degraded in endosomes or recycled back to the cell surface. The internalization is therefore a process contributing to the resensitization of the receptor. Internalization reduces the continuing migration and chemotactic activity of leukocytes under inflammatory conditions. High concentrations of CXCL11 were shown to rearrange actin cytoskeleton, a process in which the third intracellular loop of CXCR3 is necessary. This actin polymerization enhances the adhesion of cells to the extracellular membrane and to integrin ligands and therefore prevents the cell migration (Dagan-Berger et al., 2006; Ferguson et al., 1996).

Three functional isoforms of human CXCR3 are known: CXCR3-A and CXCR3-B are generated by alternative splicing and CXCR3-alt by translation of a truncated transcript of CXCR3. Figure 4 shows a scheme of the isoforms. CXCR3-alt is a truncated variant of CXCR3 (267 aa) that does not contain the second exon of the CXCR3 open reading frame, therefore it shows a dramatically different structure and consists of only four or five transmembrane domains, but still mediates functional activity even though CXCR3-alt responds only to CXCL11. Compared to the full-size CXCR3 isoform, the CXCR3-alt mRNA and protein expression is low and the functional relevance is not yet clearly identified (Billottet et al., 2013; Ehlert et al., 2004).

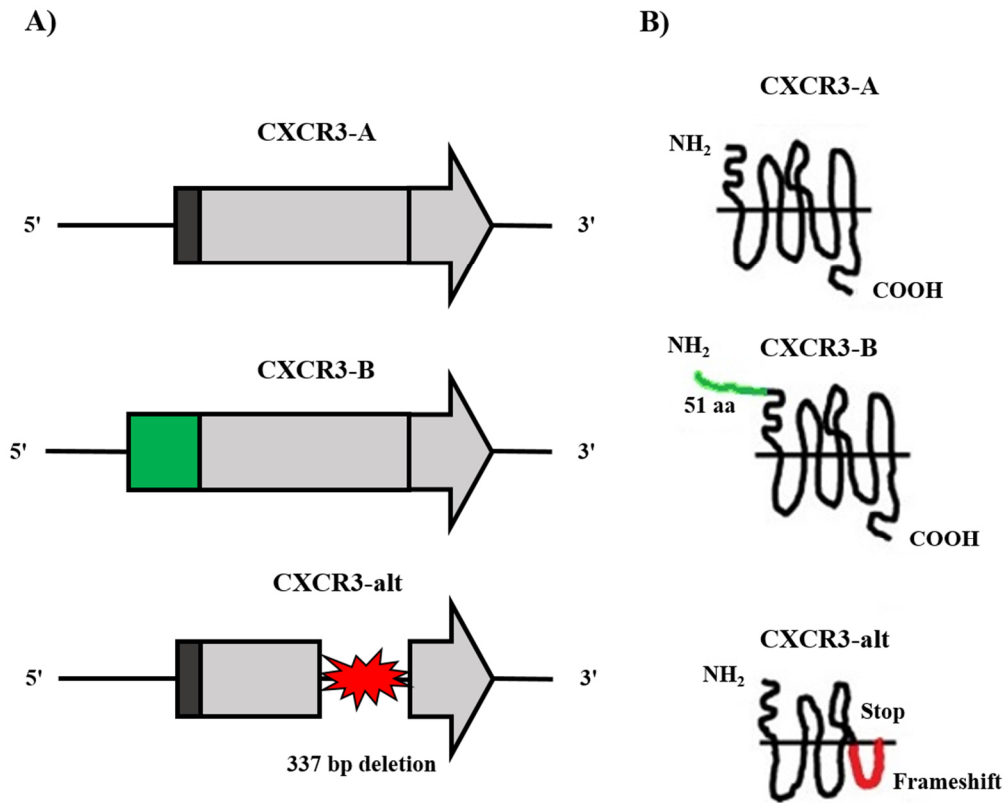


Figure 4: Variants of the CXCR3 receptor

Structure of CXCR3-A, CXCR3-B and CXCR3-alt **A)** gene and **B)** protein. Common mRNA sequences to all variants are indicated with gray boxes. The longer extracellular domain of the N-terminus of CXCR3-B mRNA is displayed in green, the classical N-terminus of CXCR3-A mRNA with a black box. The missing 337 base pairs in CXCR3-alt mRNA are shown in red, as well as the predicted 6th transmembrane domain where the CXCR3-alt mRNA forms a stop codon. (modified from Furuya et al., 2011).

CXCR3-A is the main isoform and found in most cell types (Liu et al., 2011). The ligands CXCL9, CXCL10 and CXCL11 all bind to CXCR3-A and CXCR3-B. Another chemokine, CXCL4, binds weakly to CXCR3-B. The CXCR3-A isoform codes for a protein of 368 aa and mediates chemotaxis, proliferation and anti-apoptotic effects, whereas CXCR3-B mediates the angiostatic effects of the CXCR3 ligands, so that is the preferred receptor isoform to be expressed on endothelial cells. It also mediates anti-proliferative and pro-apoptotic effects. The CXCR3-B isoform shares the identical 3'-sequence with CXCR3-A, but displays a longer extracellular amino-terminus, so that it codes for a larger protein of 415 aa (Billottet et al., 2013; Campanella et al., 2010; Lasagni et al., 2003). CXCR3-A and CXCR3-B share the common G protein catalytic subtypes G β and G γ , but differ in their coupled regulatory α subtypes. CXCR3-A is mainly linked to G proteins of the subtype G α i or G α q, whereas CXCR3-B is coupled to G α s. Activation of the receptor and thus these G

proteins results in the different signaling pathways. The chemotactic, proliferative, migratory, invasive, survival and tumor growth enhancing effects of CXCR3-A signaling are mediated through $G_{\alpha q}$ activation of phospholipase C β (PLC β) and through $G_{\alpha i}$ stimulation of phosphatidylinositol-3-kinase (PI3K)/Akt and MAPK/ERK pathways. Signaling through the $G_{\alpha s}$ protein coupled to CXCR3-B inhibits cell proliferation, angiogenesis and metastasis and enhances apoptosis via activation of the cyclic adenosine monophosphate (cAMP)-dependent pathway (Figure 5) (Billottet et al., 2013). CXCR3-B and CXCR3-alt do not exist in mice, CXCR3-A is expressed as the only isoform of murine CXCR3 (Ehlert et al., 2004; Leibovich-Rivkin et al., 2013).

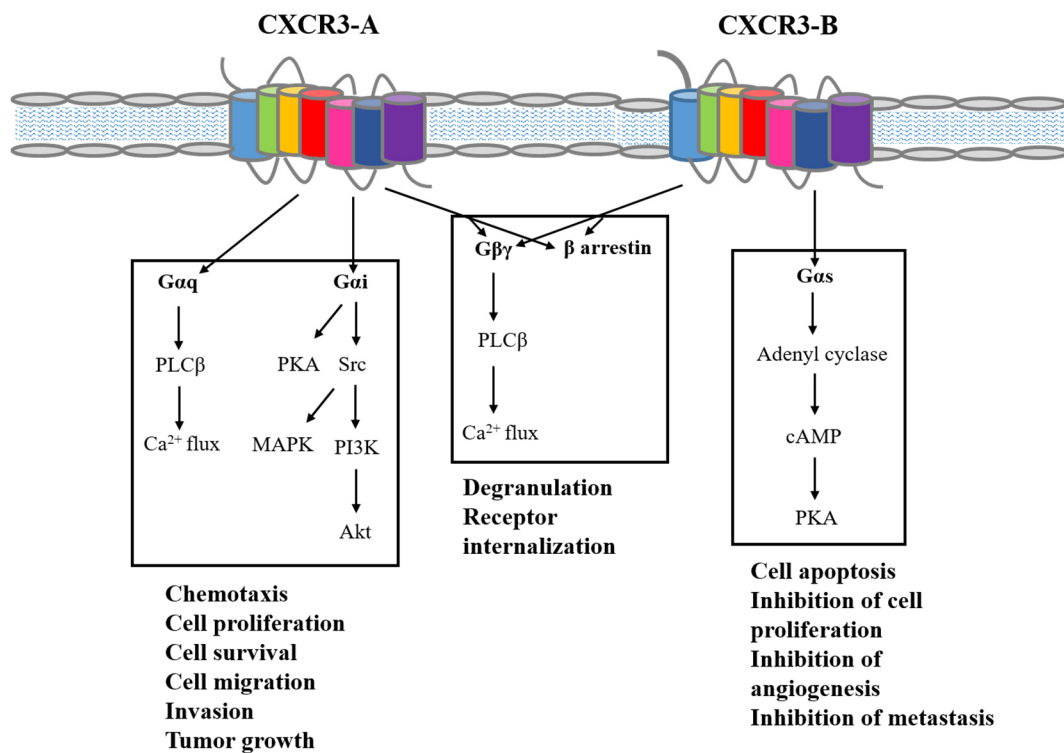


Figure 5: CXCR3-A and CXCR3-B intracellular signaling

CXCR3-A is mainly linked to $G_{\alpha q}$ or $G_{\alpha i}$ proteins, that activates pathways such as PLC β , MAPK or PI3K/Akt, resulting in chemotaxis and enhanced cell proliferation, survival, migration, invasion and also tumor growth. CXCR3-B is coupled to $G_{\alpha s}$ proteins, that mediate cell apoptosis and inhibits cell proliferation, angiogenesis and metastasis through the cAMP-dependent pathway. Both receptor isoforms bind the G protein subunits $G\beta$ and $G\gamma$ resulting in degranulation and receptor internalization (modified from Billottet et al., 2013)

3.3. CXCL9 and CXCL10 expression in cancer

The angiostatic chemokines CXCL9 and CXCL10 attract leukocytes to sites of inflammation and on that account also to the tumor microenvironment. Hence the

recruitment of CXCR3⁺ NK and T cells to tumors, the generation of tumor-specific cytotoxic T lymphocyte responses, together with the angiostatic effects are potent anti-malignant activities of CXCL9 and CXCL10 that result in tumor suppression and control of metastasis (Rossi et al., 2000). Several studies have investigated the antitumor role of the chemokine ligand expression in experimental murine cancer models. The transfection of a highly invasive murine mammary cancer cell line with CXCL9 inhibited tumor growth in a T cell dependent manner and decreased the growth of lung metastases NK cell-dependently (Walser et al., 2007). Transfection of a murine mammary cancer cell line with CXCL10 also inhibited tumor growth, enhanced the survival of the treated mice and increased the tumor-specific T cell infiltration (Yang et al., 2006). Tumor-derived CXCL9 was critical for T cell-mediated suppression of cutaneous fibrosarcomas, and the loss of CXCL9 expression was proposed to be an immune escape mechanism of tumors (Gorbachev et al., 2007). This tumor immune evasion mechanism was further investigated and it was shown that fibrosarcomas growing under IFN γ -mediated stress cease CXCL9 expression that results in a more aggressive tumor growth rate, as well as an increased resistance to antitumor T cell immunity and a poor recruitment of T and NK cells into these tumors (Petro et al., 2013). Dorsey et al. systemically administered recombinant human CXCL10 to mice bearing highly malignant mammary tumors and showed a significant tumor growth inhibition, an effect that was partially reversed by adding anti-CXCL10 antibodies. The tumor growth inhibition was accompanied by an increasing CD4⁺ T cell infiltration (Dorsey et al., 2002).

Analysis of human patient samples revealed a high expression of CXCL9 and CXCL10 as favorable prognostic factors in renal cell carcinoma, associated with decreased tumor size and increased CD8⁺ T cell infiltration (Kondo et al., 2004), as well as high CXCL9 expression being associated with a longer disease-free survival in breast cancer patients treated with a cyclophosphamide, methotrexate and 5-fluorouracile (CMF)-based chemotherapy (Specht et al., 2009).

Thus, mechanisms that increase the levels of CXCL9 and CXCL10 in the tumor microenvironment have shown to promote effective cell-mediated anti-tumor activity through the CXCR3 expressing effector NK and/or T lymphocytes. While the studies mentioned above demonstrate the favorable anti-tumor activity mediated by CXCL9 and CXCL10, regulatory T cells also express CXCR3, and analysis of breast cancer

samples revealed an association of CXCL10 expression with increased CXCR3⁺FOXP3⁺ regulatory T cells (Mulligan et al., 2013). The antibody-mediated neutralization of CXCL10 inhibited migration of regulatory T cells to breast tumor sites *in vivo* in a mouse tumor model (Ye et al., 2013). Furthermore, while the presence of intratumoral CD3⁺ T cells in epithelial ovarian cancer was beneficial for survival, tumor-infiltrating CD4⁺ T lymphocytes were shown to be correlated with an unfavorable outcome and to influence the beneficial effects of CD8⁺ tumor infiltration. A high ratio of CD8⁺/CD4⁺ TIL compared to a low ratio was associated with a prolonged overall survival (Sato et al., 2005; Zhang et al., 2003). Hence, recruitment of these CD4⁺ suppressor cells into the tumor could lead to pro-tumor effects.

3.4. CXCR3 expression in cancer

The expression of the chemokine receptor CXCR3 on immune effector cells can mediate effective anti-tumor activities by chemokine ligand-mediated infiltration of CXCR3⁺ lymphocytes into the tumor microenvironment, where they can exert their cytotoxic functions. But CXCR3 is also expressed by tumor cells, where it induces distinct effects that are considerably pro-malignant. Several studies have explored that endogenous CXCR3 expression enhances tumor growth, tumor cell migration and metastasis resulting in a poor prognosis for cancer patients. Ma et al. demonstrated that tumor CXCR3 expression promoted metastasis in a murine model of breast cancer and high CXCR3 expression correlated with poor overall survival in early breast cancer patients (Ma et al., 2009). In a murine model of melanoma, the metastatic frequency to lymph nodes was dramatically decreased by transfecting melanoma cells with CXCR3-shRNA or by treating glioma bearing mice with antibodies against CXCL9 and CXCL10 (Kawada et al., 2004). The same group showed that CXCR3-overexpressing human colon cancer cells expanded more rapidly in mice and formed more metastases in the draining lymph nodes. Moreover, a high CXCR3 expression was associated with a poorer prognosis for colon cancer patients (Kawada et al., 2007). These results were verified by Wu et al., describing a poorer overall survival for patients with colorectal cancer and an association of high CXCR3 expression in human colorectal cancer samples with tumor size and differentiation, as well as lymph node and distant metastasis (Wu et al., 2012). Pharmacological antagonism of CXCR3 inhibited lung metastasis of breast cancer cells in a murine model (Walser et al., 2006) and inhibited lung metastasis of colon carcinoma cells (Cambien et al., 2009).

The impact of CXCR3 expression is therefore a paradox: while the expression of CXCR3 on immune cells and its recruitment by the ligands is correlated with a better patient survival, the expression of CXCR3 on cancer cells is associated with a poor outcome. Liu et al. found that glioma-bearing CXCR3-deficient mice showed a decreased median survival time together with reduced numbers of tumor-infiltrating NK and NKT cells, whereas a pharmacological antagonism of CXCR3 resulted in a prolonged median survival time and did not impact lymphocytic tumor infiltration (Liu et al., 2011). There are several hypotheses that could explain this paradox. On the one hand are the CXCR3⁺ immune cells that are recruited by chemokine ligands to the tumor site, where the T lymphocytes and NK cells can exert their biological functions, namely kill the cancer cells. The angiostatic ligands CXCL9 and CXCL10 can inhibit the tumor angiogenesis. Furthermore, a ligand gradient towards the tumor bed can possibly hold back CXCR3⁺ cancer cells at the tumor site. On the other hand is CXCR3 responsible for the homing of CXCR3⁺ cancer cells into organs with abundant chemokine ligand expression such as lymph nodes (Kawada et al., 2011), lung (Pradelli et al., 2009) and liver (Murakami et al., 2013) by exploiting distant chemokine ligand gradients. In this context CXCL10 was shown to facilitate the trafficking of CXCR3⁺ breast cancer and melanoma cells to bone and to promote osteolytic bone metastasis (Lee et al., 2012). The CXCR3⁺ cancer cells could further serve as decoy receptors, meaning they bind intratumoral ligands which limits their ability to recruit immune effector cells. An activation of CXCR3 on cancer cells was also shown to induce the expression of proteases such as MMP-1, MMP-2, MMP-3 or MMP-9 (Kawada et al., 2007; Shen et al., 2015). Moreover, it is important, which splice variant of CXCR3 is expressed. CXCR3-A is known to promote migration and invasion of several cancer types, whereas CXCR3-B inhibits migration, proliferation and growth, induces apoptosis and has no chemotactic function. It is postulated, that CXCR3-B supports a cancer stem-like cell phenotype (Li et al., 2015). In some cells, CXCR3-B is downregulated by the oncogene Ras to promote tumor cell proliferation (Datta et al., 2006).

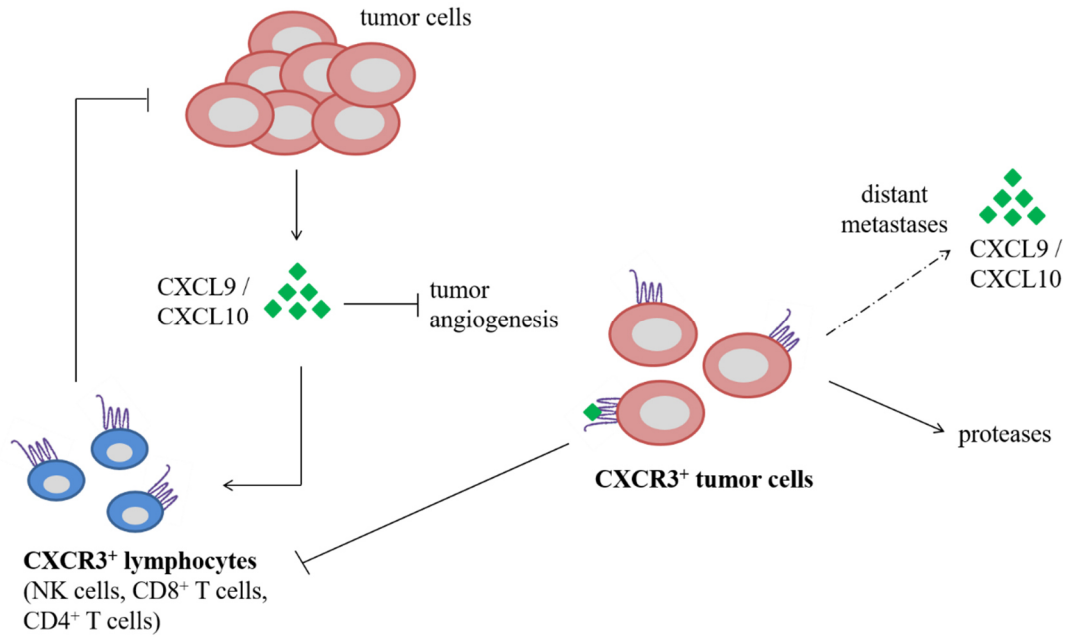


Figure 6: CXCR3 expression on lymphocytes and cancer cells

CXCR3⁺ lymphocytes are recruited by the angiostatic chemokines CXCL9 and CXCL10 to the tumor microenvironment. CXCR3⁺ tumor cells bind the chemokine ligands, thus limiting their ability to recruit lymphocytes. Moreover CXCR3⁺ tumor cells can upregulate proteases and can exploit chemokine gradients to migrate to distant organs and metastasize (modified from Cerny et al., 2014).

To date, only little is known about the role of CXCR3 and its ligands in serous ovarian cancer and the association of the expression of CXCR3, CXCL9 and CXCL10 with histopathological and clinical parameters. CXCR3 was found to be upregulated in clear cell ovarian cancer cells, but not in normal ovarian tissue (Furuya et al., 2007; Furuya et al., 2011). Moreover, a high expression of CXCR3 could be associated with tumor grade and lymph node metastasis in patients with primary ovarian cancer. In this study, ovarian cancer tissues from 78 patients were analyzed and 45 were expressing high CXCR3. The analyzed collective was composed of several ovarian cancer subtypes, only approximately 40% were serous ovarian cancers and around 60% were clear cell, endometrioid or mucinous ovarian cancers, which are the rarer subtypes of ovarian cancer. No correlation between CXCR3 expression and survival was performed (Lau et al., 2014).

III. AIMS OF THE STUDY

The aim of this study was to identify the expression, function and clinical relevance of CXCR3 and its ligands in high-grade serous ovarian cancer. In detail, the following topics are investigated:

- In several cancer types the chemokine ligands CXCL9 and CXCL10 have an anti-malignant role by recruiting CXCR3⁺ tumor-suppressive T lymphocytes and NK cells to the tumor microenvironment. What kind of role play CXCL9 and CXCL10 in the pathophysiology of ovarian cancer, especially in the regulation of the intratumoral immune infiltration?
- The expression of the receptor CXCR3 is known to promote pro-malignant functions. What kind of role plays CXCR3 in the pathophysiology of ovarian cancer and does the expression of CXCR3 correlate with clinical parameters like overall and progression-free survival?
- Which chemoattractants induce ovarian cancer cell detachment from the primary tumor and metastasis and does the CXCR3 system has an impact on the migration of cancer cells? Is CXCR3 involved in the peritoneal spread of ovarian cancer? If this is the case, the question raises, if it is possible to suppress the peritoneal metastasis by blocking the CXCR3 receptor, making thus CXCR3 a potential therapeutic target, and if this has an impact on the therapeutic important CXCR3-dependent immune cell infiltration?

IV. MATERIAL

1. Human tissue and ascites samples and patient cohort

1.1. Immunohistochemically used human tissue samples and patient cohort

For the immunohistochemical studies two collectives of formalin-fixed, paraffin-embedded specimens from patients with high-grade serous ovarian cancer stage FIGO III or IV were used. All patients were treated at the Department of Gynecology and Obstetrics, Klinikum rechts der Isar, Technische Universität München and underwent standard debulking surgery, including pelvic and paraaortic lymphadenectomy and partial resection of the small and large intestine if indicated, peritonectomies and upper abdominal surgery. All patients were adjuvantly treated according to consensus recommendations at that time and received platinum-based chemotherapy. Written informed consent was obtained from all patients. Table 2 and 3 show the patient characteristics of the different collectives. A pathologist reviewed the histological slides from all patients to confirm the high-grade serous subtype. Immunohistochemical staining was performed on slides from suitable paraffin blocks with sufficiently large tumor areas.

Table 2: Patient characteristics of the discovery and validation collectives for the immunohistochemical CXCL9 and CXCL10 staining.

Characteristic	Discovery set (n=70)	Validation set (n=114)	Both collectives (n=184)
Median age at diagnosis [years]	63	63.5	63
(range)	(35-82)	(28-88)	(28-88)
≤65	41 (59%)	67 (59%)	108 (59%)
>65	29 (41%)	41 (41%)	76 (41%)
Median follow-up time [months]	31.5	34	33
(range)	(3-166)	(1-242)	(1-242)
FIGO stage			
III	57 (81%)	80 (70%)	137 (74%)
IV	13 (19%)	34 (30%)	47 (26%)
Postsurgical residual tumor mass			
Optimal (0 cm)	18 (26%)	38 (33%)	56 (30%)
Suboptimal	52 (74%)	75 (66%)	127 (69%)
No data available	0 (0%)	1 (1%)	1 (1%)

Characteristic	Discovery set (n=70)	Validation set (n=114)	Both collectives (n=184)
Nodal status			
Negative (pN0)	17 (25%)	36 (32%)	53 (29%)
Positive (pN1)	38 (54%)	66 (58%)	104 (56%)
No data available	15 (21%)	12 (10%)	27 (15%)

Table 3: Patient characteristics of the discovery and validation collectives for the immunohistochemical CXCR3 staining.

Characteristic	Discovery set (n=60)	Validation set (n=127)	Both collectives (n=187)
Median age at diagnosis [years] (range)	62 (35-81)	63 (28-88)	63 (28-88)
≤65	36 (59%)	76 (59.8%)	112 (59.6%)
>65	25 (41%)	51 (40.2%)	76 (40.4%)
Median follow-up time PFS [months] (range)	13.5 (1-86)	15 (2-118)	14 (1-118)
Median follow-up time OS [months] (range)	31 (3-154)	36 (1-253)	35 (1-253)
FIGO stage			
III	47 (78.3%)	89 (70.1%)	136 (72.7%)
IV	13 (21.7%)	38 (29.9%)	51 (27.3%)
Postsurgical residual tumor mass			
Optimal (0 cm)	19 (31.7%)	44 (34.6%)	63 (33.7%)
Suboptimal	41 (68.3%)	81 (63.8%)	122 (65.2%)
No data available	0 (0%)	2 (1.6%)	2 (1.1%)
Nodal status			
Negative (pN0)	14 (23.3%)	40 (31.5%)	54 (28.9%)
Positive (pN1)	35 (58.3%)	75 (59.1%)	110 (58.8%)
No data available	11 (18.3%)	12 (9.4%)	23 (12.3%)

Furthermore, 34 formalin-fixed, paraffin-embedded metastatic lymph node samples from patients with ovarian cancer were immunohistochemically stained for CXCR3. The patients that were treated at the Department of Gynecology and Obstetrics, Klinikum rechts der Isar, Technische Universität München. Written informed consent was obtained from all patients.

1.2. Human ascites samples for ELISA

For the protein determination in ascitic fluid 166 ascites samples from ovarian cancer patients were used. From these 166 ascites samples, only 102 were derived from

patients with high-grade serous ovarian carcinoma (FIGO III and FIGO IV) and therefore only these 102 samples were taken into further analysis. The patients were treated at the Department of Gynecology and Obstetrics, Klinikum rechts der Isar, Technische Universität München and at the Department of Gynecology and Obstetrics, Kreisklinik Ebersberg between 1998 and 2012. Written informed consent was obtained from all patients. The median patient age at diagnosis was 63.7 years (range, 27-86). The ascitic fluid was obtained either by puncture or during surgery and stored at -80 °C before analysis.

1.3. Human ascites samples for migration assay

For the analysis of cell migration towards ascitic fluid, 10 different ascites samples were randomly chosen from the cohort in 1.2, including samples with both high and low CXCL9 and CXCL10 concentrations. The patients were treated at the Department of Gynecology and Obstetrics, Klinikum rechts der Isar, Technische Universität München. Written informed consent was obtained from all patients. The ascites was obtained by either puncture or during surgery between 1999 and 2012 and stored at -80 °C before assay performance. The median patient age at ascites puncture was 66 years (range, 48-78). The patient and tumor characteristics are shown in Table 4.

Table 4: Ascites for migration assay: patient and tumor characteristics

Patient #	Age	Histology	FIGO	G	R	N	CTX
1	48	serous	Ic	n.a.	0	n.a.	no chemotherapy
2	55	serous	n.a.	2	0	0	n.a.
3	76	serous	III	3	0	1	6x carboplatin/ paclitaxel
4	68	serous	III	3	1	n.a.	6x carboplatin/ paclitaxel
5	51	serous	IV	3	1	1	6x carboplatin/ paclitaxel
6	62	serous	IV	3	1	1	6x carboplatin/ paclitaxel
7	78	serous	III	3	1	n.a.	no chemotherapy, died after surgery
8	70	serous	III	3	1	1	6x carboplatin/ paclitaxel
9	68	serous	IV	3	1	1	chemotherapy, not further described
10	65	serous	III	3	1	1	neoadjuvant chemotherapy

1.4. Human ascites samples for the generation of primary cells

To obtain primary epithelial ovarian cancer (EOC) cells, ascites was freshly isolated from six patients with high-grade ovarian cancer. The patients were treated at the Department of Gynecology and Obstetrics, Klinikum rechts der Isar, Technische Universität München. Written informed consent was obtained from all patients. The median patient age at ascites puncture was 77 years (range, 69-93). The patient and tumor characteristics are shown in Table 5.

Table 5: Ascites for isolation of primary epithelial ovarian cancer cells: patient and tumor characteristics

EOC #	Age	Histology	FIGO	G	R	N	CTX
1	93	adeno-carcinoma	IV	n.a.	1	n.a.	no chemotherapy
2	Isolation was not successful						
3	69	serous	III	3	0	1	6x carboplatin/ paclitaxel
4	73	serous	III	3	1	n.a.	carboplatin/ paclitaxel
5	Isolation was not successful						
6	72	serous	III	3	0	1	6x carboplatin/ paclitaxel

2. Eukaryotic cell lines

All used cell lines were obtained from the American Type Culture Collection (ATCC), Manassas, VA, USA, except ID8. ID8 were obtained from Katherine F. Roby, PhD, Kansas City, MO, USA (Roby et al., 2000).

Cell line	ATCC® no.	Tissue	Disease
ID8 (MOSEC)	-	murine ovarian surface epithelial cells	serous
OVCAR-3	HTB-161	human ovary	adenocarcinoma
Phoenix-ECO	CRL-3214	second-generation retrovirus producer line, ecotropic	-
SKOV-3	HTB-77	human ovary: ascites	adenocarcinoma

2.1. Culture media for eukaryotic cell lines

Medium	Cell line	Company
DMEM (1x) + Gluta MAX™-I Dulbecco's Modified Eagle Medium [+] 4.5 g/l D-Glucose [-] Pyruvate	ID8, Phoenix, SKOV-3	Life Technologies, Carlsbad, CA, USA
RPMI Medium 1640 (1x) [+] L-Glutamine	OVCAR-3	Life Technologies, Carlsbad, CA, USA

2.2. Supplements in 500 ml culture medium

Component	Cell line
10% (w/v) fetal calf serum (heat inactivated at 57 °C, 30 min)	all cell lines
10 mM HEPES buffer solution	
0.550 mM L-Arginine	
0.272 mM L-Asparagine	
0.01% (w/v) Insulin Solution from Bovine Pancreas	only used for OVCAR-3
1% (w/v) Insulin-Transferrin-Selenium	only used for ID8

2.3. Culture media for primary epithelial ovarian cancer cells

Component	Company
44.5% (v/v) MCDB 105 Medium, pH 7.4	Sigma, St. Louis, MN, USA
44.5% (v/v) Medium 199 (1x) [+] Earle's Salt [+] L-Glutamine	Life Technologies, Carlsbad, CA, USA
10% (w/v) fetal calf serum (heat inactivated at 57 °C, 30 min)	Life Technologies, Carlsbad, CA, USA
1% (w/v) Penicillin-Streptomycin	Sigma, St. Louis, MN, USA

2.4. Cell culture solutions

Solution	Composition
Detachment solution	95% (v/v) PBS 5% (v/v) EDTA
Freezing medium	95% (v/v) FCS 5% (v/v) DMSO
Puromycin selection medium	5 µg/ml puromycin in growth medium

Solution	Composition
Serum-free medium	culture medium with all supplements, but without FCS
Transfected cell clone picking solution/ detachment solution	90% (v/v) PBS 0.05% (v/v) Trypsin 0.02% (v/v) EDTA

3. Proteins

All recombinant proteins were dissolved in 0.1% BSA/PBS.

Protein	Company
Recombinant human CXCL9	Peprtech, Rocky Hill, NJ, USA
Recombinant human CXCL10	Peprtech, Rocky Hill, NJ, USA
Recombinant murine CXCL10	Peprtech, Rocky Hill, NJ, USA

4. Antibodies

Primary antibody	Clone	Clonality, species	Company, order no.	Application
Anti-CXCL9	49801	Monoclonal mouse IgG ₁	R&D Systems, MAB392	IHC
Anti-CXCL10	H-95	Monoclonal mouse IgG _{2b}	Santa Cruz Biotechnology, sc-101500	IHC
Anti-CXCR3	49801	Monoclonal mouse IgG ₁	R&D Systems, MAB160	IHC, western blot, migration assay, FACS
Anti-GAPDH	-	Monoclonal mouse IgG ₁	Merck, MAB374	Western blot
Anti-mCXCR3	-	Polyclonal rabbit IgG	Santa Cruz Biotechnology, sc-13951	Western blot
Anti- α -tubulin	B-7	Monoclonal mouse IgG _{2a}	Santa Cruz Biotechnology, sc-5286	Western blot
IgG ₁ isotype control	11711	Monoclonal mouse IgG ₁	R&D Systems, MAB002	Migration assay, FACS

Secondary antibody	Isotype	Company, order no.	Application
Goat anti-mouse HRP	Polyclonal IgG (H+L)	Jackson ImmunoResearch, 115-035-003	Western blot
Goat anti-rabbit HRP	Polyclonal IgG (H+L)	Invitrogen, G-21234	Western blot
AlexaFluor® 488 goat anti-mouse	IgG (H+L)	Life Technologies, A11001	FACS

5. Technical devices

Device	Application	Company
Bandelin Sonopuls	Ultrasonic homogenizer	Bandelin electronic, Berlin, Germany
Cawomat 2000 IR	X-ray film processor	Cawo, Schrobenhausen, Germany
Centrifuge 54 24 R	Centrifuge	Eppendorf AG, Hamburg, Germany
EV231	Electrophoresis power supply	Consort bvba, Turnhout, Belgium
FACSCalibur	FACS	Becton Dickinson, Franklin Lakes, NJ, USA
Fast Blot	Semi-dry western blot chamber	Biometra, Göttingen, Germany
HERACELL 150i	Cell Incubator	Thermo Fisher Scientific, Waltham, MA, USA
Herasafe	Laminar flow	Thermo Fisher Scientific, Waltham, MA, USA
IKA MAG® REO	Stirring plate	IKA Labortechnik, Staufen, Germany
Incubator	Slide Incubator	Memmert GmbH, Schwabach, Germany
Mini-Protean® 3 Cell	SDS-PAGE chamber	Biorad, Hercules, CA, USA
MS1 Minishaker	Vortex mixer	Carl Roth, Karlsruhe, Germany
Multiskan FC	ELISA Reader	Thermo Fisher Scientific, Waltham, MA, USA
NanoZoomer Digital Pathology RS	Slide scanner	Hamamatsu, Hamamatsu, Japan
Olympus CK30	Light microscope (cell culture)	Olympus, Tokyo, Japan
pH-Meter Lab 850	pH adjustment	Schott, Mainz, Germany
Polymax 2040	Shaking platform	Heidolph Instruments GmbH & Co. KG, Schwabach, Germany

Device	Application	Company
Power Pac 300	Electrophoresis power supply	Biorad, Hercules, CA, USA
Purelab classic	High-purity water	Elga GmbH, Wien, Austria
Rotina 48 R	Centrifuge	Hettich Zentrifugen, Tuttlingen, Germany
Sartorius basic	Scale	Sartorius AG, Göttingen, Germany
Sartorius BP 1200	Scale	Sartorius AG, Göttingen, Germany
SLT Spectra ELISA Reader, Software easyWIN fitting E 5.0 a	ELISA reader	SLT, Crailsheim, Germany
Vortex Genie 2™	Vortex mixer	Bender & Hobein AG, Zurich, Switzerland
WMF Schnellkochtopf® PERFECT	Pressure cooker	WMF, Geislingen an der Steige, Germany
Zeiss Axio Observer A1	Fluorescence microscope (Migration assay)	Zeiss, Jena, Germany
Zeiss Axioskop	Light microscope (Immunohistochemistry)	Zeiss, Jena, Germany

6. Consumables

Consumables	Company
Blotting paper MN 8273	Macherey-Nagel, Düren, Germany
Cell culture flasks	Greiner bio-one, Kremsmünster, Austria
Cell culture plates	Becton Dickinson Labware, Franklin Lakes, NJ, USA
Cell scrapers	Becton Dickinson Labware, Franklin Lakes, NJ, USA
Combitips® plus 2.5/5 ml	Eppendorf AG, Hamburg, Germany
Coverslips	R. Langenbrinck, Emmendingen, Germany
Cryogenic vials	NALGENE® Labware, Thermo Fisher Scientific, Roskilde, Denmark
96-well ELISA Microplates, PS, F-bottom, MICROCOLON® 200, med. binding	Greiner bio-one, Kremsmünster, Austria
FACS vials conical	Greiner bio-one, Kremsmünster, Austria
Feather Disposable Scalpel	Feather Safety Razor Co. LTD, Osaka, Japan
Microscope slides	R. Langenbrinck, Emmendingen, Germany
Minisart® sterile filter 0.1/0.2 µm	Sartorius AG, Göttingen, Germany

Consumables	Company
Nitrocellulose Transfer Membrane Protran BA 85, pore size 0.45 µm	Schleicher & Schuell, Dassel, Germany
Neubauer counting chamber	LO Laboroptik, Lancing, UK
Nunc-immuno™ 96-well plates	Nunc, Thermo Fisher Scientific, Roskilde, Denmark
Pasteur pipettes glass	Hirschmann Laborgeräte, Eberstadt, Germany
Pipette tips	Sarstedt, Nümbrecht, Germany
Polystyrene Round Bottom Tube 5ml	Corning Incorporated, Corning, NY, USA
PVDF Transfer Membrane ROTI®-PVDF, pore size 0.45 µm	Millipore, Schwalbach, Germany
Reaction tubes (1,5/2 ml)	Sarstedt, Nümbrecht, Germany
Serological pipettes (2/5/10/25/50 ml)	Greiner bio-one, Kremsmünster, Austria
Sterile syringes	Braun, Melsungen, Germany
6.5 mm Transwell® with 8.0 µm Pore Polycarbonate Membrane Insert	Corning Incorporated, Corning, NY, USA
Tubes (15/50 ml)	Greiner bio-one, Kremsmünster, Austria
X-ray films CEA RP-new	Agfa HealthCare NV, Mortsel, Belgium

7. Laboratory chemicals and reagents

Chemical	Application	Company
7AAD Viability staining solution	FACS	eBioscience, San Diego, CA, USA
Ammonium persulfate (APS)	SDS-PAGE	Carl Roth, Karlsruhe, Germany
Antibody diluent	Immunohistochemistry	Zytomed Systems GmbH, Berlin, Germany
Aprotinin	Protease array	Sigma, St. Louis, MN, USA
Bovine Serum Albumin (BSA)	ELISA, cell culture, reconstitution of reagents	Sigma, St. Louis, MN, USA
Bromphenolblue	Sample buffer	Serva, Heidelberg, Germany
Citric acid monohydrate	Immunohistochemistry	Sigma, St. Louis, USA
C&L Entwickler Typ E	X-ray film developer solution	C&L GmbH, Planegg, Germany
Complete + EDTA Protease Inhibitor Cocktail	Cell lysis	Roche Diagnostics GmbH, Mannheim, Germany
DAPI (4'-6-diamidino-2-phenylindole, dihydrochloride)	Migration assay	Life Technologies, Carlsbad, CA, USA

Chemical	Application	Company
Dimethyl sulfoxide (DMSO) Hybri-Max [®]	Cell culture	Sigma, St. Louis, MN, USA
Disodium hydrogen phosphate dihydrate (Na ₂ HPO ₄ ·2H ₂ O)	ELISA	Carl Roth, Karlsruhe, Germany
DMEM (1x) + Gluta MAXTM_1 Dulbecco's Modified Eagle Medium [+] 4.5 g/l D-Glucose [-] Pyruvate	Cell culture	Life Technologies, Carlsbad, CA, USA
Dulbecco's Phosphate buffered saline (PBS)	Cell culture	Life Technologies, Carlsbad, CA, USA
Dulbecco's Phosphate buffered saline (PBS) [+] CaCl ₂ [+] MgCl ₂	Migration assay	Life Technologies, Carlsbad, CA, USA
EC-Fixierer F 1000	X-ray film fixer solution	Ernst Christiansen GmbH, Planegg, Germany
Ethylenediaminetetraacetic acid (EDTA) (Versen) 1% in PBS, w/o Ca ²⁺ , w/o Mg ²⁺	Cell culture	Biochrom AG, Berlin, Germany
Ethanol (70%)	Immunohistochemistry	In-house Ethanol provided by Department of Pathology, Technical University of Munich
Ethanol (96%)	Immunohistochemistry	In-house Ethanol provided by Department of Pathology, Technical University of Munich
Ethanol (99.9%)	Western blot	Merck, Darmstadt, Germany
Fetal calf serum (FCS)	Cell culture	Life Technologies, Carlsbad, CA, USA
Geneticin [®] G 418 Sulfate, Potency: 708 µg/mg	Cell culture	Life Technologies, Carlsbad, CA, USA
Glycine	Buffers	Carl Roth, Karlsruhe, Germany
β-glycerol phosphate	Cell lysis	Sigma, St. Louis, MN, USA
Goat serum (normal)	Immunohistochemistry	Dako, Glostrup, Denmark
HEPES buffer solution 1M (4- (2-hydroxyethyl)-1- piperazineethanesulfonic acid)	Cell culture	Life Technologies, Carlsbad, CA, USA
Hydrogen chloride (HCl)	pH adjustment	Carl Roth, Karlsruhe, Germany
Hydrogen chloride fuming 37%	Buffer	Merck, Darmstadt, Germany
Hydrogen peroxide 30%	Immunohistochemistry	Merck, Darmstadt, Germany
Igepal [®] CA-630	Protease array	Sigma, St. Louis, MN, USA

Chemical	Application	Company
Insulin Solution from Bovine Pancreas, 10 mg/ml, 25 mM HEPES, pH 8.2	Cell culture	Sigma, St. Louis, MN, USA
Insulin-Transferrin-Selenium (100x), prepared in EBSS	Cell culture	Life Technologies, Carlsbad, CA, USA
Isopropyl alcohol	Immunohistochemistry	Department of Pathology, Technical University of Munich
Isopropyl alcohol	Western blot	Merck, Darmstadt, Germany
L-Arginine	Cell culture	Sigma, St. Louis, MN, USA
L-Asparagine	Cell culture	Sigma, St. Louis, MN, USA
Leupeptin	Protease array	Tocris, Bristol, United Kingdom
Lipofectin [®] Reagent	Cell culture	Life Technologies, Carlsbad, CA, USA
Mayer's hematoxylin solution	Immunohistochemistry	Carl Roth, Karlsruhe, Germany
MCDB 105 Medium, pH 7.4	Cell culture	Sigma, St. Louis, MN, USA
Medium 199 (1x) [+] Earle's Salt [+] L-Glutamine	Cell culture	Life Technologies, Carlsbad, CA, USA
Methanol	Migration assay	Carl Roth, Karlsruhe, Germany
β -Mercaptoethanol	Sample buffer	Merck, Darmstadt, Germany
PageRuler [™] Prestained Protein Ladder	SDS-PAGE	Pierce Biotechnology, Thermo Fisher Scientific, Rockford, IL USA
Penicillin-Streptomycin (10000 units Penicillin and 10 mg Streptomycin per ml)	Cell culture	Sigma, St. Louis, MN, USA
Pepstatin A	Protease array	Sigma, St. Louis, MN, USA
Pertex mounting medium	Immunohistochemistry	Medite GmbH, Burgdorf, Germany
Ponceau S	Western blot	AppliChem, Darmstadt, Germany
Polybrene	Cell culture	Santa Cruz Biotechnology, Dallas, TX, USA
Potassium chloride (KCl)	ELISA	RdH Laborchemikalien, Seelze, Germany
Potassium dihydrogen phosphate (KH ₂ PO ₄)	ELISA	Merck, Darmstadt, Germany
Puromycin 10 mg/ml	Cell culture	Life Technologies, Carlsbad, CA, USA

Chemical	Application	Company
Rotiphorese 40 (Acrylamide)	SDS-PAGE	Carl Roth, Karlsruhe, Germany
RPMI Medium 1640 (1x) [+] L-Glutamine	Cell culture	Life Technologies, Carlsbad, CA, USA
Skimmed milk powder	Western blot	Sigma, St. Louis, MN, USA
Sodium chloride (NaCl)	Buffers	Carl Roth, Karlsruhe, Germany
Sodium dodecyl sulfate (SDS) Pellets	Western blot	Carl Roth, Karlsruhe, Germany
Sodium fluoride (NaF)	Cell lysis	Carl Roth, Karlsruhe, Germany
Sodium hydroxide solution	pH adjustment	Merck, Darmstadt, Germany
Sodium orthovanadate	Cell lysis	Sigma, St. Louis, MN, USA
Sodium pyrophosphate	Cell lysis	Sigma, St. Louis, MN, USA
Sulfuric acid (H ₂ SO ₄)	ELISA	Carl Roth, Karlsruhe, Germany
N,N,N',N'-Tetramethylethylenediamine (TEMED)	Western blot	AppliChem, Darmstadt, Germany
Tris (Ultra Pure)	Buffers	Carl Roth, Karlsruhe, Germany
Tris hydrochloride	Buffers	Carl Roth, Karlsruhe, Germany
Triton X-100	Cell lysis Buffers	Sigma, St. Louis, MN, USA
TRIZMA [®] Base	Immunohistochemistry	Sigma, St. Louis, MN, USA
Trypan blue solution 0.4%	Cell culture	Sigma, St. Louis, MN, USA
Trypsin/EDTA solution (10x) 0.5%/0.2% (w/v) in PBS, w/o Ca ²⁺ , w/o Mg ²⁺	Cell culture	Biochrom AG, Berlin, Germany
Tween [®] -20	Buffers	Sigma, St. Louis, MN, USA
Vectashield mounting medium for fluorescence	Migration assay	Vector, Burlingame, CA, USA
Xylene	Immunohistochemistry	Department of Pathology, Technical University of Munich

8. Buffers and solutions

Solution	Composition	Application
Blocking buffer	TBS 1x pH 7.4 5% (w/v) skimmed milk powder 0.1% Tween®-20	Western blot
Blocking solution	PBS 1x pH 7.4 1% BSA	ELISA
Citrate buffer (pH 6.0)	10 mM Citric acid monohydrate pH 6.0 adjusted with 2 N NaOH	Immunohistochemistry
Electrophoresis buffer 10x	1.6 M glycine 0.25 M Tris 1% (w/v) SDS	SDS-PAGE
FACS buffer	PBS 1x pH 7.4 0.5% (w/v) FCS 0.01% (w/v) sodium azide	FACS
Laemmli buffer	150 mM 1 M Tris/HCl pH 6,8 45% glycerol 17% β-mercaptoethanol 15% SDS 0.01% bromphenol blue	Western blot
Lysis buffer	TBS 1x pH 7.4 1% Triton X-100 0.1% (w/v) Complete™ + EDTA 50 mM NaF 10 mM sodium pyrophosphate 1 mM sodium orthovanadate 1 mM β-glycerol-phosphate	Cell lysis
Lysis buffer	PBS 1x pH 7.4 137 mM NaCl 20 mM Tris-HCl (pH 8.0) 2 mM EDTA 10% glycerol 1% Igepal CA-630 10 µg/ml Aprotinin 10 µg/ml Leupeptin 10 µg/ml Pepstatin	Protease array
PBS 10x (pH 7,4)	1.4 M NaCl 61.8 mM·Na ₂ HPO ₄ 2H ₂ O 26.83 mM KCl 14.7 mM KH ₂ PO ₄	ELISA
PBST	PBS 1x pH 7.4 0.05% (v/v) Tween®-20	ELISA
Ponceau S dye	5% (v/v) acetic acid 0,1% (w/v) Ponceau S	Western blot

Solution	Composition	Application
Sample buffer	150 mM Tris-HCl 1 M pH 6,8 45% (v/v) glycerol 17% (v/v) β -mercaptoethanol 15% (w/v) SDS 0,01% (w/v) bromphenolblue	SDS-PAGE
Semi-Dry buffer	50 mM Tris 30 mM glycine 20% (v/v) Ethanol 4‰ (w/v) SDS	Western blot
Separating gel 12%	375 mM Tris-HCl 1.5 M pH 8.8 12% (v/v) acrylamide 0.1% (w/v) SDS 0.05% (w/v) APS 0.05% (v/v) TEMED	SDS-PAGE
Stacking gel (4%)	129 mM Tris-HCl 0.5 M pH 6.8 5% (v/v) acrylamide 0.1% (w/v) SDS 0.1% (w/v) APS 0.1% (v/v) TEMED	SDS-PAGE
Stripping solution pH 2.2	160 mM glycine 1% (v/v) Tween®-20 0.1% (w/v) SDS	Western blot
TBS 10x (pH 7.4)	1.4 M NaCl 0.1 M Tris-HCl	Western blot Cell lysis
TBS 10x (pH 7.6)	1.5 M NaCl 0.5 M Trizma Base pH 7.6 adjusted with HCl fuming 37%	Immunohistochemistry
TBST	TBS 1x pH 7.4 0.1% (v/v) Tween-20	Western blot
TBSTT	TBS 1x pH 7.4 0.1% (v/v) Triton X-100 0.05% (v/v) Tween®-20	Protein determination

9. Kits

Kit name	Application	Company
Avidin Biotin Kit	Immunohistochemistry	Zytomed Systems GmbH, Berlin, Germany
Pierce™ BCA Protein Assay Kit	Protein determination	Pierce Biotechnology, Thermo Fisher Scientific, Rockford, IL USA
DAB substrate kit high contrast	Immunohistochemistry	Zytomed Systems GmbH, Berlin, Germany
DuoSet® Human CXCL9/MIG	ELISA	R&D, Minneapolis, USA

Kit name	Application	Company
DuoSet [®] Human CXCL10/IP-10	ELISA	R&D, Minneapolis, USA
Pierce [™] BCA Protein Assay Kit	Protein determination	Pierce Biotechnology, Thermo Fisher Scientific, Rockford, IL USA
Pierce [®] ECL Western Blotting Substrate	Western blot	Pierce Biotechnology, Thermo Fisher Scientific, Rockford, IL USA
Proteome Profiler Arrays: Human Protease Array	Protease array	R&D, Minneapolis, USA
TMB Microwell Peroxidase Substrate System	ELISA	KPL, Gaithersburg MD, USA
ZytoChem Plus HRP Broad Spectrum Bulk Kit	Immunohistochemistry	Zytomed Systems GmbH, Berlin, Germany

10. Plasmids

Plasmid	Company
Cxcr3 Mouse, unique 29mer shRNA constructs in retroviral untagged vector pRS	OriGene, Rockville, MD, USA
Construct name	Sequence
TR500382B	TGAACGTCAAGTGCTAGATGCCTCGGACT
TR500382D	CCAACACTACGATCAGCGCCTCAATGCCACC

V. METHODS

1. Cell culture

1.1. Cultivation of cells

All cells were cultivated at 37 °C and 5% CO₂ in a cell incubator in a water saturated atmosphere. The cell specific culture medium was replaced every 3-4 days, until the cells reached a density of 70%. For detachment, the cells were washed with PBS, incubated with 0.05% EDTA in PBS, washed off with PBS and transferred into 15 ml tubes. After centrifugation at 330 g for 3 min, the cell pellet was resuspended in culture medium and a certain part, depending on cell type and growth rate, was passed into a new cell culture flask.

1.2. Freezing and thawing of cells

For freezing and storing, the cells were detached with 0.05% EDTA in PBS, washed off with PBS and centrifuged at 330 g for 3 min. The cell pellet was resuspended in 1 ml freezing solution containing 5% DMSO in FCS and transferred into sterile cryogenic vials, which were placed into a freezing box at -80 °C. For long-term storage, the frozen cells were transferred to liquid nitrogen at -196 °C.

For thawing cells, the frozen cells were quickly washed with cold culture medium, centrifuged at 330 g for 3 min, resuspended with culture medium and transferred into a cell culture flask that had been coated before with FCS. After 24 h, the excess of FCS and culture medium was aspirated and replaced by fresh culture medium.

1.3. Primary culture of ascites derived epithelial ovarian cancer cells

To obtain primary epithelial ovarian cancer (EOC) cells from the ascitic fluid isolated from patients with high-grade ovarian cancer, the protocol by Shepherd et al. was applied (Shepherd et al., 2006). The following culture medium was prepared and used: powdered MCDB 105 medium was suspended in a final volume of 1 l of tissue culture grade water and the pH was adjusted to 7.2. The medium was sterilized by filtering through a sterile membrane filter with a pore size of 0,1 µm. 225 ml of the final MCDB 105 medium were mixed with 225 ml of Medium 199, 50 ml FCS and 5 ml 100x Penicillin-Streptomycin.

Ascitic fluid was freshly isolated from patients and received in a sterile container. 24 ml of the ascites was equally transferred to 6 tissue culture flasks and an equal volume of MCDB105/M199 culture medium was added. Additional ascitic fluid was transferred to sterile tubes and centrifuged at 3200 g for 10 min at 4 °C. The supernatant was distributed to several tubes and frozen at -80 °C for archival purposes. The cells were placed in an incubator and left undisturbed for 4 days, when the first change of culture medium took place. The EOC cells were bound to the tissue culture surface of the flasks, whereas erythrocytes were removed by a PBS washing step and the change of culture medium. The culture medium was changed every 2-3 days until the cells were confluent. They were passaged at a 1:2-1:3 dilution with 5% EDTA/PBS. Numerous vials of passage-1 cells were frozen for archival purposes. According to the protocol, the isolated cells are epithelial ovarian cancer cells, a contamination with fibroblasts is very rare and these cells could be morphologically distinguished from the cancer cells.

1.4. Stable knockdown of a target gene in ID8 cells

For the stable knockdown of a target gene, cells were transfected with short hairpin RNA (shRNA) constructs in a retroviral vector. The shRNA is a double-stranded RNA with a tight hairpin that is used to silence gene expression via RNA interference. It either leads to cleavage of the complementary target mRNA or to a repression of the mRNA translation, both cases leading to gene silencing (Moore et al., 2010).

Phoenix-ECO cells were used, as they are a retrovirus producer cell line for the generation of ecotropic retroviruses that is highly transfectable. The cells were seeded in a density of $4 \cdot 10^5$ cells per 6 cm dish, so that they reached a confluence of 70-80% the next day, when the transfection was carried out. Lipofectin (2, 6 or 10 μ l) and the vector DNA (1, 3 or 5 μ g, respectively) were added to separate polystyrene round-bottom tubes containing DMEM medium without additives, the tubes were then left undisturbed for 45 min. Afterwards, the DNA solution was added to the Lipofectin-solution and left undisturbed for 15 min. In the meantime, the 6 cm dishes were washed twice with PBS and filled with culture medium. The whole Lipofectin-DNA-solution was then added drop by drop to the cells. Culture medium was changed the next day in the morning. In the evening, as well as in the morning and in the evening of the third day, the supernatant from the cell culture dishes was taken off, collected in a tube and stored at 4 °C, when fresh culture medium was added to the cells. To the

retrovirus containing supernatant 10 µg/ml Polybrene was added. ID8 cells were seeded in a density of $1 \cdot 10^5$ per 6 cm dish in culture medium and were covered the next day with retroviral phage solution in the morning and in the evening. The day after, the retroviral solution was aspirated and replaced by culture medium. For selection of positive cell clones, cells were incubated with culture medium containing 5 µg/ml puromycin. The surviving cell clones were lightly detached with 0.05% Trypsin/0.02% EDTA in PBS and transferred to cell culture plates. Cell clones were tested for successful knockdown via flow cytometry.

2. Migration assay

To determine the migratory capacity of cancer cells towards chemoattractants cell migrations were assayed in 24-well modified Boyden chambers, the so called Transwells[®], with 8.0 µm pore size polycarbonate membranes. Membranes were first hydrated with 500 µl serum-free culture medium in each chamber for 1 h. Then cancer cells were detached, washed and seeded in the upper chamber of the inserts in a density of $5 \cdot 10^4$ cells per well in 500 µl serum-free medium. 500 µl serum-free medium with chemoattractant (40 ng/ml rh-CXCL9, 40 ng/ml rh-CXCL10 or 0.1% BSA/PBS as a control) or 500 µl ascitic fluid was added to the lower chamber. In a neutralization assay, 30 min before the chemoattractant was added to the lower chamber, either the α -CXCR3 antibody or the IgG₁ isotype control was added to the cells in the upper chamber in a concentration of 1 µg/ml. After 4 h of migration the membranes were washed in PBS and non-migrated cells were scraped off with cotton swabs. The membranes were fixed and stained with 1 µg/ml DAPI in methanol for 15 min. After washing in PBS containing Ca²⁺ and Mg²⁺ and high-purity water, the membranes were dried, cut out with a scalpel and sealed on microscope slides with coverslips, using Vectashield mounting medium and nail polish. The migrated cells were visualized and counted in five different fields with the Zeiss Axio Observer A1 fluorescence microscope. Migration was normalized by division through the spontaneous migration.

3. Proliferation assay

To analyze their proliferative activity cells were seeded in three 24-well plates ($2 \cdot 10^4$ OVCAR-3 or EOC cells per well; $1.5 \cdot 10^4$ SKOV-3 cells per well). For analyzing the impact of chemokine stimulation, OVCAR-3 and SKOV-3 cells were starved the next

day for 6h with serum-free culture medium and stimulated afterwards with 100 ng/ml rh-CXCL9, 100 ng/ml rhCXCL10 or 0.1% BSA/PBS as a control. After 24 h, 48 h and 72 h cells were detached with increasing volumes of 0.05% Trypsin/0.02% EDTA in PBS (200 μ l, 300 μ l or 400 μ l respectively). After addition of 50 μ l trypan blue solution cells were counted manually using a Neubauer counting chamber and the Olympus CK30 microscope.

4. Flow cytometry

Cells were seeded in 6-well plates at a density of $2 \cdot 10^5$ per well the day before measurement. The cells were then detached, resuspended in PBS and transferred to conical FACS vials. After washing with FACS buffer, immunostaining was performed by incubating the cells with 20 μ g/ml α -CXCR3 antibody diluted in FACS buffer, as well as with monoclonal mouse IgG₁ isotype control for 1 h on ice, followed by detection with 2,86 μ g/ml (1:700 dilution) Alexa488-conjugated goat anti-mouse secondary antibody for 30 min on ice in the dark. Dead cells were stained with 0.4% (v/v) 7AAD viability staining solution in FACS buffer. The measurements were performed using the Becton Dickinson FACSCalibur and the software CellQuest Pro from Becton Dickinson, the data was analyzed with Flowing Software version 2.5.1 by Perttu Torhu, Turku Centre of Biotechnology, University of Turku, Finland.

5. Protease array

To determine the protease expression in chemokine stimulated cells, $5 \cdot 10^5$ cells were seeded in 6 cm cell culture dishes, starved the next day and stimulated 24 h later with either 100 ng/ μ l rhCXCL9 or 0.1% BSA/PBS as a control. 48 h post-stimulation, cells were rinsed with PBS and solubilized in protease array lysis buffer. Therefore, the lysates were rocked gently at 4 °C for 30 min and then centrifuged at 14000 g for 5 min. The supernatants were transferred into new tubes and 200 μ g lysate per array were assayed immediately according to the Proteome Profiler Human Protease Array Kit instructions. A densitometric analysis was performed using ImageJ 1.50i by Wayne Rasband, National Institutes of Health, USA.

6. Enzyme-linked immunosorbent assay (ELISA)

The ELISA was performed according to the manufacturer's protocol. Briefly, 96-well

microtiter plates (Nunc) were coated with 100 μ l of capture antibody diluted in PBS and incubated over night at room temperature. After washing three times with PBST, the wells were coated with 200 μ l 1% BSA/PBS and incubated for 1 h to block unspecific antibody binding. Next, the plates were washed three times with PBST and 100 μ l of ascites or standard dilutions were applied. Twofold serial dilutions of CXCL9 or CXCL10 stock solutions diluted in 1% BSA/PBS served as standard to obtain a seven-point standard curve. After 2 h of incubation, the plates were washed and incubated with 100 μ l of detection antibody diluted in 1% BSA/PBS for 2 h. Subsequently, plates were washed and incubated with streptavidin conjugated horseradish peroxidase diluted in 1% BSA/PBS for 20 min in the dark. After three additional washes, 3,3',5,5'-tetramethylbenzidine (TMB) substrate was applied to the wells and incubated for 20 min in the dark. 50 μ l 0.5 M H₂SO₄ stopped the reaction and enhanced the signal. Absorbance at 450 nm was subsequently measured using an ELISA Reader (SLT-Spectra).

7. Western blot

7.1. Cell lysis

For protein isolation the cells were kept on ice. Lysis buffer was freshly prepared. The cells were washed twice with 1 ml ice cold PBS. 250 μ l lysis buffer was added to the cells per 6 cm cell culture dish. Afterwards, the cells were homogenized, treated with ultrasound for 10 sec and put back on ice for 20 min. The samples were stored at -20 °C.

7.2. Determination of protein concentration

The samples were diluted with TBSTT and the protein concentration was measured with the Pierce™ BCA protein kit according to the manufacturer's protocol. Absorbance at 570 nm was recorded using an ELISA Reader (Multiskan FC).

7.3. Immunoblot analysis

The protein lysates were adjusted to 40-60 μ g/ μ l with 3x Laemmli-buffer and PBS, the samples were denatured at 96 °C for 5 min and afterwards kept on ice. Protein separation was performed with a SDS polyacrylamide gel electrophoresis (SDS-PAGE) (gel percentage depending on the protein size ranging from 8-15%) in electrophoresis buffer at 120 V in a PAGE-chamber.

Protein transfer to a PVDF or nitrocellulose membrane was performed in semi-dry buffer at 75 mA per membrane for 2 h in a semi-dry blotting chamber.

After transfer, membranes were washed with TBST and stained with Ponceau S dye to check the protein load. To block any unspecific antibody binding the membranes were incubated with 5% skim milk powder in TBST. Afterwards, the membranes were incubated with primary antibody in 5% skim milk in TBST over night at 4 °C. On the next day, the membranes were washed 3x10 min with TBST and incubated with the species-specific HRP-coupled secondary antibody in 5% skim milk in TBST for 1 h at room temperature. After three washing steps with TBST, the protein bands were visualized using the ECL western blotting detection reagents and X-ray films.

The used antibody concentrations were as follows:

Primary antibody	Isotype	Final conc.	Membrane
Anti-CXCR3	Monoclonal mouse IgG ₁	0,67 µg/ml	Nitrocellulose
Anti-mCXCR3	Polyclonal rabbit IgG	0,267 µg/ml	PVDF
Anti-GAPDH	Monoclonal mouse IgG ₁	0.1 µg/ml	Nitrocellulose or PVDF
Anti- α -tubulin	Monoclonal mouse IgG _{2a}	0.2 µg/ml	Nitrocellulose or PVDF

Secondary antibody	Isotype	Final conc.	Membrane
Goat anti-mouse HRP	Polyclonal IgG (H+L)	Dilution 1:10000	Nitrocellulose or PVDF
Goat anti-rabbit HRP	Polyclonal IgG (H+L)	Dilution 1:10000	PVDF

8. Immunohistochemistry

8.1. Immunohistochemical staining

Formalin-fixed paraffin-embedded sections (3-4 µm) were deparaffinized in xylene twice for 10 min and rehydrated in decreasing alcohol (2x 100% isopropyl alcohol, 1x 96% ethanol, 1x 70% ethanol; 5 min each). The slides were washed with TBS for 5 min with an intervening buffer change, like all the following TBS washing steps were performed. For antigen retrieval, slides were pressure cooked in citrate buffer

(pH 6.0) for 1-4 min, depending on the antibody. The slides were cooled down with tap water and washed with TBS. To quench endogenous peroxidase activity, sections were incubated with 3% H₂O₂ for 20 min, then washed first with tap water for 5 min and then with TBS. To block unspecific antibody binding, slides were incubated in avidin solution, biotin solution (both from the Vector avidin biotin blocking kit; not done for CXCL9 staining) and in 5% secondary antibody specific serum (normal goat serum; all stainings) in TBS for 10 min each with TBS washing steps in between. The goat serum was just rinsed down and thereafter, slides were incubated with primary antibody in antibody diluent for 1 h at room temperature. After washing with TBS, the biotinylated secondary antibody from the Zytocem Plus HRP Broad Spectrum Bulk Kit was applied for 20 min at room temperature followed by streptavidin-HRP conjugate from the same kit for 20 min at room temperature after washing with TBS. Signal detection for all stainings was performed with the DAB kit according to the manufacturer's protocol. Subsequently, the slides were counterstained with Mayer's hematoxylin solution for 50 sec, washed for 5 min with tap water and transferred into deionized water. The slides were dehydrated in the ascending alcohol row (70% ethanol, 96% ethanol, 2x 100% isopropyl alcohol, 2x xylene, 3 min each) and the cover glass lid sealing with Pertex mounting medium was followed. Histological images were taken with the Hamamatsu digital slide scanner NanoZoomer Digital Pathology RS.

The antibody concentrations, pressure cooking times and the use of avidin biotin blocking solution were as follows:

Antibody	Final conc.	Pressure cooking time	Avidin biotin block	Detection system
Anti-CXCL9	20 µg/ml	4 min	-	LSAB
Anti-CXCL10	1 µg/ml	4 min	✓	LSAB
Anti-CXCR3	0.5 µg/ml	1 min	✓	LSAB

8.2. Scoring of immunostaining

All used antibodies showed no considerable intratumoral heterogeneity, so that the staining intensity alone was used to immunohistochemically assess the protein expression. Staining was evaluated semi-quantitatively by a pathologist and scored as

absent (0), weak (1+), moderate (2+) or strong (3+).

During establishment of the staining protocols negative controls (without primary antibody) were used to verify that there is no background staining.

For each antibody a control tissue that was previously scored as 2+ was stained together with the patient samples to test for intra- and inter-run staining intensity differences. Unaffected fallopian tube tissue served for this control.

Scoring of the immunohistochemical stainings was performed by Dr. Stefanie Avril (Institute of pathology, Technische Universität München, Munich, Germany) and Dr. Holger Bronger (Department of Gynecology and Obstetrics, Technische Universität München, Munich, Germany). Dr. Holger Bronger also provided the clinical (follow-up) data on the patients.

9. Statistics

For each type of experiment adequate statistical analysis methods were applied and all statistical tests were performed on two-sided 5% significance levels. For quantitative data mean \pm standard deviation or median and range are used to describe normally and nonnormally distributed data. The distribution of qualitative data is described by absolute and relative frequencies. Univariate survival analyses were plotted using the Kaplan-Meier method and analyzed with the log-rank test or by using a Cox proportional hazard model. For multivariate survival analyses a Cox proportional hazard regression model was used. Results of the migration experiments were evaluated using mean values taken from at least two independent experiments performed in triplicates each and analyzed using t-tests. Results are given as mean \pm standard error of the mean, if not indicated otherwise. Spearman's rank coefficient and t-tests were used to describe correlations between the chemokines present in ascites. Statistical significance was defined as * $p \leq 0.05$, ** $p \leq 0.005$, or *** $p \leq 0.001$. IBM SPSS Statistics 22 and 23 (SPSS Inc., Chicago, IL, USA) was used for statistical analysis.

VI. RESULTS

1. Expression analyses of CXCR3 chemokines in ovarian cancer

1.1. Expression of CXCL9 and CXCL10 and prognostic impact

High-grade serous ovarian cancer samples were immunohistochemically stained for the chemokine ligands CXCL9 and CXCL10. The chemokines were predominantly localized in the cytoplasm of tumor cells. Some endothelial cells, leukocytes and the extracellular matrix showed weak background staining (Figure 8 and 9).

1.1.1. Discovery set

The staining of the 70 tumor tissues of the first collective was scored microscopically and compared to fallopian tube tissue as an intra- and inter-run control.

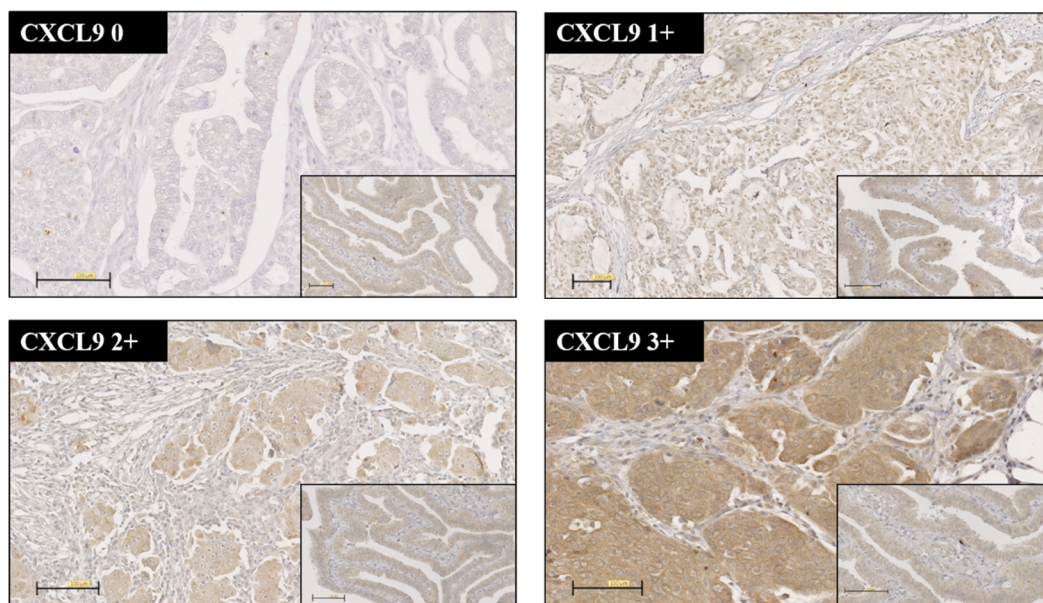


Figure 8: Immunohistochemical staining and scoring of CXCL9 in ovarian cancer tissue

The four different scores are shown for CXCL9. Small boxes: fallopian tube tissue as intratumoral control scored previously as 2+. Scale: 100 μ m.

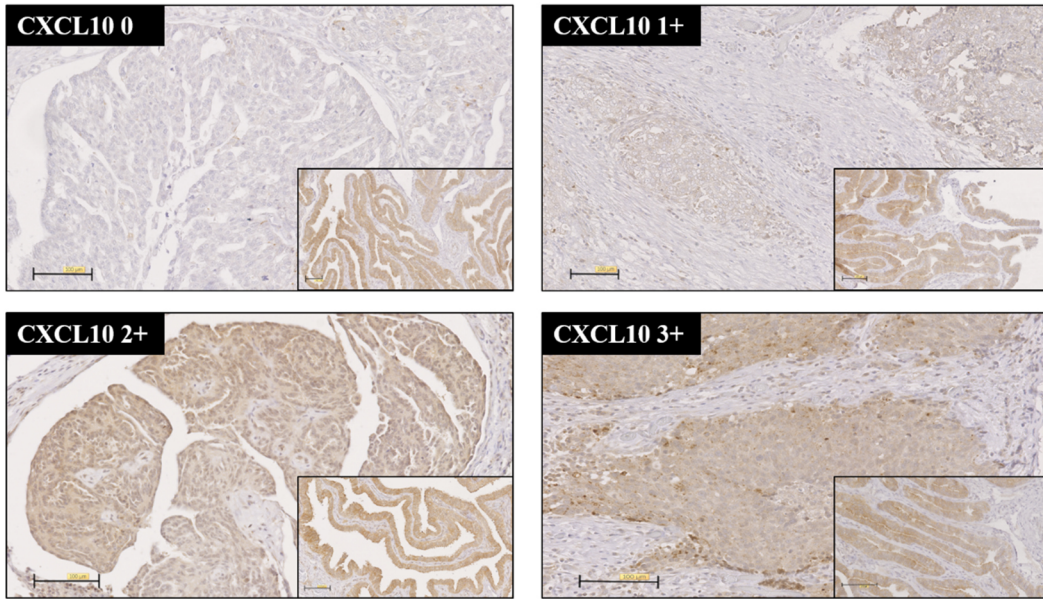


Figure 9: Immunohistochemical staining and scoring of CXCL10 in ovarian cancer tissue

The four different scores are shown for CXCL10. Small boxes: fallopian tube tissue as intratumoral control scored previously as 2+. Scale: 100 μ m.

The staining intensity and therefore expression of tumor CXCL9 and CXCL10 was scored as shown in Table 6, due to technical difficulties the expression of CXCL10 was not assessable in six cases. Depending on the score, tumors were grouped in low expressing tumors (score 0 or 1+) and high expressing tumors (score 2+ or 3+). The majority of high-grade serous ovarian cancer samples showed a high expression of both chemokines, 79% for CXCL9 and 66% for CXCL10. The immunohistochemical expression of CXCL9 and CXCL10 showed no correlation with each other.

The tumors were further grouped into three combined subtypes depending on a combined low or high expression of both CXCL9 and CXCL10. 8% were ‘double-low’ (CXCL9^{low} and CXCL10^{low}) tumors, 56% were ‘double-high’ (CXCL9^{high} and CXCL10^{high}) tumors and 36% were tumors that strongly expressed only one chemokine (CXCL9^{high} or CXCL10^{high}).

Table 6: CXCL9 and CXCL10 expression in ovarian cancer (discovery set)

Shown are the numbers and percentage per immunohistochemical staining and score. Score 0 and 1+ are summarized as ‘low’, score 2+ and 3+ are summarized as ‘high’. Due to technical difficulties the expression of CXCL10 was not assessable in six cases.

CXCL9			CXCL10		
score	percentage	counts	score	percentage	counts
low	21%	15/70	low	34%	22/64
high	79%	55/70	high	66%	42/64
‘double low’ CXCL9 ^{low} and CXCL10 ^{low}				8%	5/64
‘single-high’ CXCL9 ^{high} or CXCL10 ^{high}				36%	23/64
‘double-high’ CXCL9 ^{high} and CXCL10 ^{high}				56%	36/64

In a univariate analysis, both CXCL9 and CXCL10 overexpression was associated with a significantly better, approximately doubled, overall survival, (CXCL9: HR 0.42, 95% CI 0.23-0.78, $p=0.006$; CXCL10: HR 0.47, 95% CI 0.26-0.85, $p=0.012$). Expression of both chemokines was furthermore associated with a significantly longer progression-free survival, albeit not reaching statistical significance. The combined overexpression of both chemokines was associated with even a better prognosis, as the ‘double-high’ tumors (CXCL9^{high} and CXCL10^{high}) were correlated with a significant better patient progression-free and overall survival than tumors overexpressing only one of the two chemokines (PFS: HR 0.24, 95% CI 0.09-0.65, $p=0.005$; OS: HR 0.14, 95% CI 0.05-0.39, $p<0.001$). The worst prognosis had patients whose tumors expressed both chemokines at a low level (CXCL9^{low}/CXCL10^{low}) with a median overall survival of only 14 months. Between the ‘single-high’ tumors (CXCL9^{high}/CXCL10^{low} or CXCL9^{low}/CXCL10^{high}) no statistically significant difference was observed for both overall and progression-free survival.

Table 7: Median progression-free and overall survival according to CXCL9 and/or CXCL10 expression (discovery set) – univariate analysis

Median progression-free survival				
Variable	Median (months)	hazard ratio	95% C.I.	p-value
CXCL9 expression				
low	13 ± 1.93	1		
high	17 ± 1.72	0.64	0.35-1.17	0.151
CXCL10 expression				
low	15 ± 1.55	1		
high	16 ± 3.20	0.64	0.36-1.13	0.120
CXCL9 ^{low} /CXCL10 ^{low}	9 ± 1.10	1		0.019
CXCL9 ^{high} /CXCL10 ^{low} or CXCL9 ^{low} /CXCL10 ^{high}	17 ± 2.08	0.29	0.11-0.82	0.019
CXCL9 ^{high} /CXCL10 ^{high}	16 ± 3.37	0.24	0.09-0.65	0.005
Median overall survival				
Variable	Median (months)	hazard ratio	95% C.I.	p-value
CXCL9 expression				
low	18 ± 5.80	1		
high	47 ± 3.47	0.42	0.23-0.78	0.006
CXCL10 expression				
low	27 ± 7.28	1		
high	49 ± 3.80	0.47	0.26-0.85	0.012
CXCL9 ^{low} /CXCL10 ^{low}	14 ± 4.38	1		<0.001
CXCL9 ^{high} /CXCL10 ^{low} or CXCL9 ^{low} /CXCL10 ^{high}	30 ± 12.81	0.27	0.10-0.75	0.012
CXCL9 ^{high} /CXCL10 ^{high}	52 ± 10.26	0.14	0.05-0.39	<0.001

The results were confirmed by a Kaplan-Meier estimate. An overexpression of the ligands CXCL9 or CXCL10 was associated with a prolonged overall survival (CXCL9: $p=0.005$; CXCL10: $p=0.010$) (Figure 10A-D). The combined overexpression of both chemokines CXCL9 and CXCL10 was correlated with an even better progression-free and overall survival compared to the overexpression of only one chemokine and the low expression of both ligands was associated with a poor progression-free and overall survival (PFS: $p=0.008$; OS: $p<0.001$) (Figure 10E-F).

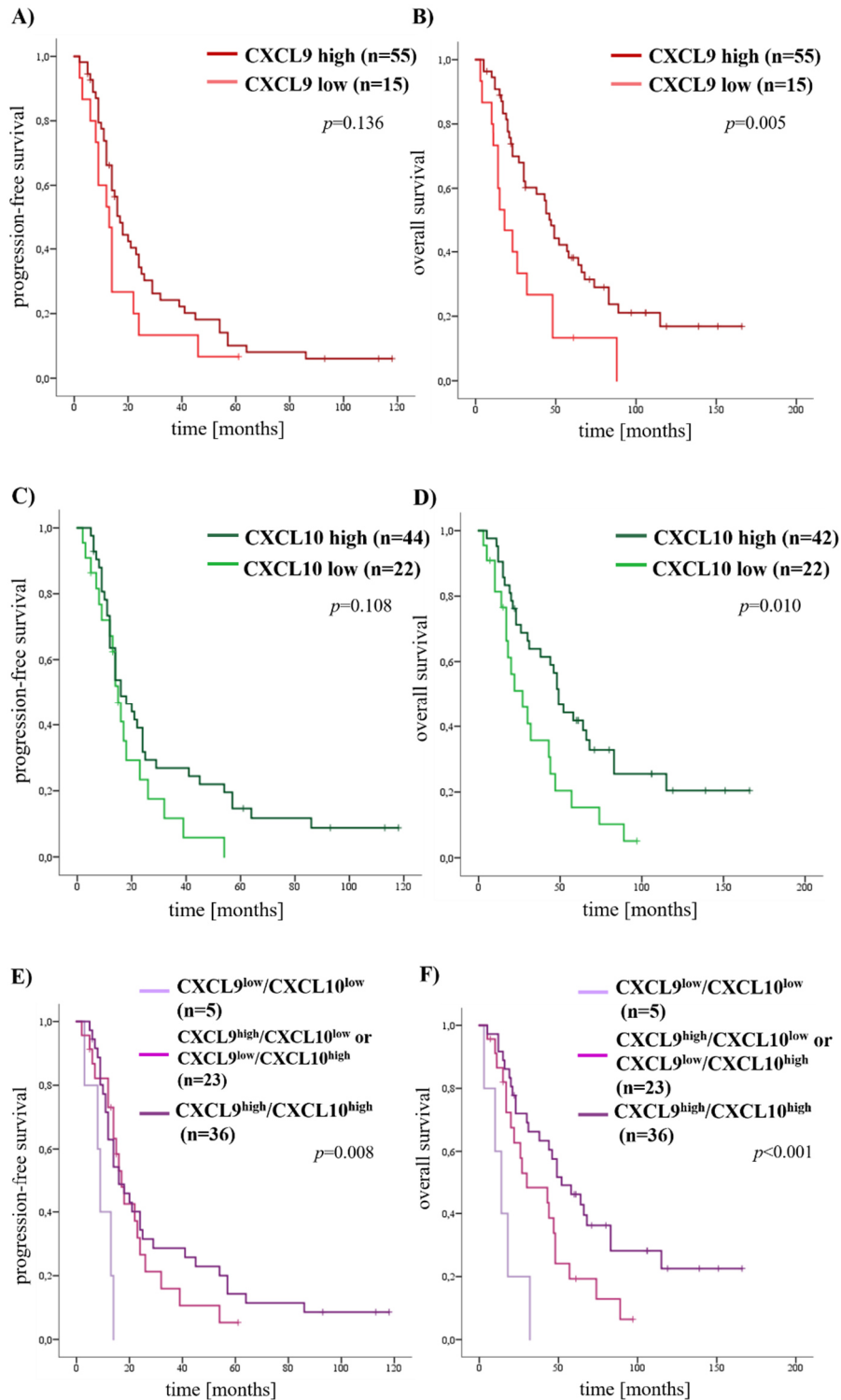


Figure 10: Prognostic significance of CXCL9 and CXCL10 expression in high-grade serous ovarian cancer (discovery set)

Shown are Kaplan-Meier curves for **A)** progression-free survival and **B)** overall survival comparing tumors with low (light red line) and high (red line) CXCL9 expression, for **C)** progression-free survival and **D)** overall survival comparing tumors with low (light green line) and high (green line) CXCL10 expression and for **E)** progression-free survival and **F)** overall survival comparing tumors that express both CXCL9 and CXCL10 at a low level (light purple line), that either highly express CXCL9 or CXCL10 (pink line) or that highly express both CXCL9 and CXCL10 (purple line). Time is given in months, statistical significance (p -value) is stated (log rank).

Next, a multivariate analysis using a COX proportional hazard model was performed, including postsurgical residual tumor mass and lymph node metastasis as covariates. CXCL9 and CXCL10 were identified as independent markers for a better overall survival in high-grade serous ovarian cancer (Table 8).

Even when both chemokines were included into the same multivariate analysis, they remained independent prognostic factors for overall survival (CXCL9: HR 0.39, 95% CI 0.17-0.77, $p=0.009$; CXCL10: HR 0.44, 95% CI 0.22-0.89, $p=0.022$).

Furthermore, the overexpression of both chemokines was identified as an independent prognostic factor for both progression-free and overall survival and the expression of both chemokines at a low level was correlated with a poor outcome (Table 8).

Table 8: Cox multivariate analysis for the progression-free and overall survival (discovery set)

Residual tumor below 1 cm is defined as ‘optimal’, residual tumor above 1 cm as ‘suboptimal’.

Median progression-free survival				
Variable	<i>n</i>	hazard ratio	95% C.I.	<i>p</i>-value
CXCL9 expression				
low	11	1		
high	44	0.52	0.24-1.14	0.102
Postsurgical residual tumor				
optimal	18	1		
suboptimal	37	2.78	1.42-5.44	0.003
Nodal status				
pN0	17	1		
pN1	38	0.98	0.50-1.95	0.961
CXCL10 expression				
low	15	1		
high	37	0.65	0.33-1.30	0.223
Postsurgical residual tumor				
optimal	18	1		
suboptimal	34	2.64	1.35-5.18	0.005
Nodal status				
pN0	15	1		
pN1	37	0.76	0.38-1.50	0.429

Median progression-free survival				
Variable	n	hazard ratio	95% C.I.	p-value
CXCL9 ^{low} /CXCL10 ^{low}	3	1		0.049
CXCL9 ^{low} /CXCL10 ^{high} or CXCL9 ^{high} /CXCL10 ^{low}	18	0.25	0.07-0.99	0.048
CXCL9 ^{high} /CXCL10 ^{high}	31	0.20	0.06-0.73	0.015
Postsurgical residual tumor				
optimal	18	1		
suboptimal	34	2.61	1.32-5.17	0.006
Nodal status				
pN0	15	1		
pN1	37	0.75	0.36-1.54	0.433
Median overall survival				
Variable	n	hazard ratio	95% C.I.	p-value
CXCL9 expression				
low	11	1		
high	44	0.36	0.17-0.77	0.009
Postsurgical residual tumor				
optimal	18	1		
suboptimal	37	4.86	2.15-11.01	<0.001
Nodal status				
pN0	17	1		
pN1	38	0.88	0.43-1.78	0.716
CXCL10 expression				
low	15	1		
high	37	0.44	0.22-0.89	0.022
Postsurgical residual tumor				
optimal	18	1		
suboptimal	34	4.82	2.12-10.97	<0.001
Nodal status				
pN0	15	1		
pN1	37	0.75	0.36-1.53	0.425
CXCL9 ^{low} /CXCL10 ^{low}	3	1		0.006
CXCL9 ^{low} /CXCL10 ^{high} or CXCL9 ^{high} /CXCL10 ^{low}	18	0.43	0.12-1.58	0.204
CXCL9 ^{high} /CXCL10 ^{high}	31	0.17	0.05-0.65	0.009

Median overall survival				
Variable	n	hazard ratio	95% C.I.	p-value
Postsurgical residual tumor				
optimal	18	1		
suboptimal	34	4.94	2.14-11.38	<0.001
Nodal status				
pN0	15	1		
pN1	37	0.74	0.35-1.55	0.421

1.1.2. Validation set

In a validation collective, 114 high-grade serous ovarian tumor tissues were immunohistochemically stained for CXCL9 and CXCL10, scored microscopically and compared to fallopian tube tissue as an intra- and inter-run control. Table 9 shows the results of the scored CXCL9 and CXCL10 expression. Due to technical difficulties the expression of CXCL9 was not assessable in one case and CXCL10 was not assessable in three cases. Tumors were grouped in low expressing tumors (score 0 or 1+) and high expressing tumors (score 2+ or 3+), for the CXCL9 staining this grouping was only possible for 104 cases due to technical reasons. A high expression of the chemokines was shown for the majority of high-grade serous ovarian cancer samples, 58.7% for CXCL9 and 69.4% for CXCL10. Furthermore, 14.9% of the tumors were ‘double-low’ (CXCL9^{low} and CXCL10^{low}) tumors, 40.6% were ‘double-high’ (CXCL9^{high} and CXCL10^{high}) tumors and 44.5% were tumors that strongly expressed only one chemokine (CXCL9^{high} or CXCL10^{high}) (Table 9).

Table 9: CXCL9 and CXCL10 expression in ovarian cancer (validation set)

Shown are the numbers and percentage per immunohistochemical staining and score. Score 0 and 1+ are summarized as ‘low’, score 2+ and 3+ are summarized as ‘high’. Due to technical difficulties the expression of CXCL9 was not assessable in one case and the expression of CXCL10 was not assessable in three cases. For the stratification to CXCL9 low and high expressing tumors, ten cases had to be eliminated due to technical reasons.

CXCL9			CXCL10		
score	percentage	counts	score	percentage	counts
low	41.3%	43/104	low	30.6%	34/111
high	58.7%	61/104	high	69.4%	77/111
‘double low’ CXCL9 ^{low} and CXCL10 ^{low}			14.9%	15/101	
‘single-high’ CXCL9 ^{high} or CXCL10 ^{high}			40.6%	41/101	
‘double-high’ CXCL9 ^{high} and CXCL10 ^{high}			44.5%	45/101	

To determine the association of the tumor expression of CXCL9 and CXCL10 with patient survival, a univariate analysis was performed (Table 10). Both CXCL9 and CXCL10 overexpression were associated with a significantly better overall survival, it was doubled for CXCL9 and 1.5-fold longer for CXCL10 (CXCL9: HR 0.60, 95% CI 0.39-0.92, $p=0.019$; CXCL10: HR 0.52, 95% CI 0.33-0.82, $p=0.005$). In the high expression groups, the progression-free survival was longer, but this correlation was not statistically significant. The combined overexpression of both chemokines was associated with even a better prognosis as the ‘double-high’ tumors (CXCL9^{high} and CXCL10^{high}) were correlated with a significant better patient overall survival than tumors overexpressing only one of the two chemokines ($p=0.008$), this correlation was not statistically significant for the progression-free survival. Between the ‘single-high’ tumors (CXCL9^{high}/CXCL10^{low} or CXCL9^{low}/CXCL10^{high}) there was no statistically significant difference for both overall and progression-free survival.

Table 10: Median progression-free and overall survival according to CXCL9 and/or CXCL10 expression (validation set) – univariate analysis

Median progression-free survival				
Variable	Median (months)	hazard ratio	95% C.I.	p-value
CXCL9 expression				
low	17 ± 4.73	1		
high	16 ± 3.54	0.99	0.60-1.63	0.958
CXCL10 expression				
low	13 ± 2.31	1		
high	20 ± 2.48	0.76	0.46-1.25	0.283
CXCL9 ^{low} /CXCL10 ^{low}	24 ± 9.75	1		0.343
CXCL9 ^{high} /CXCL10 ^{low} or CXCL9 ^{low} /CXCL10 ^{high}	11 ± 1.85	1.55	0.68-3.58	0.300
CXCL9 ^{high} /CXCL10 ^{high}	22 ± 3.62	1.11	0.49-2.53	0.801
Median overall survival				
Variable	Median (months)	hazard ratio	95% C.I.	p-value
CXCL9 expression				
low	24 ± 3.93	1		
high	48 ± 5.95	0.60	0.39-0.92	0.019
CXCL10 expression				
low	31 ± 5.47	1		
high	46 ± 6.12	0.52	0.33-0.82	0.005
CXCL9 ^{low} /CXCL10 ^{low}	24 ± 7.73	1		0.010
CXCL9 ^{high} /CXCL10 ^{low} or CXCL9 ^{low} /CXCL10 ^{high}	27 ± 6.75	0.74	0.39-1.41	0.364
CXCL9 ^{high} /CXCL10 ^{high}	52 ± 6.37	0.41	0.21-0.79	0.008

Also in the Kaplan-Meier estimate an overexpression of the ligands CXCL9 or CXCL10 was associated with a prolonged overall survival (CXCL9: $p=0.017$; CXCL10: $p=0.004$) (Figure 11B and 11D). The combined overexpression of both chemokines CXCL9 and CXCL10 was correlated with an even better overall survival, compared to the overexpression of only one chemokine and the low expression of both ligands was associated with a poor overall survival ($p=0.007$) (Figure 11F). The progression-free survival could not be correlated in a statistically significant way with the chemokine expression.

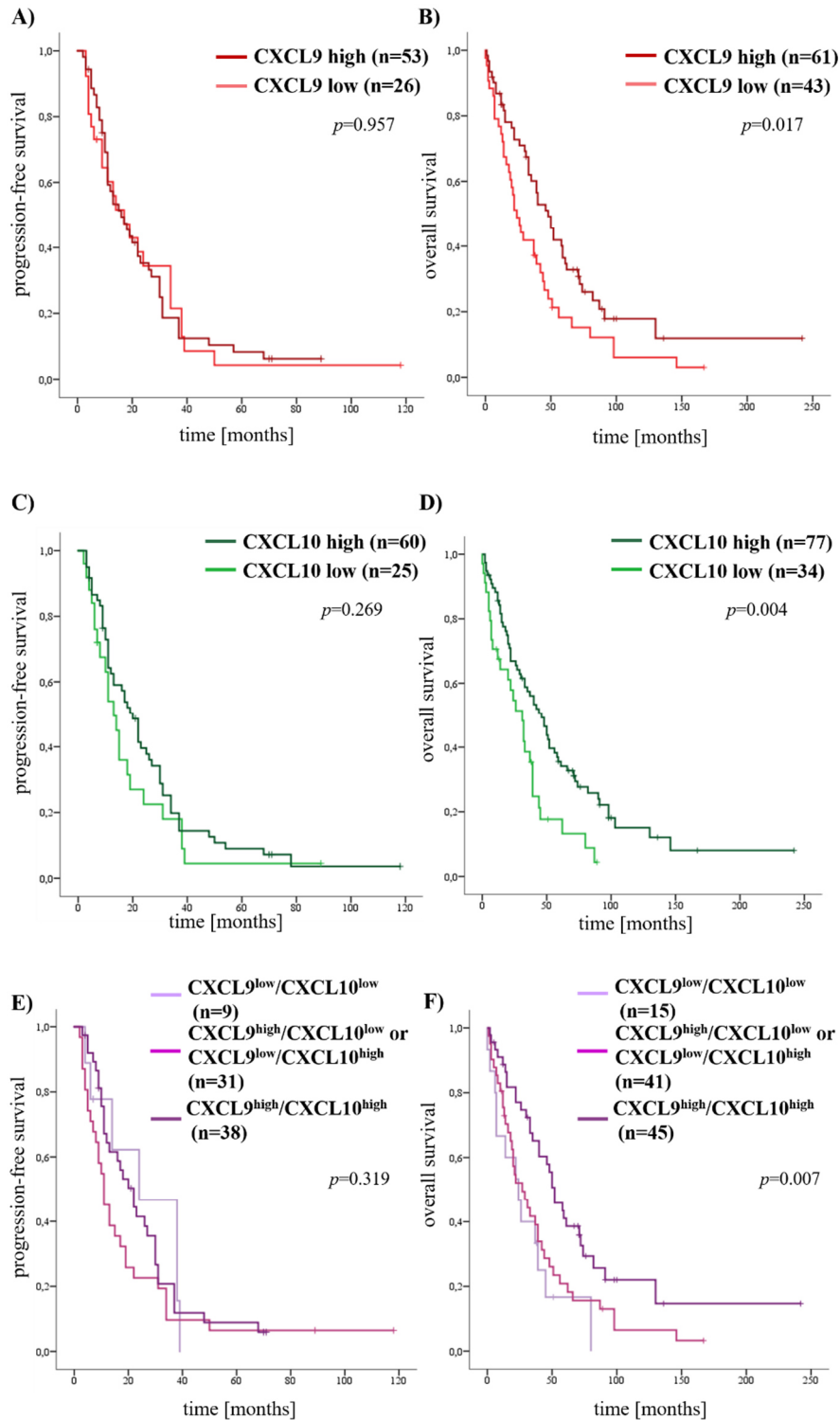


Figure 11: Prognostic significance of CXCL9 and CXCL10 expression in high-grade serous ovarian cancer (validation set)

Shown are Kaplan-Meier curves for **A)** progression-free survival and **B)** overall survival comparing tumors with low (light red line) and high (red line) CXCL9 expression, for **C)** progression-free survival and **D)** overall survival comparing tumors with low (light green line) and high (green line) CXCL10 expression and for **E)** progression-free survival and **F)** overall survival comparing tumors that express both CXCL9 and CXCL10 at a low level (light purple line), that either highly express CXCL9 or CXCL10 (pink line) or that highly express both CXCL9 and CXCL10 (purple line). Time is given in months, statistical significance (p -value) is stated (log rank).

In a multivariate analysis using a COX proportional hazard model, including postsurgical residual tumor mass and lymph node metastasis as covariates, CXCL10 was identified as independent marker for a better overall survival in high-grade serous ovarian cancer (Table 11). This could not be determined for progression-free survival. Also CXCL9 or the combined expression of both chemokines were no independent markers for overall and progression-free survival.

Table 11: Cox multivariate analysis for the progression-free and overall survival (validation set)

Residual tumor below 1 cm is defined as ‘optimal’, residual tumor above 1 cm as ‘suboptimal’.

Median progression-free survival				
Variable	n	hazard ratio	95% C.I.	p-value
CXCL9 expression				
low	21	1		
high	48	1.23	0.69-2.17	0.482
Postsurgical residual tumor				
optimal	28	1		
suboptimal	41	2.14	1.26-3.64	0.005
Nodal status				
pN0	26	1		
pN1	43	1.10	0.64-1.89	0.736
CXCL10 expression				
low	19	1		
high	55	0.83	0.46-1.50	0.531
Postsurgical residual tumor				
optimal	30	1		
suboptimal	44	2.10	1.25-3.52	0.005
Nodal status				
pN0	29	1		
pN1	45	1.04	0.62-1.73	0.893
CXCL9 ^{low} /CXCL10 ^{low}	6	1		0.100
CXCL9 ^{low} /CXCL10 ^{high} or CXCL9 ^{high} /CXCL10 ^{low}	27	3.22	1.05-9.83	0.040
CXCL9 ^{high} /CXCL10 ^{high}	35	2.32	0.78-6.93	0.130
Postsurgical residual tumor				
optimal	28	1		
suboptimal	40	2.56	1.47-4.45	0.001

Median progression-free survival				
Variable	n	hazard ratio	95% C.I.	p-value
Nodal status				
pN0	26	1		
pN1	42	1.44	0.84-2.50	0.189
Median overall survival				
Variable	n	hazard ratio	95% C.I.	p-value
CXCL9 expression				
low	37	1		
high	55	0.74	0.46-1.19	0.215
Postsurgical residual tumor				
optimal	35	1		
suboptimal	57	3.55	2.07-6.08	<0.001
Nodal status				
pN0	33	1		
pN1	59	0.95	0.59-1.54	0.829
CXCL10 expression				
low	26	1		
high	72	0.55	0.32-0.94	0.029
Postsurgical residual tumor				
optimal	36	1		
suboptimal	62	3.13	1.87-5.25	<0.001
Nodal status				
pN0	36	1		
pN1	62	0.84	0.53-1.34	0.468
CXCL9 ^{low} /CXCL10 ^{low}				
	11	1		0.173
CXCL9 ^{low} /CXCL10 ^{high} or CXCL9 ^{high} /CXCL10 ^{low}				
	36	0.98	0.46-2.10	0.955
CXCL9 ^{high} /CXCL10 ^{high}				
	42	0.62	0.28-1.35	0.225
Postsurgical residual tumor				
optimal	34	1		
suboptimal	55	3.46	2.00-5.99	<0.001
Nodal status				
pN0	33	1		
pN1	56	0.95	0.59-1.54	0.842

1.1.3. Combined cohorts

Next, both collectives were analyzed together in order to achieve a sufficient number of events for multivariate analyses. 66.7% of all tumors showed a high expression of CXCL9 and 68% were high CXCL10 expressing tumors. 49.1% overexpressed both chemokines, 38.8% highly expressed either CXCL9 or CXCL10 and 12.1% expressed both chemokines at a low level (Table 12).

Table 12: CXCL9 and CXCL10 expression in ovarian cancer (combined cohorts)

Shown are the numbers and percentage per immunohistochemical staining and score. Score 0 and 1+ are summarized as 'low', score 2+ and 3+ are summarized as 'high'.

CXCL9			CXCL10		
score	percentage	counts	score	percentage	counts
low	33.3%	58/174	low	32.0%	56/175
high	66.7%	116/174	high	68.0%	119/175
'double low' CXCL9 ^{low} and CXCL10 ^{low}			12.1%	20/165	
'single-high' CXCL9 ^{high} or CXCL10 ^{high}			38.8%	64/165	
'double-high' CXCL9 ^{high} and CXCL10 ^{high}			49.1%	81/165	

The univariate analysis comparing chemokine expression levels and survival data revealed a significant association between CXCL9 and CXCL10 overexpression and a longer overall survival (CXCL9: HR 0.53, 95% CI 0.38-0.75, $p < 0.001$; CXCL10: HR 0.50, 95% CI 0.35-0.72, $p < 0.001$), a high CXCL10 expression was furthermore correlated with a longer progression-free survival reaching borderline significance ($p = 0.056$). The combined overexpression of both chemokines was associated with an even better overall survival ($p < 0.001$). The worst prognosis had patients whose tumors expressed both chemokines at a low level (OS $p < 0.001$) (Table 13).

Table 13: Median progression-free and overall survival according to CXCL9 and/or CXCL10 expression (combined cohorts) – univariate analysis

Median progression-free survival				
Variable	Median (months)	hazard ratio	95% C.I.	p-value
CXCL9 expression				
low	14 ± 1.01	1		
high	17 ± 2.06	0.82	0.56-1.20	0.297
CXCL10 expression				
low	14 ± 1.04	1		
high	18 ± 2.46	0.70	0.48-1.01	0.056
CXCL9 ^{low} /CXCL10 ^{low}	14 ± 2.65	1		0.210
CXCL9 ^{high} /CXCL10 ^{low} or CXCL9 ^{low} /CXCL10 ^{high}	14 ± 2.01	0.91	0.48-1.72	0.772
CXCL9 ^{high} /CXCL10 ^{high}	18 ± 3.03	0.68	0.36-1.26	0.219
Median overall survival				
Variable	Median (months)	hazard ratio	95% C.I.	p-value
CXCL9 expression				
low	22 ± 3.26	1		
high	48 ± 4.59	0.53	0.38-0.75	<0.001
CXCL10 expression				
low	27 ± 4.37	1		
high	48 ± 3.53	0.50	0.35-0.72	<0.001
CXCL9 ^{low} /CXCL10 ^{low}	19 ± 8.94	1		<0.001
CXCL9 ^{high} /CXCL10 ^{low} or CXCL9 ^{low} /CXCL10 ^{high}	29 ± 5.98	0.61	0.35-1.04	0.068
CXCL9 ^{high} /CXCL10 ^{high}	52 ± 4.81	0.32	0.18-0.55	<0.001

Confirming these results, an overexpression of the ligands CXCL9 or CXCL10 was associated with a prolonged overall survival in a log rank test (CXCL9: PFS $p=0.041$; OS $p<0.001$; CXCL10: PFS $p=0.023$; OS $p<0.001$), the overexpression of CXCL10 was furthermore associated with a better progression-free survival reaching borderline significance ($p=0.050$) (Figure 12C). The combined overexpression of both chemokines CXCL9 and CXCL10 was correlated with an even better overall survival compared to the overexpression of only one chemokine and the low expression of both ligands was associated with a poor overall survival ($p<0.001$) (Figure 12E-F).

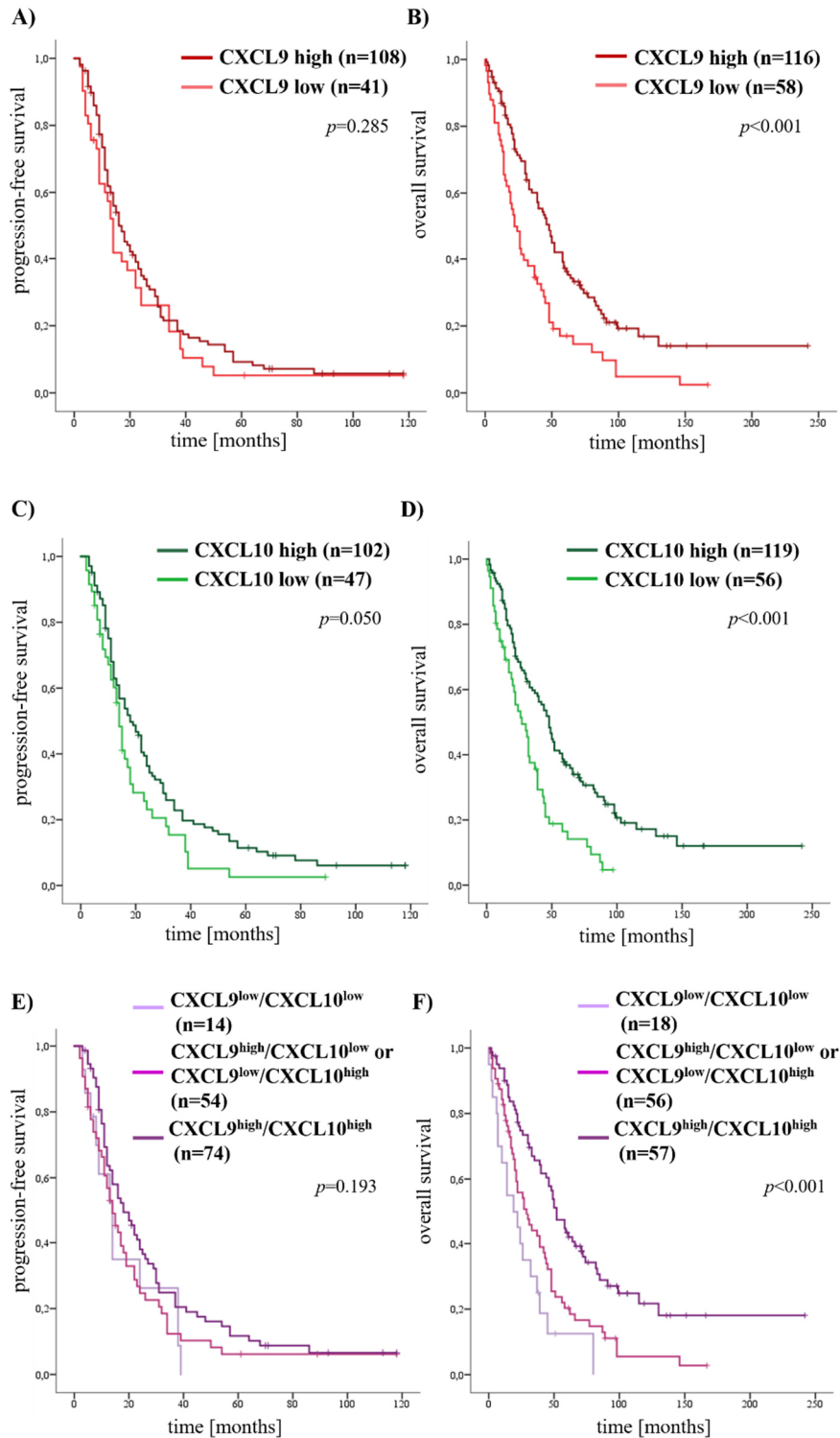


Figure 12: Prognostic significance of CXCL9 and CXCL10 expression in high-grade serous ovarian cancer (combined cohorts)

Shown are Kaplan-Meier curves for **A)** progression-free survival and **B)** overall survival comparing tumors with low (light red line) and high (red line) CXCL9 expression, for **C)** progression-free survival and **D)** overall survival comparing tumors with low (light green line) and high (green line) CXCL10 expression and for **E)** progression-free survival and **F)** overall survival comparing tumors that express both CXCL9 and CXCL10 at a low level (light purple line), that either highly express CXCL9 or CXCL10 (pink line) or that highly express both CXCL9 and CXCL10 (purple line). Time is given in months, statistical significance (p -value) is stated (log rank).

The Cox multivariate analysis including residual tumor mass and lymph node metastasis revealed CXCL9 and CXCL10 as independent markers for a better overall survival in high-grade serous ovarian cancer. The combined overexpression of both chemokines was associated with an even better outcome (Table 14).

Table 14: Cox multivariate analysis for the progression-free and overall survival (combined cohorts)

Residual tumor below 1 cm is defined as ‘optimal’, residual tumor above 1 cm as ‘suboptimal’.

Median progression-free survival				
Variable	n	hazard ratio	95% C.I.	p-value
CXCL9 expression				
low	32	1		
high	92	0.88	0.56-1.38	0.587
Postsurgical residual tumor				
optimal	46	1		
suboptimal	78	2.32	1.54-3.50	<0.001
Nodal status				
pN0	43	1		
pN1	81	1.01	0.67-1.53	0.972
CXCL10 expression				
low	34	1		
high	92	0.73	0.47-1.13	0.162
Postsurgical residual tumor				
optimal	48	1		
suboptimal	78	2.30	1.53-3.45	<0.001
Nodal status				
pN0	44	1		
pN1	82	0.91	0.61-1.35	0.625
CXCL9 ^{low} /CXCL10 ^{low}				
	9	1		0.296
CXCL9 ^{low} /CXCL10 ^{high} or CXCL9 ^{high} /CXCL10 ^{low}				
	45	1.39	0.61-3.20	0.434
CXCL9 ^{high} /CXCL10 ^{high}				
	66	1.00	0.45-2.23	0.996
Postsurgical residual tumor				
optimal	46	1		
suboptimal	74	2.45	1.61-3.73	<0.001

Median progression-free survival				
Variable	n	hazard ratio	95% C.I.	p-value
Nodal status				
pN0	41	1		
pN1	79	1.08	0.70-1.65	0.738
Median overall survival				
Variable	n	hazard ratio	95% C.I.	p-value
CXCL9 expression				
low	48	1		
high	99	0.58	0.39-0.86	0.007
Postsurgical residual tumor				
optimal	53	1		
suboptimal	94	3.71	2.38-5.77	<0.001
Nodal status				
pN0	48	1		
pN1	99	0.90	0.61-1.34	0.605
CXCL10 expression				
low	41	1		
high	109	0.51	0.34-0.78	0.002
Postsurgical residual tumor				
optimal	54	1		
suboptimal	96	3.42	2.23-5.27	<0.001
Nodal status				
pN0	51	1		
pN1	99	0.77	0.52-1.13	0.184
CXCL9 ^{low} /CXCL10 ^{low}				
	14	1		0.003
CXCL9 ^{low} /CXCL10 ^{high} or CXCL9 ^{high} /CXCL10 ^{low}				
	54	0.82	0.43-1.57	0.546
CXCL9 ^{high} /CXCL10 ^{high}				
	73	0.43	0.22-0.83	0.012
Postsurgical residual tumor				
optimal	52	1		
suboptimal	89	3.64	2.31-5.71	<0.001
Nodal status				
pN0	48	1		
pN1	93	0.86	0.58-1.29	0.463

1.2. Expression of CXCR3 and correlation with survival data

The tumor tissues of both collectives were further stained for the chemokine receptor CXCR3, scored microscopically and compared to fallopian tube tissue as an intra- and inter-run control. CXCR3 was predominantly localized in the cytoplasm of tumor cells and on the cytoplasmic membrane (Figure 13). It was also located on the membrane of lymphocytes, but only tumor CXCR3 was included into evaluation and scoring. Moreover, it was noted, that in several cases the invasive tumor front revealed a stronger staining and on that account a higher expression of CXCR3 compared with tumor center.

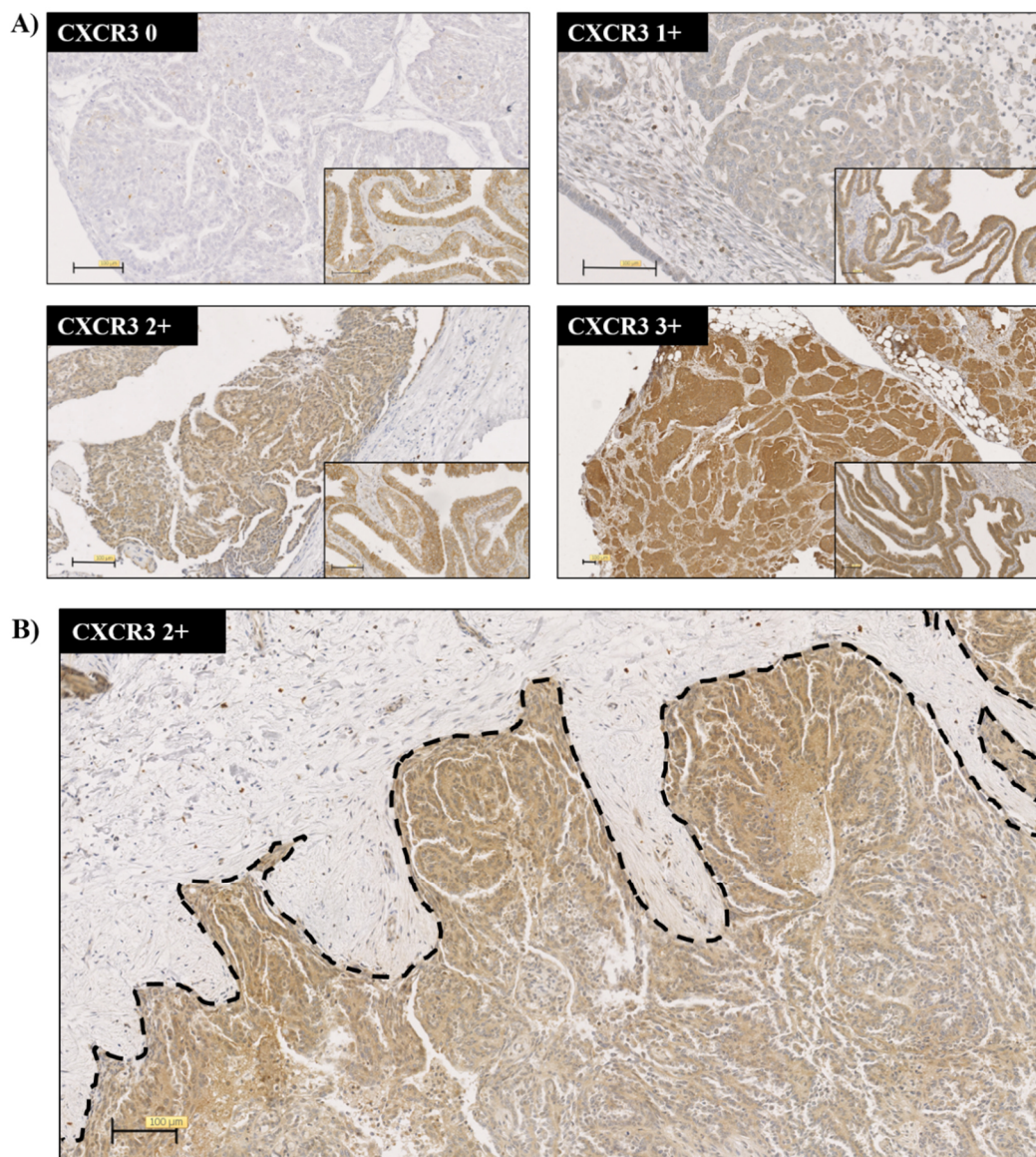


Figure 13: Immunohistochemical staining and scoring of CXCR3 in tumor cells

A) Different scores of the immunohistochemical staining. Small boxes: fallopian tube tissue as intratumoral control scored previously as 2+. Scale: 100 μm . **B)** Stronger staining indicating higher CXCR3 expression at the invasive tumor front (dashed line). Scale: 100 μm .

To validate the results and to test the specificity of the α -CXCR3 antibody, six tumor lysates from different ovarian cancers were applied under reducing conditions to a SDS-gel. After gel electrophoresis, the proteins were transferred to a nitrocellulose membrane by using a semi-dry western blot chamber. Immunostaining with the monoclonal antibody directed against CXCR3 revealed the expression of the receptor CXCR3 in all tumor lysates (Figure 14). Moreover, all tumor lysates expressed both receptor isoforms CXCR3-A and CXCR3-B. As endogenous control the membrane was stained for the housekeeping gene GAPDH.

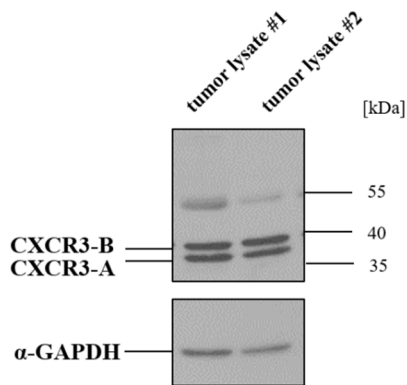


Figure 14: Protein expression of CXCR3 in tumor lysates

Representative western blot with lysates from two different tumor lysates immunostained with CXCR3 antibody and GAPDH antibody as endogenous control.

1.2.1. Discovery set

In the discovery set, 60 high-grade serous ovarian tumor tissues were immunohistochemically stained for CXCR3. Table 15 shows the results of the scored CXCR3 expression. Tumors that were scored 0, 1+ or 2+ were grouped to CXCR3 low expressing tumors and CXCR3 high expressing tumors were scored 3+. The majority of the examined tumors were low CXCR3 expressing (72%).

Table 15: CXCR3 expression in ovarian cancer (discovery set)

Shown are the numbers and percentage per immunohistochemical staining and expression grade. Score 0, 1+ and 2+ are summarized as 'low', score 3+ is defined as 'high'.

CXCR3 in ovarian tumor		
score	percentage	counts
CXCR3 low	72%	43/60
CXCR3 high	28%	17/60

Furthermore, the association of the CXCR3 tumor expression with patient survival was statistically determined. In the Cox univariate analysis, the tumor cell CXCR3 overexpression was significantly associated with a worse overall survival (HR 2.41, 95% CI 1.26-4.62, $p=0.008$). A worse progression-free survival could be correlated with an CXCR3 overexpression reaching borderline significance ($p=0.059$) (Table 16).

Table 16: Median progression-free and overall survival according to CXCR3 expression (discovery set) – univariate analysis

Median progression-free survival				
Variable	Median (months)	hazard ratio	95% C.I.	<i>p</i>-value
CXCR3 expression				
low	16 ± 2.51	1		
high	11 ± 1.60	1.88	0.98-3.61	0.059
Median overall survival				
Variable	Median (months)	hazard ratio	95% C.I.	<i>p</i>-value
CXCR3 expression				
low	52 ± 7.85	1		
high	17 ± 1.85	2.41	1.26-4.62	0.008

A tumor CXCR3 overexpression was associated with a worse overall and progression-free survival that was statistically significant in the log rank test (PFS: $p=0.045$; OS: $p=0.006$) (Figure 15).

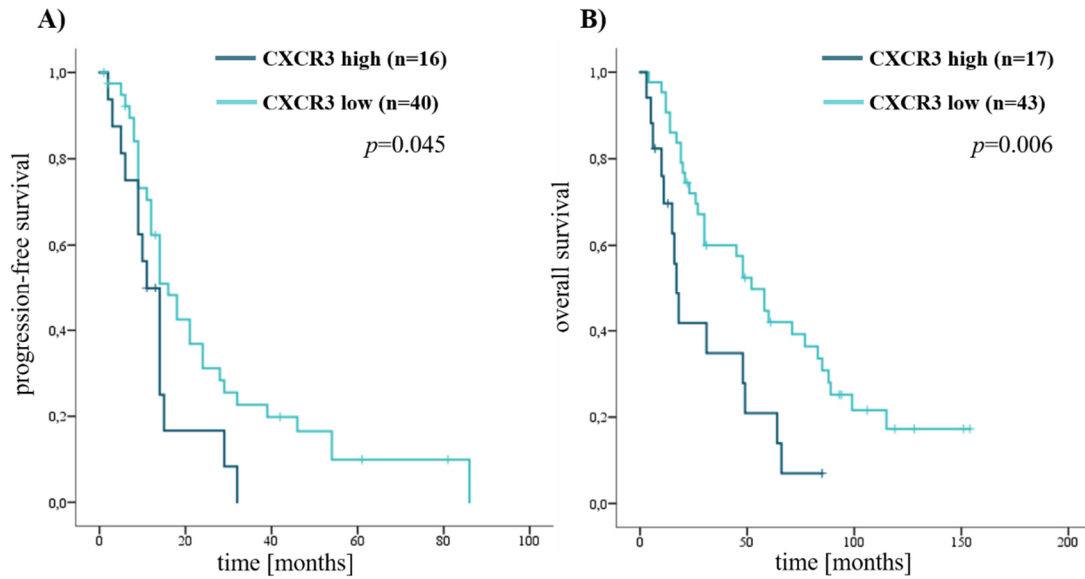


Figure 15: Prognostic significance of CXCR3 expression in high-grade serous ovarian cancer (discovery set)

Shown are Kaplan-Meier curves for **A)** progression-free survival and **B)** overall survival comparing tumors with low (light blue line) and high (dark blue line) CXCR3 expression. Time is given in months, statistical significance (p -value) is stated (log rank).

A multivariate analysis using a COX proportional hazard model including postsurgical residual tumor mass and lymph node metastasis as covariates identified CXCR3 as an independent marker for a worse overall survival in high-grade serous ovarian cancer ($p=0.016$) (Table 17).

Table 17: Cox multivariate analysis for the progression-free and overall survival (discovery set)

Residual tumor below 1 cm is defined as ‘optimal’, residual tumor above 1 cm is defined as ‘suboptimal’.

Median progression-free survival				
Variable	<i>n</i>	hazard ratio	95% C.I.	<i>p</i>-value
CXCR3 expression				
low	33	1		
high	12	1.52	0.66–3.51	0.330
Postsurgical residual tumor				
optimal	17	1		
suboptimal	28	3.76	1.56–9.02	0.003

Median progression-free survival				
Variable	<i>n</i>	hazard ratio	95% C.I.	<i>p</i>-value
Nodal status				
pN0	13	1		
pN1	32	0.88	0.41–1.92	0.754
Median overall survival				
Variable	<i>n</i>	hazard ratio	95% C.I.	<i>p</i>-value
CXCR3 expression				
low	36	1		
high	13	2.71	1.21–6.07	0.016
Postsurgical residual tumor				
optimal	18	1		
suboptimal	31	2.81	1.24–6.40	0.014
Nodal status				
pN0	14	1		
pN1	35	0.84	0.39–1.83	0.658

1.2.2. Validation set

In a validation collective, 127 high-grade serous ovarian tumor tissues were immunohistochemically stained for CXCR3. Table 18 shows the results of the scored CXCR3 expression. Due to technical difficulties the expression of CXCR3 was not assessable in ten cases, so that only 117 cases were taken into further analysis. As in the discovery set, tumors that were scored 0, 1+ or 2+ were grouped to CXCR3 low expressing tumors and CXCR3 high expressing tumors were scored 3+. The majority of the examined tumors were low CXCR3 expressing (76.1%).

Table 18: CXCR3 expression in ovarian cancer (validation set)

Shown are the numbers and percentage per immunohistochemical staining and expression grade. Score 0, 1+ and 2+ are summarized as 'low', score 3+ is defined as 'high'.

CXCR3 in ovarian tumor		
score	percentage	counts
CXCR3 low	76.1%	89/117
CXCR3 high	23.9%	28/117

In the Cox univariate analysis, the CXCR3 overexpression was correlated with a poor progression-free and overall survival (PFS: HR 2.37, 95% CI 1.37-4.09, $p=0.002$; OS: HR 2.16, 95% CI 1.32-3.52, $p=0.002$) (Table 19).

Table 19: Median progression-free and overall survival in relation to CXCR3 expression (validation set) – univariate analysis

Median progression-free survival and overall survival of the different expression grades of CXCR3 in months, including hazard ratio, 95% confidence interval and statistical significance (p -value).

Median progression-free survival				
Variable	Median (months)	hazard ratio	95% C.I.	p-value
CXCR3 expression				
low	22 ± 2.19	1		
high	11 ± 1.27	2.37	1.37-4.09	0.002
Median overall survival				
Variable	Median (months)	hazard ratio	95% C.I.	p-value
CXCR3 expression				
low	44 ± 6.29	1		
high	22 ± 3.44	2.16	1.32-3.52	0.002

A tumor cell CXCR3 overexpression was associated with a worse overall and progression-free survival, that was highly statistically significant in the Kaplan-Meier function (PFS and OS: $p=0.001$) (Figure 16).

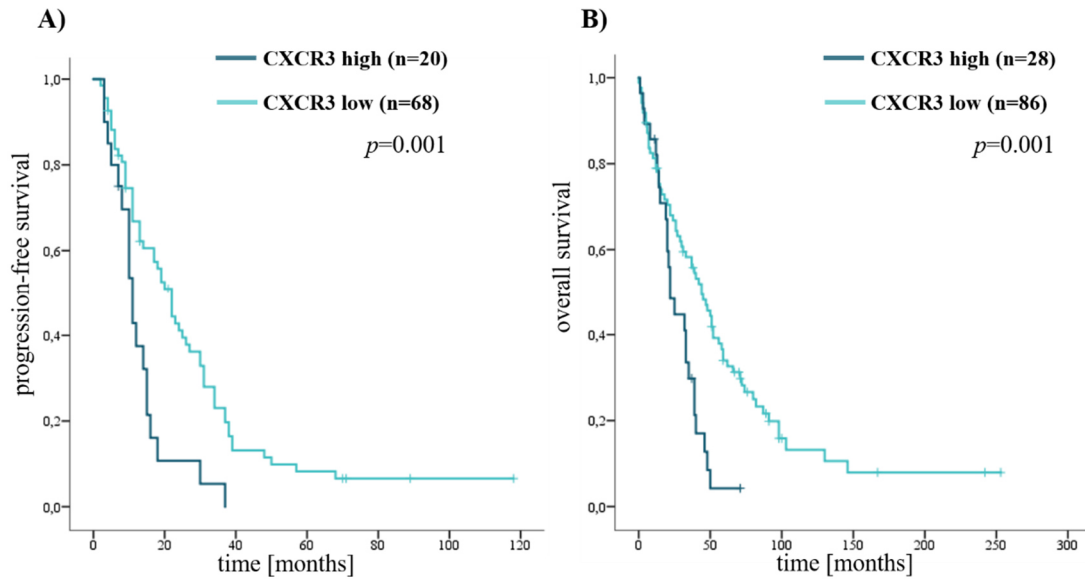


Figure 16: Prognostic significance of CXCR3 expression in high-grade serous ovarian cancer (validation set)

Shown are Kaplan-Meier curves for **A)** progression-free survival and **B)** overall survival comparing tumors with low (light blue line) and high (dark blue line) CXCR3 expression. Time is given in months, statistical significance (p -value) is stated (log rank).

Moreover, CXCR3 overexpression was identified as an independent marker for a worse progression-free and overall survival in high-grade serous ovarian cancer (PFS and OS: $p=0.004$) in a multivariate analysis using a COX proportional hazard model (Table 20).

Table 20: Cox multivariate analysis for the progression-free and overall survival (validation set)

Residual tumor below 1 cm is defined as ‘optimal’, residual tumor above 1 cm is defined as ‘suboptimal’.

Median progression-free survival				
Variable	<i>n</i>	hazard ratio	95% C.I.	<i>p</i>-value
CXCR3 expression				
low	59	1		
high	18	2.40	1.31–4.37	0.004
Postsurgical residual tumor				
optimal	31	1		
suboptimal	46	2.15	1.30–3.55	0.003

Median progression-free survival				
Variable	<i>n</i>	hazard ratio	95% C.I.	<i>p</i>-value
Nodal status				
pN0	30	1		
pN1	47	0.97	0.58–1.62	0.910
Median overall survival				
Variable	<i>n</i>	hazard ratio	95% C.I.	<i>p</i>-value
CXCR3 expression				
low	75	1		
high	25	2.21	1.28–3.80	0.004
Postsurgical residual tumor				
optimal	37	1		
suboptimal	63	3.22	1.95–5.32	<0.001
Nodal status				
pN0	37	1		
pN1	63	0.93	0.59–1.48	0.770

1.2.3. Combined cohorts

The combined analysis of both collectives showed a high expression of CXCR3 in 25.4% of all tumors, 74.6% expressed the chemokine receptor at a low level (Table 21).

Table 21: CXCR3 expression in ovarian cancer (combined cohorts)

Shown are the numbers and percentage per immunohistochemical staining and expression grade. Score 0, 1+ and 2+ are summarized as ‘low’, score 3+ is defined as ‘high’.

CXCR3 in ovarian tumor		
score	percentage	counts
CXCR3 low	74.6%	132/177
CXCR3 high	25.4%	45/177

Furthermore, the association of the CXCR3 tumor expression with patient survival was statistically determined. In the Cox univariate analysis, the CXCR3 overexpression was associated with a worse progression-free and overall survival that was highly

statistical significant (PFS: HR 2.19, 95% CI 1.44-3.33, $p<0.001$; OS: HR 2.16, 95% CI 1.47-3.19, $p<0.001$) (Table 22).

Table 22: Median progression-free and overall survival in relation to CXCR3 expression (combined cohorts) – univariate analysis

Median progression-free survival				
Variable	Median (months)	hazard ratio	95% C.I.	<i>p</i>-value
CXCR3 expression				
low	19 ± 2.08	1		
high	11 ± 1.09	2.19	1.44-3.33	<0.001
Median overall survival				
Variable	Median (months)	hazard ratio	95% C.I.	<i>p</i>-value
CXCR3 expression				
low	48 ± 4.24	1		
high	22 ± 3.17	2.16	1.47-3.19	<0.001

Also in the log rank test a tumor CXCR3 overexpression was statistically significant associated with a worse overall and progression-free survival (PFS and OS $p<0.001$) (Figure 17).

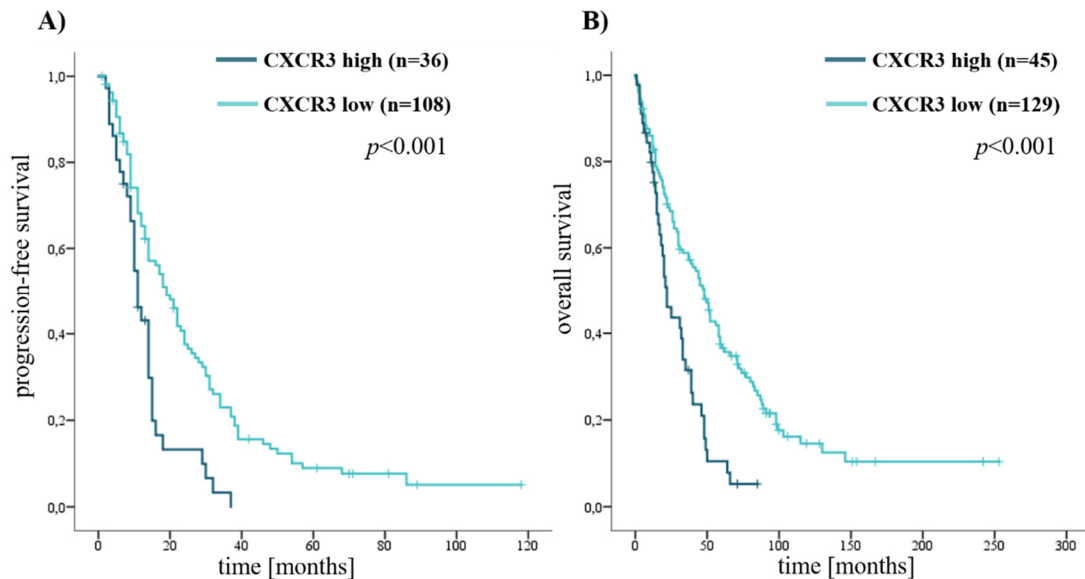


Figure 17: Prognostic significance of CXCR3 expression in high-grade serous ovarian cancer (combined cohorts)

Shown are Kaplan-Meier curves for **A)** progression-free survival and **B)** overall survival comparing tumors with low (light blue line) and high (dark blue line) CXCR3 expression. Time is given in months, statistical significance (p -value) is stated (log rank).

CXCR3 was furthermore identified as an independent marker for a worse progression-free and overall survival in high-grade serous ovarian cancer in a multivariate analysis using a COX proportional hazard model, including postsurgical residual tumor mass and lymph node metastasis as covariates (PFS: $p=0.003$; OS: $p<0.001$) (Table 23).

Table 23: Cox multivariate analysis for the progression-free and overall survival (combined cohorts)

Residual tumor below 1 cm is defined as ‘optimal’, residual tumor above 1 cm is defined as ‘suboptimal’.

Median progression-free survival				
Variable	<i>n</i>	hazard ratio	95% C.I.	<i>p</i>-value
CXCR3 expression				
low	92	1		
high	30	2.11	1.30–3.43	0.003
Postsurgical residual tumor				
optimal	48	1		
suboptimal	74	2.51	1.64–3.84	<0.001
Nodal status				
pN0	43	1		
pN1	79	0.98	0.64–1.49	0.921
Median overall survival				
Variable	<i>n</i>	hazard ratio	95% C.I.	<i>p</i>-value
CXCR3 expression				
low	111	1		
high	38	2.21	1.43–3.42	<0.001
Postsurgical residual tumor				
optimal	55	1		
suboptimal	94	3.16	2.06–4.83	<0.001
Nodal status				
pN0	51	1		
pN1	98	0.85	0.58–1.26	0.419

1.2.4. CXCR3 expression in lymph node metastases

Additional to the CXCR3 expression in tumor tissue the receptor expression in lymph node metastases was also investigated by immunohistochemically staining of 34

metastatic lymph node samples. The staining was scored microscopically (Figure 18).

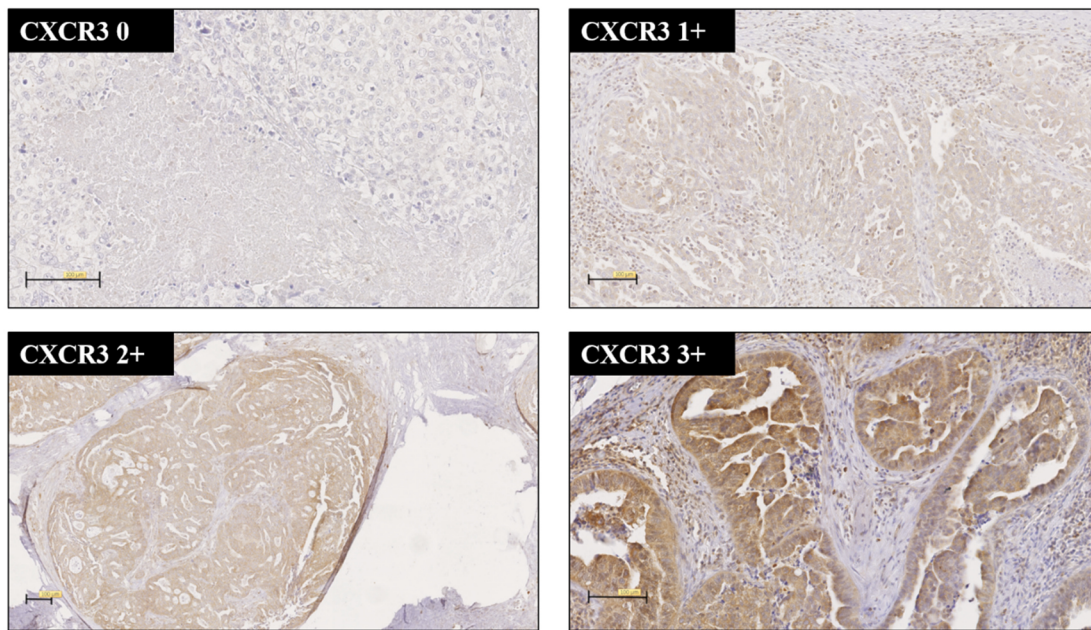


Figure 18: CXCR3 expression in metastatic lymph nodes

Different scores of the immunohistochemical staining. Scale: 100 µm.

About 94% of the analyzed lymph node metastases were CXCR3 positive, 44% were low CXCR3 expressing and 56% were high CXCR3 expressing metastases.

Table 24: CXCR3 expression in lymph node metastases

Shown are the numbers and percentage per immunohistochemical staining and expression grade. Score 0 and 1+ are summarized as 'low', score 2+ and 3+ are summarized as 'high'.

CXCR3 in LN		
score	percentage	counts
0	6%	2/34
1+	38%	13/34
2+	32%	11/34
3+	24%	8/34
CXCR3 low	44%	15/34
CXCR3 high	56%	19/34

1.3. Combined expression of receptor and ligand

1.3.1. Discovery set

The combined expression of both ligands and receptor was analyzed in the discovery set of high-grade serous ovarian carcinomas. Only a small portion expressed CXCL9 or CXCL10 at a low level and concomitantly CXCR3 at a high level. The majority of the cancer samples were high ligand/low receptor expressing.

Table 25: CXCL9, CXCL10 and CXCR3 in ovarian tumor (discovery set)

Shown are the numbers and percentage per combined ligand and receptor group.

CXCL9, CXCL10 and CXCR3 in ovarian tumor		
group	percentage	counts
CXCL9 ^{high} /CXCR3 ^{high} or CXCL9 ^{low} /CXCR3 ^{low}	41.7%	25/60
CXCL9 ^{low} /CXCR3 ^{high}	3.3%	2/60
CXCL9 ^{high} /CXCR3 ^{low}	55.0%	33/60
CXCL10 ^{high} /CXCR3 ^{high} or CXCL10 ^{low} /CXCR3 ^{low}	37.0%	20/54
CXCL10 ^{low} /CXCR3 ^{high}	13.0%	7/54
CXCL10 ^{high} /CXCR3 ^{low}	50.0%	27/54

A univariate analysis demonstrated an association of tumor CXCR3 overexpression and a simultaneous low CXCL9 expression with a worse overall and progression-free survival, that was statistically significant (PFS: HR 11.88, 95% CI 2.22-63.69, $p=0.004$; OS: HR 12.45, 95% CI 2.36-65.73, $p=0.003$). The longest overall survival had patients, whose tumors expressed low CXCR3 and high CXCL9 or CXCL10 (CXCL9: HR 0.37, 95% CI 0.20-0.69, $p=0.002$; CXCL10: HR 0.44, 95% CI 0.23-0.84, $p=0.013$), this correlation did not reach statistical significance for the progression-free survival. An either double high expression or a double low expression of both ligand and receptor was correlated with an intermediate progression-free and overall survival (Table 26).

Table 26: Median progression-free and overall survival in relation to CXCR3 and CXCL9 or CXCL10 (discovery set) – univariate analysis

Median progression-free survival				
Variable	Median (months)	hazard ratio	95% C.I.	p-value
CXCL9 ^{high} /CXCR3 ^{high} or CXCL9 ^{low} /CXCR3 ^{low}	14 ± 1.01	1		0.003
CXCL9 ^{low} /CXCR3 ^{high}	3	11.88	2.22-63.69	0.004
CXCL9 ^{high} /CXCR3 ^{low}	18 ± 3.09	0.66	0.36-1.21	0.180
CXCL10 ^{high} /CXCR3 ^{high} or CXCL10 ^{low} /CXCR3 ^{low}	14 ± 1.73	1		0.363
CXCL10 ^{low} /CXCR3 ^{high}	14 ± 5.00	0.98	0.36-2.69	0.971
CXCL10 ^{high} /CXCR3 ^{low}	18 ± 4.30	0.63	0.32-1.23	0.178
Median overall survival				
Variable	Median (months)	hazard ratio	95% C.I.	p-value
CXCL9 ^{high} /CXCR3 ^{high} or CXCL9 ^{low} /CXCR3 ^{low}	19 ± 7.06	1		<0.001
CXCL9 ^{low} /CXCR3 ^{high}	3	12.45	2.36-65.73	0.003
CXCL9 ^{high} /CXCR3 ^{low}	60 ± 12.98	0.37	0.20-0.69	0.002
CXCL10 ^{high} /CXCR3 ^{high} or CXCL10 ^{low} /CXCR3 ^{low}	27 ± 12.30	1		0.037
CXCL10 ^{low} /CXCR3 ^{high}	17 ± 18.64	0.96	0.32-2.83	0.936
CXCL10 ^{high} /CXCR3 ^{low}	60 ± 17.74	0.44	0.23-0.84	0.013

The Kaplan-Meier estimate also demonstrated the good outcome of a simultaneous low CXCR3 and high CXCL9 expression, the intermediate survival time for patients with tumors that express both ligand and receptor either double high or double low and the poor outcome of a high receptor expression with a combined low ligand expression for the overall and progression-free survival. For CXCL10 and CXCR3, the different groups were not so easily distinguishable as for CXCL9 and CXCR3. Only the CXCL10^{high}/CXCR3^{low} expressing tumors showed a clearly better overall survival (Figure 19).

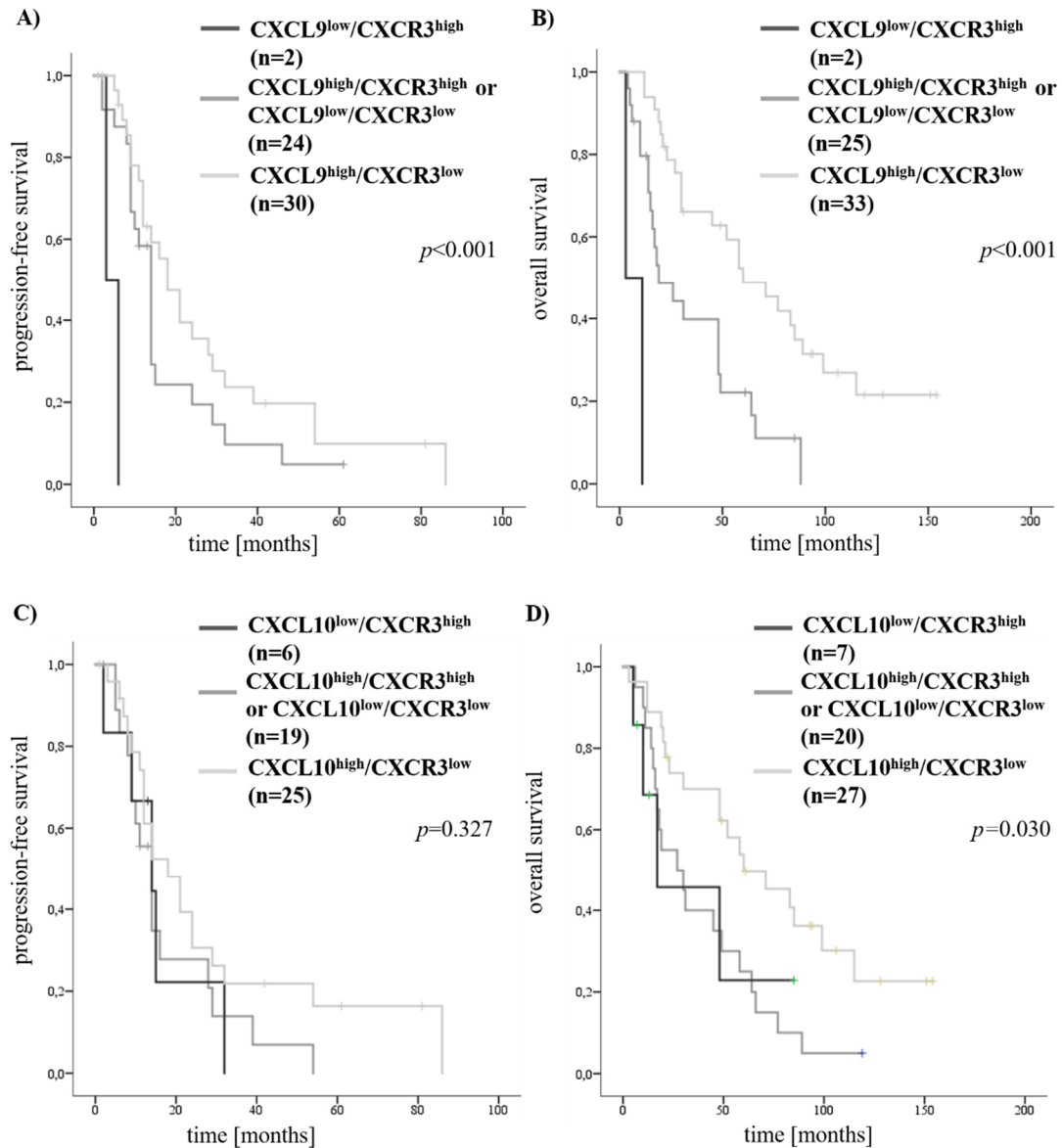


Figure 19: Prognostic significance of combined CXCR3 and CXCL9 or CXCL10 expression in high-grade serous ovarian cancer (discovery set)

Shown are Kaplan-Meier curves for **A)** progression-free survival and **B)** overall survival comparing tumors that either express low CXCL9 and high CXCR3 (black line), both high CXCL9 and CXCR3 or both low CXCL9 and CXCR3 (grey line) and high CXCL9 and low CXCR3 (light grey line) and for **C)** progression-free survival and **D)** overall survival comparing tumors that either express low CXCL10 and high CXCR3 (black line), both high CXCL10 and CXCR3 or both low CXCL10 and CXCR3 (grey line) and high CXCL10 and low CXCR3 (light grey line). Time is given in months, statistical significance (p -value) is stated (log rank).

1.3.2. Validation set

In the validation set of high-grade serous ovarian carcinomas, the majority of the cancer samples were either CXCL9/CXCR3 double high or low expressing or expressed CXCL10 at a high level and simultaneously CXCR3 at a low level. Only a small portion expressed CXCL9 or CXCL10 at a low level and concomitantly CXCR3

at a high level (Table 27).

Table 27: CXCL9, CXCL10 and CXCR3 in ovarian tumor (validation set)

Shown are the numbers and percentage per combined ligand and receptor group.

CXCL9, CXCL10 and CXCR3 in ovarian tumor		
group	percentage	counts
CXCL9 ^{high} /CXCR3 ^{high} or CXCL9 ^{low} /CXCR3 ^{low}	48.0%	49/102
CXCL9 ^{low} /CXCR3 ^{high}	8.8%	9/102
CXCL9 ^{high} /CXCR3 ^{low}	43.1%	44/102
CXCL10 ^{high} /CXCR3 ^{high} or CXCL10 ^{low} /CXCR3 ^{low}	39.6%	42/106
CXCL10 ^{low} /CXCR3 ^{high}	8.5%	9/106
CXCL10 ^{high} /CXCR3 ^{low}	51.9%	55/106

In the univariate analysis, the longest overall survival had patients, whose tumors expressed low CXCR3 and concomitantly high CXCL9 (HR 0.55, 95% CI 0.35-0.88, $p=0.013$) or high CXCL10 (HR 0.43, 95% CI 0.27-0.68, $p<0.001$). An either double high expression or a double low expression of both CXCL9 and CXCR3 was correlated with an intermediate progression-free and overall survival (Table 28).

Table 28: Median progression-free and overall survival in relation to CXCR3 and CXCL9 or CXCL10 (validation set) – univariate analysis

Median progression-free survival				
Variable	Median (months)	hazard ratio	95% C.I.	<i>p</i>-value
CXCL9 ^{high} /CXCR3 ^{high} or CXCL9 ^{low} /CXCR3 ^{low}	15 ± 2.89	1		0.064
CXCL9 ^{low} /CXCR3 ^{high}	4 ± 2.67	3.21	0.95-10.90	0.061
CXCL9 ^{high} /CXCR3 ^{low}	22 ± 3.71	0.77	0.48-1.26	0.299
CXCL10 ^{high} /CXCR3 ^{high} or CXCL10 ^{low} /CXCR3 ^{low}	12 ± 1.35	1		0.018
CXCL10 ^{low} /CXCR3 ^{high}	10 ± 1.66	2.23	0.90-5.55	0.085
CXCL10 ^{high} /CXCR3 ^{low}	22 ± 1.88	0.66	0.41-1.07	0.094

Median overall survival				
Variable	Median (months)	hazard ratio	95% C.I.	p-value
CXCL9 ^{high} /CXCR3 ^{high} or CXCL9 ^{low} /CXCR3 ^{low}	33 ± 5.41	1		0.004
CXCL9 ^{low} /CXCR3 ^{high}	20 ± 1.49	1.90	0.87-4.13	0.107
CXCL9 ^{high} /CXCR3 ^{low}	58 ± 5.53	0.55	0.35-0.88	0.013
CXCL10 ^{high} /CXCR3 ^{high} or CXCL10 ^{low} /CXCR3 ^{low}	22 ± 4.42	1		<0.001
CXCL10 ^{low} /CXCR3 ^{high}	32 ± 8.14	1.35	0.62-2.93	0.452
CXCL10 ^{high} /CXCR3 ^{low}	52 ± 7.09	0.43	0.27-0.68	<0.001

The good outcome of a simultaneous low CXCR3 and high CXCL9 expression, the intermediate survival time for patients with tumors that express both ligand and receptor either double high or double low and the poor outcome of a high receptor expression with a combined low ligand expression for the overall and progression-free survival could be confirmed by the Kaplan-Meier estimate. For CXCL10 and CXCR3, only the CXCL10^{high}/CXCR3^{low} expressing tumors showed clearly a better overall survival, the other groups were not so easy distinguishable as for CXCL9 and CXCR3. (Figure 20).

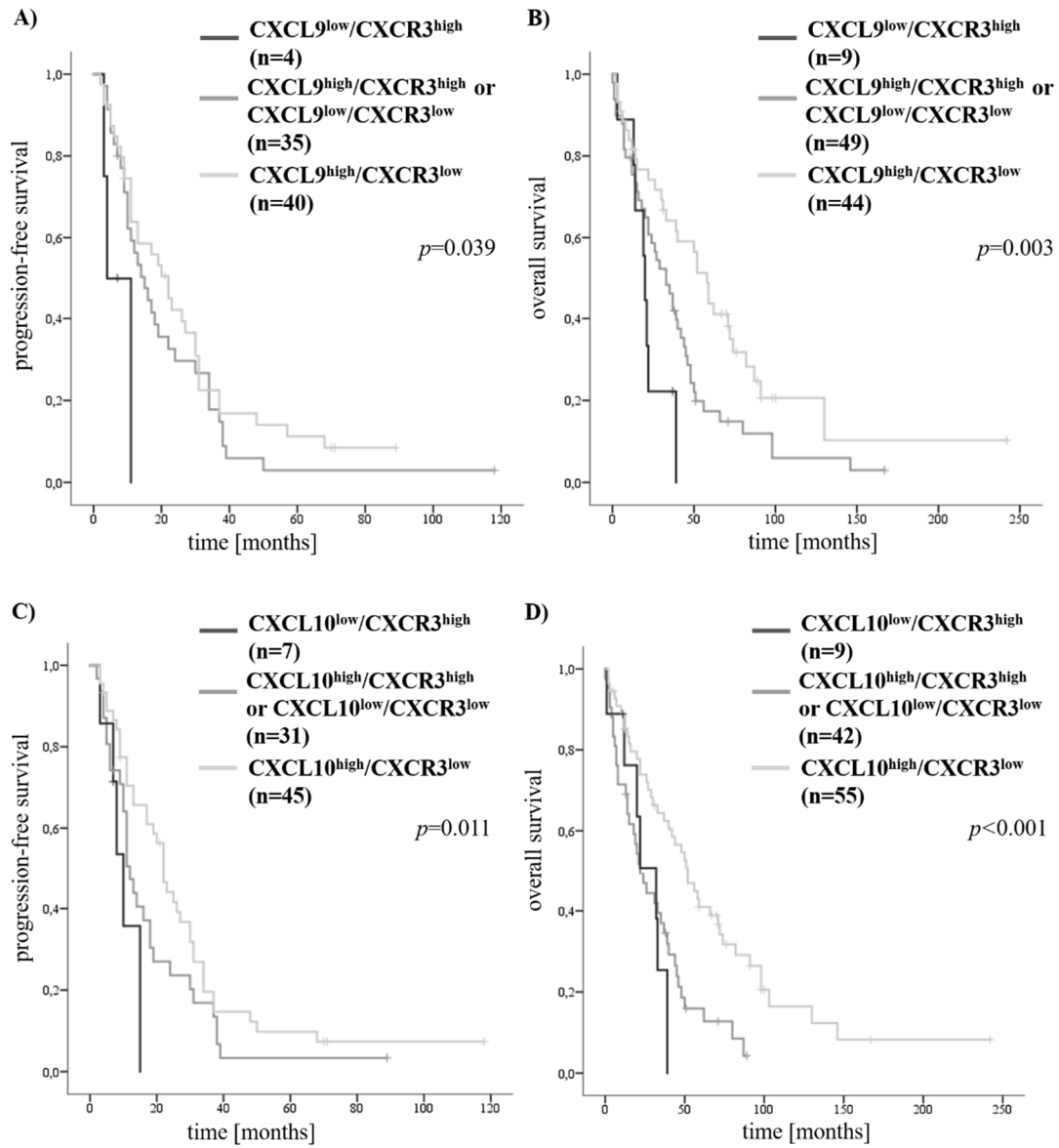


Figure 20: Prognostic significance of combined CXCR3 and CXCL9 or CXCL10 expression in high-grade serous ovarian cancer (validation set)

Shown are Kaplan-Meier curves for **A)** progression-free survival and **B)** overall survival comparing tumors that either express low CXCL9 and high CXCR3 (black line), both high CXCL9 and CXCR3 or both low CXCL9 and CXCR3 (grey line) and high CXCL9 and low CXCR3 (light grey line) and for **C)** progression-free survival and **D)** overall survival comparing tumors that either express low CXCL10 and high CXCR3 (black line), both high CXCL10 and CXCR3 or both low CXCL10 and CXCR3 (grey line) and high CXCL10 and low CXCR3 (light grey line). Time is given in months, statistical significance (p -value) is stated (log rank).

1.3.3. Combined cohorts

When both collectives were analyzed together, the majority of the cancer samples expressed the chemokine ligands CXCL9 or CXCL10 at a high level, regardless of the CXCR3 receptor status. Only approximately 7-10% of the tumors expressed CXCL9 or CXCL10 at a low level and concomitantly CXCR3 at a high level (Table 29).

Table 29: CXCL9, CXCL10 and CXCR3 in ovarian tumor (combined cohorts)

Shown are the numbers and percentage per combined ligand and receptor group.

CXCL9, CXCL10 and CXCR3 in ovarian tumor		
group	percentage	counts
CXCL9 ^{high} /CXCR3 ^{high} or CXCL9 ^{low} /CXCR3 ^{low}	46.0%	74/161
CXCL9 ^{low} /CXCR3 ^{high}	6.8%	11/161
CXCL9 ^{high} /CXCR3 ^{low}	47.2%	76/161
CXCL10 ^{high} /CXCR3 ^{high} or CXCL10 ^{low} /CXCR3 ^{low}	39.0%	62/159
CXCL10 ^{low} /CXCR3 ^{high}	10.1%	16/159
CXCL10 ^{high} /CXCR3 ^{low}	50.9%	81/159

The univariate analysis demonstrated that a tumor CXCR3 overexpression and a simultaneous low CXCL9 expression was associated with a worse overall and progression-free survival (PFS: HR 4.55, 95% CI 1.75-11.83, $p=0.002$; OS: HR 2.12, 95% CI 1.07-4.20, $p=0.031$). Patients whose tumors expressed low CXCR3 and high CXCL9 or CXCL10 had the longest overall survival (CXCL9: HR 0.49, 95% CI 0.34-0.71, $p=0.001$; CXCL10: HR 0.45, 95% CI 0.31-0.65, $p<0.001$). An either double high expression or a double low expression of both CXCL9 and CXCR3 was correlated with an intermediate progression-free and overall survival. In contrast to the CXCL9 findings, the progression-free and overall survival time was barely different for patients whose tumors had an either double high expression or a double low expression of both CXCL10 and receptor or a tumor CXCR3 overexpression and a simultaneous low CXCL10 expression. (Table 30).

Table 30: Median progression-free and overall survival in relation to CXCR3 and CXCL9 or CXCL10 (combined cohorts) – univariate analysis

Median progression-free survival				
Variable	Median (months)	hazard ratio	95% C.I.	p-value
CXCL9 ^{high} /CXCR3 ^{high} or CXCL9 ^{low} /CXCR3 ^{low}	14 ± 0.51	1		0.001
CXCL9 ^{low} /CXCR3 ^{high}	4 ± 1.84	4.55	1.75-11.83	0.002
CXCL9 ^{high} /CXCR3 ^{low}	20 ± 2.40	0.73	0.50-1.06	0.098
Median overall survival				
Variable	Median (months)	hazard ratio	95% C.I.	p-value
CXCL10 ^{high} /CXCR3 ^{high} or CXCL10 ^{low} /CXCR3 ^{low}	13 ± 1.21	1		0.019
CXCL10 ^{low} /CXCR3 ^{high}	14 ± 3.91	1.47	0.75-2.86	0.262
CXCL10 ^{high} /CXCR3 ^{low}	21 ± 1.97	0.66	0.44-0.97	0.035
Median overall survival				
Variable	Median (months)	hazard ratio	95% C.I.	p-value
CXCL9 ^{high} /CXCR3 ^{high} or CXCL9 ^{low} /CXCR3 ^{low}	29 ± 5.72	1		<0.001
CXCL9 ^{low} /CXCR3 ^{high}	19 ± 3.85	2.12	1.07-4.20	0.031
CXCL9 ^{high} /CXCR3 ^{low}	58 ± 4.78	0.49	0.34-0.71	<0.001
CXCL10 ^{high} /CXCR3 ^{high} or CXCL10 ^{low} /CXCR3 ^{low}	24 ± 6.10	1		<0.001
CXCL10 ^{low} /CXCR3 ^{high}	22 ± 10.18	1.11	0.60-2.08	0.739
CXCL10 ^{high} /CXCR3 ^{low}	52 ± 4.76	0.45	0.31-0.65	<0.001

The Kaplan-Meier estimate shown in Figure 21 also suggests that the poor outcome from an CXCR3 overexpression can be compensated by a simultaneous high expression of CXCL9. Tumors that express both ligands and receptor either at a high or at a low level show an intermediate survival. For CXCL10, this compensation is not as effective as for CXCL9. The best outcome had patients whose tumors express CXCL10^{high} and CXCR3^{low}.

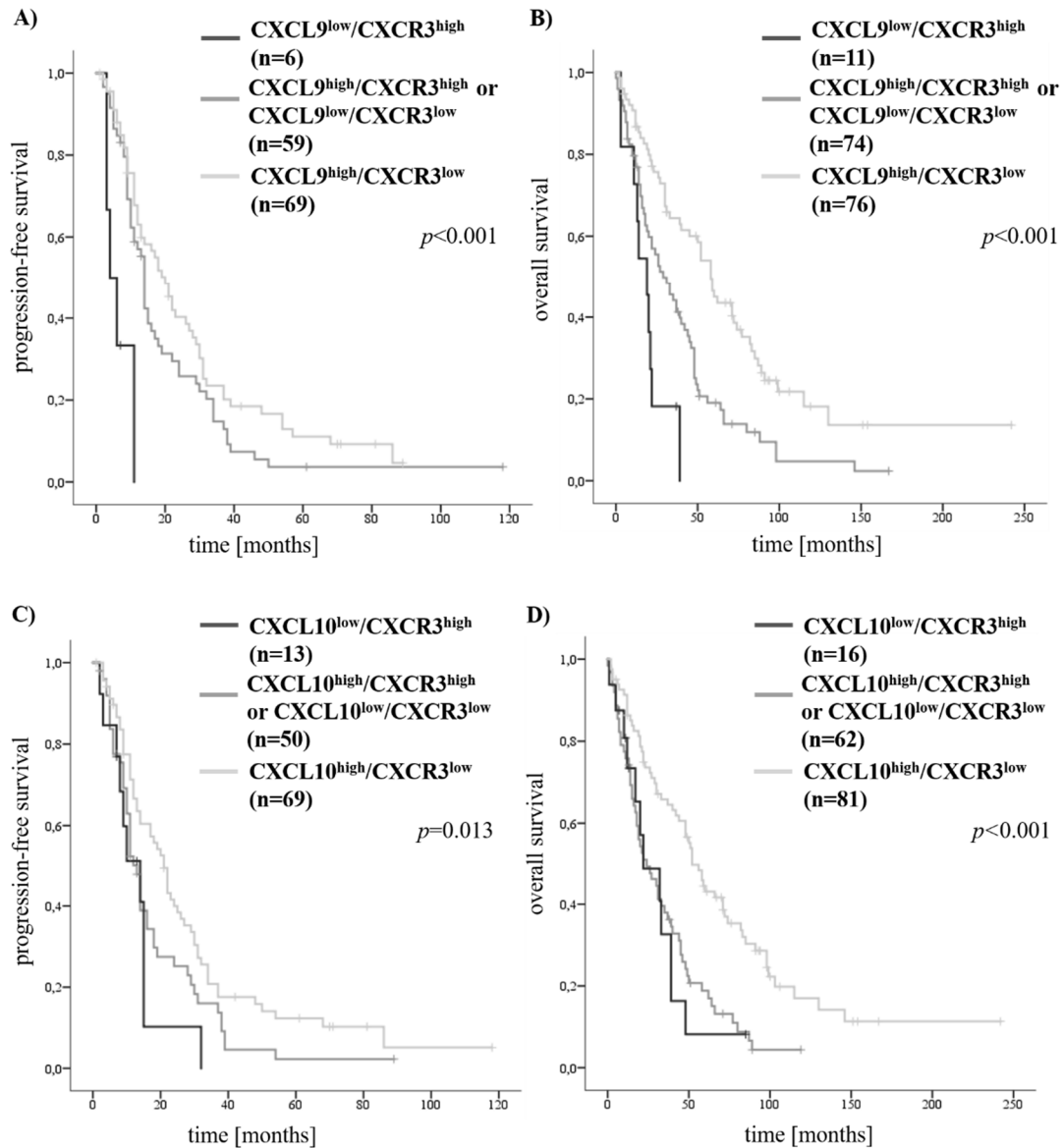


Figure 21: Prognostic significance of combined CXCR3 and CXCL9 or CXCL10 expression in high-grade serous ovarian cancer (combined collectives)

Shown are Kaplan-Meier curves for **A)** progression-free survival and **B)** overall survival comparing tumors that either express low CXCL9 and high CXCR3 (purple line), both high CXCL9 and CXCR3 or both low CXCL9 and CXCR3 (green line) and high CXCL9 and low CXCR3 (blue line) and for **C)** progression-free survival and **D)** overall survival comparing tumors that either express low CXCL10 and high CXCR3 (purple line), both high CXCL10 and CXCR3 or both low CXCL10 and CXCR3 (green line) and high CXCL10 and low CXCR3 (blue line). Time is given in months, statistical significance (p -value) is stated (log rank).

The CXCR3 overexpression and a simultaneous low CXCL9 expression could be identified as an independent marker for a poor progression-free and overall survival in high-grade serous ovarian cancer in a multivariate analysis using a COX proportional hazard model, including postsurgical residual tumor mass and lymph node metastasis as covariates (PFS: HR 6.78, 95% CI 2.44-18.80, $p < 0.001$; OS: HR 2.18, 95% CI 1.08-

4.38, $p < 0.001$). A high CXCL9 or CXCL10 expression seemed to compensate the poor outcome of the high receptor expression, leading to intermediate survival times. However, for the combined CXCL10 and CXCR3 expression, no association with the progression-free survival was possible. For the overall survival, a high CXCL10 and a concomitantly low CXCR3 expression was correlated with the best outcome (HR 0.50, 95% CI 0.33-0.77, $p = 0.001$) (Table 31).

Table 31: Cox multivariate analysis for the progression-free and overall survival (combined cohorts)

Residual tumor below 1 cm is defined as 'optimal', residual tumor above 1 cm is defined as 'suboptimal'.

Median progression-free survival				
Variable	n	hazard ratio	95% C.I.	p-value
CXCL9 ^{high} /CXCR3 ^{high} or CXCL9 ^{low} /CXCR3 ^{low}	45	1		<0.001
CXCL9 ^{low} /CXCR3 ^{high}	6	6.78	2.44-18.80	<0.001
CXCL9 ^{high} /CXCR3 ^{low}	62	0.88	0.57-1.34	0.546
Postsurgical residual tumor				
optimal	44	1		
suboptimal	69	2.72	1.75-4.25	<0.001
Nodal status				
pN0	38	1		
pN1	75	1.08	0.70-1.67	0.720
<hr/>				
CXCL10 ^{high} /CXCR3 ^{high} or CXCL10 ^{low} /CXCR3 ^{low}	40	1		0.125
CXCL10 ^{low} /CXCR3 ^{high}	10	1.71	0.78-3.78	0.182
CXCL10 ^{high} /CXCR3 ^{low}	63	0.78	0.50-1.23	0.279
Postsurgical residual tumor				
optimal	45	1		
suboptimal	68	2.58	1.64-4.04	<0.001
Nodal status				
pN0	39	1		
pN1	74	1.08	0.69-1.68	0.736

Median overall survival				
Variable	n	hazard ratio	95% C.I.	p-value
CXCL9 ^{high} /CXCR3 ^{high} or CXCL9 ^{low} /CXCR3 ^{low}	58	1		<0.001
CXCL9 ^{low} /CXCR3 ^{high}	11	2.18	1.08-4.38	0.030
CXCL9 ^{high} /CXCR3 ^{low}	69	0.56	0.37-0.85	0.006
Postsurgical residual tumor				
optimal	51	1		
suboptimal	87	3.24	2.08-5.04	<0.001
Nodal status				
pN0	46	1		
pN1	92	0.89	0.60-1.34	0.589
CXCL10 ^{high} /CXCR3 ^{high} or CXCL10 ^{low} /CXCR3 ^{low}	51	1		0.003
CXCL10 ^{low} /CXCR3 ^{high}	12	1.14	0.55-2.35	0.730
CXCL10 ^{high} /CXCR3 ^{low}	75	0.50	0.33-0.77	0.001
Postsurgical residual tumor				
optimal	51	1		
suboptimal	87	2.79	1.81-4.32	<0.001
Nodal status				
pN0	47	1		
pN1	91	0.75	0.50-1.12	0.158

2. Expression and function of CXCR3 in ovarian cancer cell lines

2.1. CXCR3 expression in human ovarian cancer cell lines

CXCR3 expression in the wildtype cell lines SKOV-3 and OVCAR-3 was examined by western blot and flow cytometry. For western blot analysis, the cells were seeded, left untreated and were lysed after they had reached a 70% confluence. Equal amounts of proteins were loaded to a SDS-gel and lysates were separated by gel electrophoresis. By using a semi-dry western blot chamber the proteins were transferred to a nitrocellulose membrane. Immunostaining with the anti-CXCR3 antibody revealed the expression of the receptor CXCR3 in both cell lines (Figure 22). The monoclonal antibody detects a domain that is shared by both CXCR3 isoforms. Hence, it cannot distinguish between the splice variants CXCR3-A and CXCR3-B, but due to the

different protein sizes, the two splice variants are detectable on the western blot membrane. The wildtype cell lines SKOV-3 and OVCAR-3 express both isoforms of the receptor CXCR3. As endogenous control the membrane was stained for the housekeeping gene α -tubulin (Figure 22).

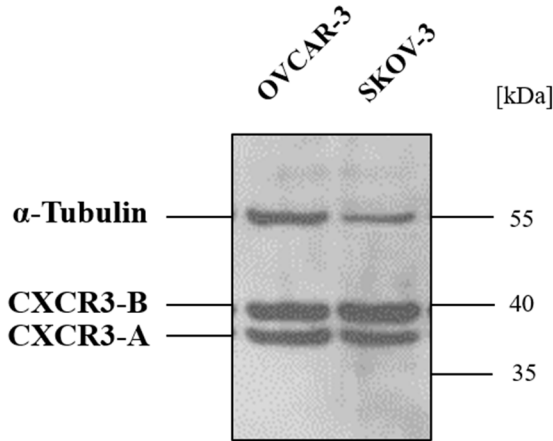


Figure 22: Protein expression of CXCR3 in SKOV-3 and OVCAR-3 cells

Western blot with lysates from OVCAR-3 cells (left lane) and SKOV-3 cells (right lane) immunostained with CXCR3 antibody and α -tubulin antibody as endogenous control

To further confirm the expression of CXCR3 in SKOV-3 and OVCAR-3 cells, the cells were immunostained with the anti-CXCR3 antibody or with an isotype control antibody, followed by an Alexa488 conjugate and analyzed by flow cytometry (Figure 23). The expression of surface CXCR3 in both ovarian cancer cell lines could be confirmed. As explained above, the anti-CXCR3 antibody cannot distinguish between the receptor splice variants and therefore the different isoforms are not detectable by flow cytometry.

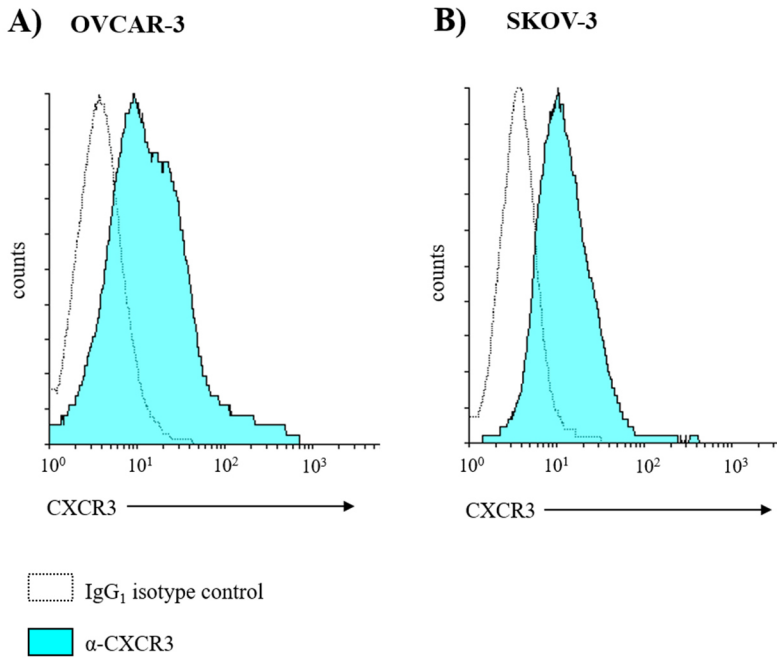


Figure 23: FACS analysis of wildtype OVCAR-3 and SKOV-3 cells

Cells were immunostained with either α -CXCR3 antibody (turquoise, right curve) or with IgG₁ isotype control (white, dotted line, left curve), both followed by an Alexa488 conjugate. Expression of CXCR3 in **A) OVCAR-3** cells and **B) SKOV-3** cells was measured by flow cytometry.

2.2. Proliferation of ovarian cancer cells upon chemokine stimulation

The impact of CXCL9 and CXCL10 stimulation on SKOV-3 and OVCAR-3 cell proliferation was analyzed by manual counting. Therefore, the cells were seeded in triplicates in 24-well plates for different time points. The cells were starved the next day with serum-free medium for 6 h and subsequently stimulated with either 100 ng/ml rhCXCL9, 100 ng/ml rhCXCL10 or 0.1% BSA/PBS as a control. 24 h, 48 h and 72 h post-stimulation the cells were detached with trypsin and counted manually in a Neubauer counting chamber using trypan blue solution. None of the chemokines had a significant effect on the proliferation of both OVCAR-3 and SKOV-3 cells (Figure 24).

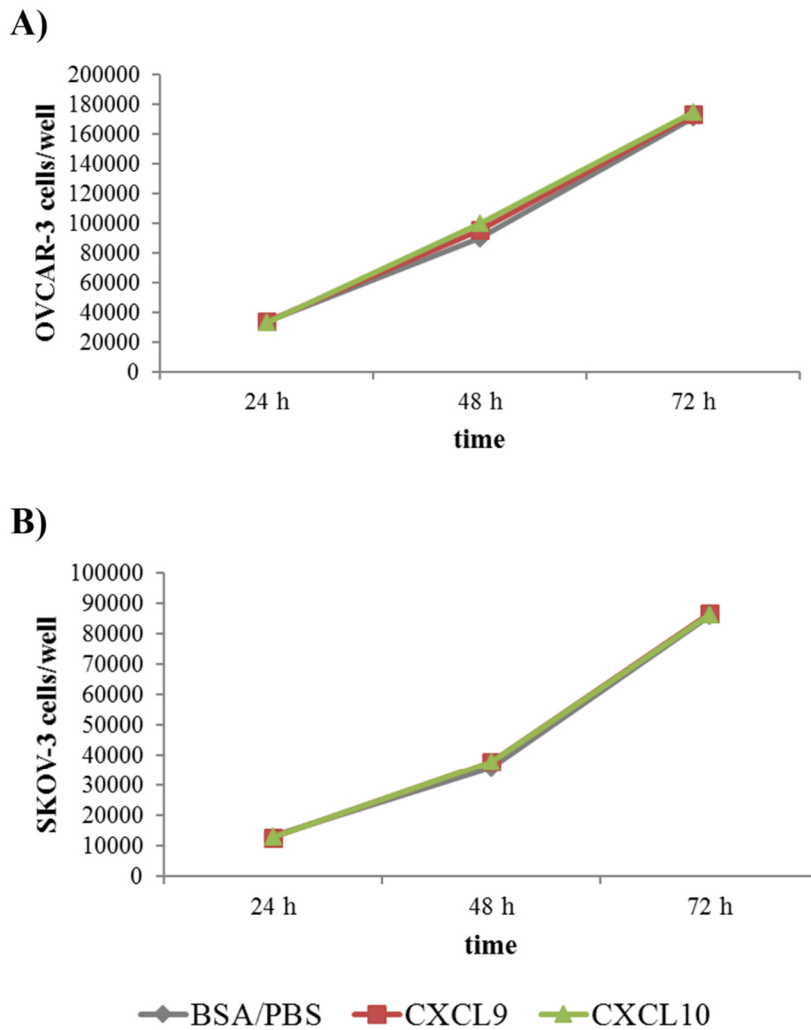


Figure 24: Proliferation of OVCAR-3 and SKOV-3 cells stimulated with chemokines

A) OVCAR-3 cells or **B)** SKOV-3 cells were stimulated with either 0.1% BSA/PBS as a control (grey line), 100 ng/ml rh-CXCL9 (red line) or 100 ng/ml rh-CXCL10 (green line). 24 h, 48 h and 72 h after stimulation proliferation was analyzed by manually counting cells.

2.3. Migration of ovarian cancer cells towards chemoattractants

To determine if the receptor CXCR3 is functionally active in human ovarian cancer cells, it was tested if chemoattraction by chemokine ligands causes migration. To this end, SKOV-3 and OVCAR-3 cells were seeded in the upper chamber of Transwell® inserts and placed in 24-well assay plates. After treatment with 1 µg/ml of either anti-CXCR3 antibody or IgG₁ isotype control antibody for 30 min, the chemoattractant was added to the lower chambers of the assay plate, either 40 ng/ml rhCXCL9 or 0.1% BSA/PBS as a control. After four hours of migration, the insert membranes were washed, fixed and stained and migrated cells were counted as described in Material

and Methods. The number of migrated cells was normalized to that of OVCAR-3 or SKOV-3 cells treated with IgG₁ isotype control which migrated towards 0.1% BSA/PBS, as this was regarded as the non-directed random baseline migration. As can be seen in Figure 25, both OVCAR-3 and SKOV-3 cells migrated towards the chemoattractant rh-CXCL9 in a statistical significant manner compared to the baseline migration ($p=0.013$ for OVCAR-3; $p=0.002$ for SKOV-3). The use of the anti-CXCR3 antibody completely blocked this movement and decreased the migration rate even below the baseline value ($p=0.006$ for OVCAR-3; $p=0.0001$ for SKOV-3).

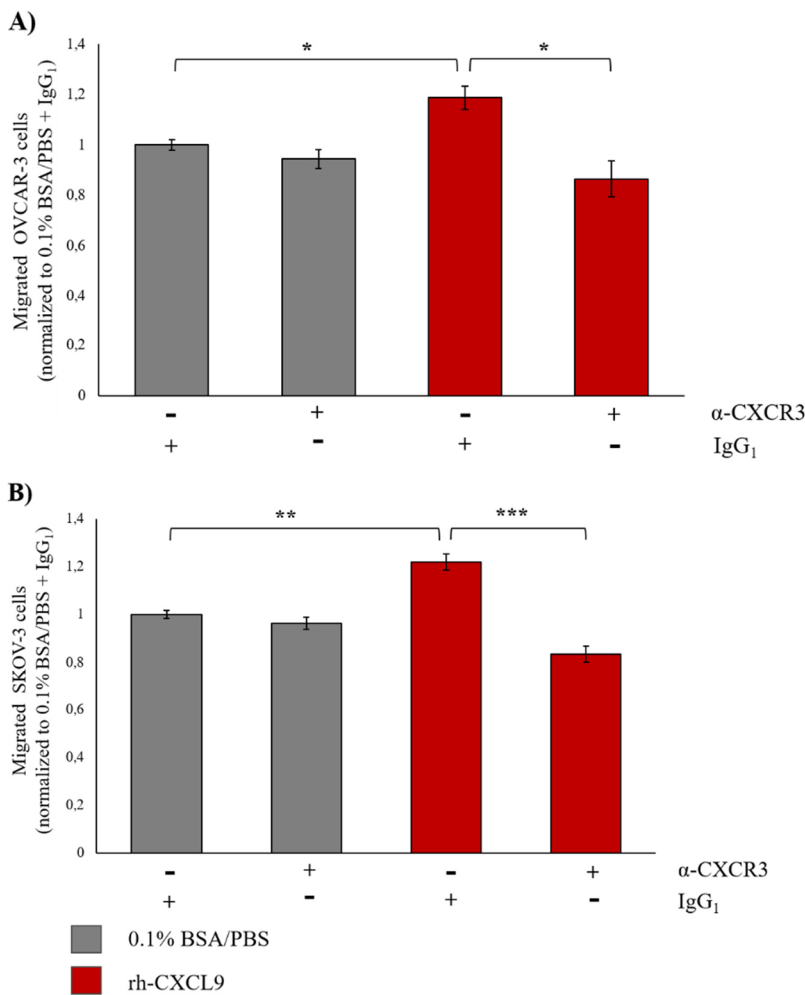


Figure 25: Migration of OVCAR-3 and SKOV-3 cells towards CXCL9

A) OVCAR-3 and B) SKOV-3 cells employ the receptor CXCR3 for migration towards the chemokine ligand CXCL9. Cells were either treated with α -CXCR3 (marked with '+') or with IgG₁ isotype control (marked with '-') and migrated towards 0.1% BSA/PBS (grey bars) as control or towards rh-CXCL9 (red bars). The number of migrated cells was normalized to the baseline migration observed from migration of control IgG₁ treated cells towards 0.1% BSA/PBS. Statistical significance was calculated and defined as * $p \leq 0.05$, ** $p \leq 0.005$, or *** $p \leq 0.001$.

To determine whether the suppression of migration upon antibody treatment was specific to chemokine ligand and receptor interaction, a migration assay with anti-

CXCR3 or IgG₁ treated cells and FCS as chemoattractant was performed. Both OVCAR-3 and SKOV-3 cells migrated rather unspecific towards FCS, but this migration could not be blocked by the use of the α -CXCR3 antibody (Figure 26).

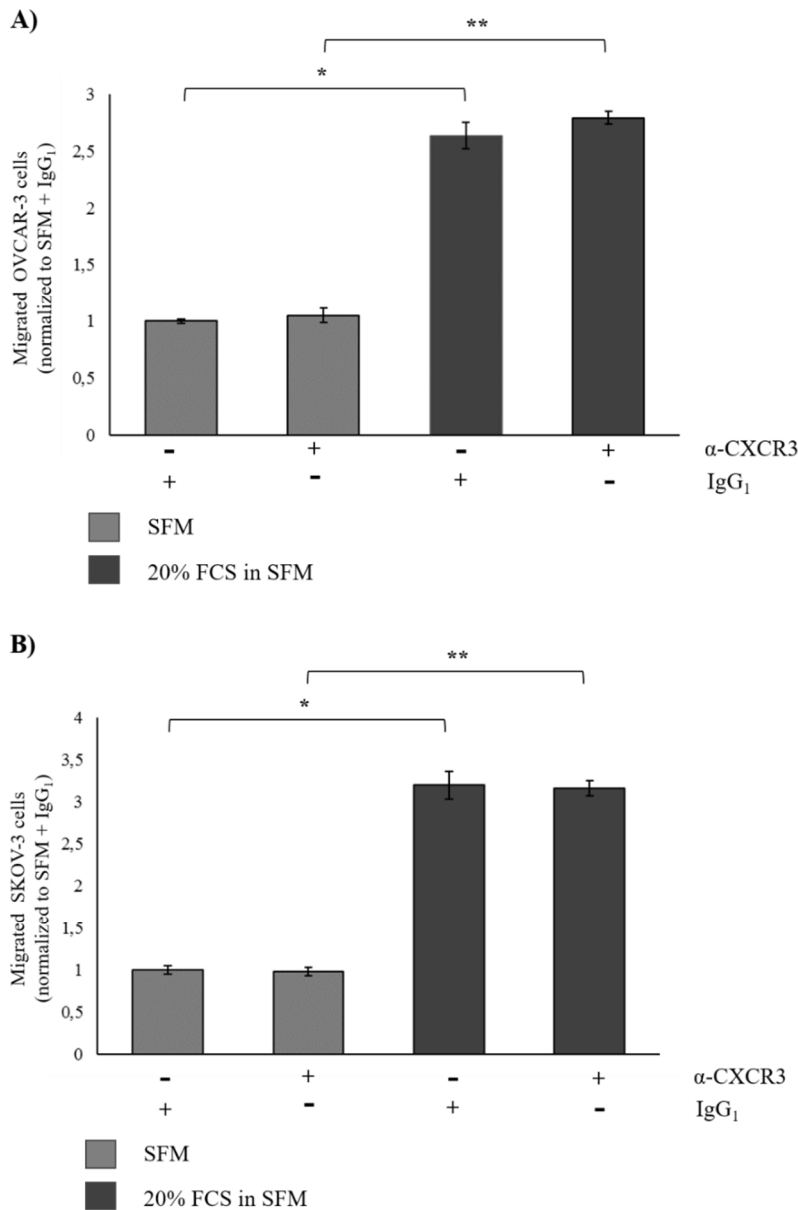
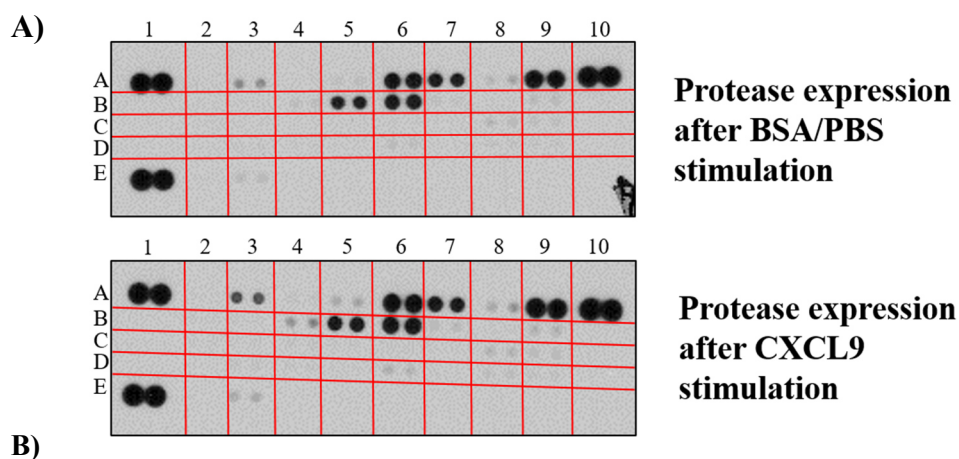


Figure 26: Migration of OVCAR-3 and SKOV-3 cells towards FCS

The migration of **A)** OVCAR-3 and **B)** SKOV-3 cells towards FCS is not dependent on CXCR3. Cells were either treated with α -CXCR3 (marked with '+') or with IgG₁ isotype control (marked with '+') and migrated towards serum-free medium (grey bars) as control or towards FCS (dark grey bars). The number of migrated cells was normalized to the baseline migration observed from migration of control IgG₁ treated cells towards serum-free medium. Statistical significance was calculated and defined as * $p \leq 0.05$, ** $p \leq 0.005$, or *** $p \leq 0.001$.

2.4. Protease expression upon chemokine stimulation

To investigate if a higher protease expression upon CXCR3 activation plays a role for the poor outcome of CXCR3 overexpression in serous ovarian cancer cells, the protease expression levels upon chemokine stimulation were determined. Therefore, the Proteome Profiler Human Protease Array Kit was used. Cell lysates were generated by seeding $5 \cdot 10^5$ OVCAR-3 cells in cell culture dishes, starving them the next day and stimulating them 24 h later with either 100 ng/ μ l rhCXCL9 or 0.1% BSA/PBS as a control. 48 h post-stimulation, cells were solubilized in protease array lysis buffer. 200 μ g lysate per array were assayed immediately according to the manufacturer's instructions. The cell's protease expression pattern can be visualized as dark spots on an X-ray film.



B)

A1	Reference spot	B2	Cathepsin E	C4	Kallikrein 10	D6	MMP-13
A2	ADAM8	B3	Cathepsin L	C5	Kallikrein 11	D7	Neprilysin / CD10
A3	ADAM9	B4	Cathepsin S	C6	Kallikrein 13	D8	Presenilin-1
A4	ADAMTS1	B5	Cathepsin V	C7	MMP-1	D9	Proprotein Convertase 9
A5	ADAMTS13	B6	Cathepsin X/Z/P	C8	MMP-2	E1	Reference spot
A6	Cathepsin A	B7	DPPIV / CD26	C9	MMP-3	E2	Proteinase 3
A7	Cathepsin B	B8	Kallikrein 3 / PSA	D2	MMP-7	E3	uPA / Urokinase
A8	Cathepsin C	B9	Kallikrein 5	D3	MMP-8	E4	Negative control
A9	Cathepsin D	C2	Kallikrein 6	D4	MMP-9		
A10	Reference spot	C3	Kallikrein 7	D5	MMP-12		

Figure 27: Protease Array

A) Protease expression pattern shown for OVCAR-3 cells stimulated with 0.1% BSA/PBS (upper panel) as control or with 100 ng/ μ l rhCXCL9 (lower panel). Darker spots indicating higher expression levels are marked by numbers and explained in the table **B)**.

The OVCAR-3 cells express mostly cathepsins and MMPs. After stimulation with CXCL9, some spots were darker compared to the control stimulation with 0.1% BSA/PBS. A densitometric evaluation revealed a darker staining of the spots A3, A5, B4, B9, C8, C9, D6, D8, D9 upon CXCL9 stimulation, referring to an upregulation of the proteases ADAM9, ADAMTS13, Cathepsin S, Kallikrein 5, MMP-2, MMP-3, MMP-13, Presenilin-1 and Proprotein Convertase 9 (Table 32).

Table 32: Upregulation of proteases upon CXCL9 stimulation

Protease	x-fold higher expression upon chemokine stimulation
ADAM9	3,3
ADAMTS13	2,9
Cathepsin S	5,0
Kallikrein 5	2,3
MMP-2	1,2
MMP-3	1,3
MMP-13	1,7
Presenilin-1	1,7
Proprotein Convertase 9	1,4

3. Expression and function of CXCR3, CXCL9 and CXCL10 in ascites

3.1. Chemokine ligand concentrations in ovarian cancer ascites

The poor outcome of a CXCR3 overexpression in ovarian tumors could be due to an enhanced peritoneal metastasis. Mediators of tumor cell migration are expected to be present in ascitic fluid. Therefore, the CXCL9 and CXCL10 concentrations in human ascites samples were measured. At first the total protein concentration in 166 ascites samples from patients with ovarian cancer were quantified using the Pierce™ BCA Protein Assay Kit. To determine the absolute and relative CXCL9 and CXCL10 concentrations enzyme-linked immunosorbent assays were performed, using the R&D DuoSet® Human CXCL9/MIG or DuoSet® Human CXCL10/IP10, respectively. From

these 166 ascites samples, only 102 were derived from patients with high-grade serous ovarian carcinoma (FIGO III and FIGO IV), so only these 102 samples were taken into further consideration. The mean protein concentrations were 44.69 mg/ml total protein, 1480.60 pg/ml CXCL9 (median 1177.54 pg/ml) and 1117.00 pg/ml CXCL10 (median 1142.90 pg/ml). The average ratio of CXCL9/total protein was 34.43 pg/mg (median 27.21 pg/mg) and the average ratio of CXCL10/total protein was 25.60 pg/mg (median 25.43 pg/mg).

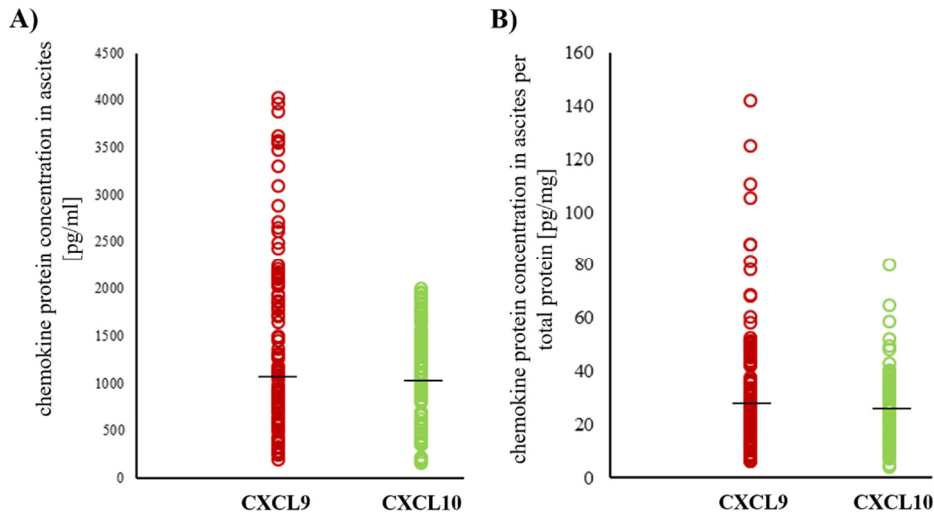


Figure 28: Chemokine concentrations in ascites from human serous ovarian cancer patients

ELISA data for CXCL9 (red dots) and CXCL10 (green dots) in 102 ascites samples. **A)** Absolute chemokine protein concentration in ascites. **B)** Relative chemokine concentrations per total protein in ascites. Horizontal bars represent median values.

To analyze the relationship between the two chemokine ligands CXCL9 and CXCL10 in human ovarian ascites the nonparametric Spearman's rank correlation was used. Moderate, but significant correlations were found between the absolute protein levels of CXCL9 and CXCL10 ($p < 0.001$), as well as between the relative chemokine levels per total protein of both ligands ($p < 0.001$) (Table 33).

Table 33: Correlations between CXCL9 and CXCL10 present in ascites

Shown is Spearman correlation coefficient and statistical significance (p) between the two chemokines and between the ratios chemokine/total protein

	CXCL9	CXCL9/total protein
CXCL10	0.62 ($p < 0.001$)	
CXCL10/total protein		0.56 ($p < 0.001$)

3.2. Correlation of chemokine concentrations in ascites with residual tumor

To determine whether a high chemokine ligand concentration in ascites is correlated with a suboptimal operable high number of peritoneal metastases, a multivariate analysis using a COX proportional hazard model including postsurgical residual tumor mass and either CXCL9 or CXCL10 expression as covariates was used. Both for overall survival and progression-free survival no association between the chemokine expression levels and survival was found. Only the postsurgical residual tumor mass was statistically significant associated with a better (R0) or worse (R1-R2) progression-free and overall survival (Table 34).

Table 34: Cox multivariate analysis for the progression-free and overall survival

Correlation between expression of CXCL9 or CXCL10 and residual tumor mass with progression-free and overall survival. No residual tumor is R0, residual tumor below 1 cm is R1, residual tumor above 1 cm is R2.

Median progression-free survival				
Variable	<i>n</i>	hazard ratio	95% C.I.	<i>p</i>-value
CXCL9 expression				
low	50	1		
high	51	1.21	0.76-1.94	0.419
Postsurgical residual tumor				
R0	23	1		0.004
R1	50	3.28	1.61-6.65	0.001
R2	28	2.94	1.38-6.28	0.005
CXCL10 expression				
low	51	1		
high	50	0.97	0.62-1.54	0.919
Postsurgical residual tumor				
R0	23	1		0.003
R1	50	3.38	1.67-6.82	0.001
R2	28	3.00	1.41-6.38	0.004

Median overall survival				
Variable	n	hazard ratio	95% C.I.	p-value
CXCL9 expression				
low	50	1		
high	51	1.16	0.73-1.85	0.522
Postsurgical residual tumor				
R0	23	1		0.005
R1	50	3.09	1.52-6.26	0.002
R2	28	3.14	1.45-6.79	0.004
CXCL10 expression				
low	51	1		
high	50	0.81	0.51-1.27	0.358
Postsurgical residual tumor				
R0	23	1		0.004
R1	50	3.18	1.58-6.40	0.001
R2	28	3.18	1.47-6.89	0.003

3.3. Migration of ovarian cancer cell lines towards ascites

The presence of CXCL9 and CXCL10 in ascitic fluid may indicate that these chemokines serve as migratory attractors of ovarian cancer cells *in vivo*. This would further explain the overexpression of the receptor CXCR3 at the invasive front of tumor cells. To analyze the migratory behavior of ovarian cancer cells towards ascitic fluid *in vitro*, SKOV-3 and OVCAR-3 cells were deployed in migration assays with ascites as chemoattractant. The cells were seeded in the upper chamber of Transwell® inserts, placed in 24-well assay plates and treated with either 1 µg/ml CXCR3 antibody or with IgG₁ isotype control antibody for 30 min. Subsequently either ascitic fluid or serum-free culture medium as chemoattractant was added to the lower chambers of the assay plate. After four hours of migration, the insert membranes were washed, fixed and stained and migrated cells were counted. The number of migrated cells was normalized to that of OVCAR-3 or SKOV-3 cells treated with IgG₁ isotype control which migrated towards serum-free culture medium, as this was regarded as the non-directed random baseline migration.

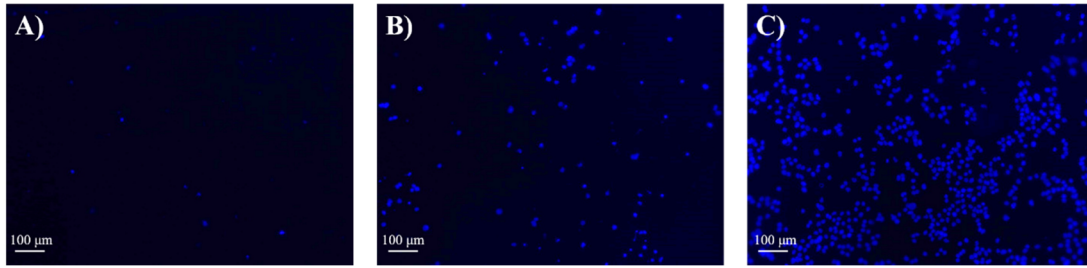


Figure 29: Microscopic evaluation of migration

OVCAR-3 migrated towards different chemoattractants. **A)** OVCAR-3 with IgG₁ towards serum-free medium, **B)** OVCAR-3 with α -CXCR3 towards ascitic fluid and **C)** OVCAR-3 with IgG₁ towards ascitic fluid.

Randomly ten different ascites samples with different chemokine concentrations were chosen out of the analyzed ascites samples from patients with serous ovarian cancer from chapter 3.1. Two samples had a low, one a moderate and seven a high chemokine concentration (Table 35).

Table 35: Ascites samples for migration assays

10 different ascites samples were used for migration assays. Shown are the absolute concentrations of CXCL9 and CXCL10 and the relative concentrations of chemokine per total protein, as well as the chemokine expression grade.

ascites sample	CXCL9 [pg/ml]	CXCL9/total protein [pg/mg]	CXCL10 [pg/ml]	CXCL10/total protein [pg/mg]	chemokine expression grade
#1	284.53	6.88	125.96	3.05	low
#2	250.15	7.13	184.80	5.27	low
#3	1308.88	25.28	828.59	16.01	moderate
#4	4032.48	78.38	1900.96	36.95	high
#5	3557.94	110.43	1894.46	58.80	high
#6	3421.63	61.50	1798.94	32.33	high
#7	2656.95	52.45	1706.02	33.68	high
#8	3624.94	52.38	1771.58	25.60	high
#9	2619.87	50.31	1762.53	33.85	high
#10	2888.87	48.81	1764.59	29.82	high

Both OVCAR-3 and SKOV-3 cells migrated towards the ten different ascites samples in a statistical significant manner compared to the baseline migration. With few exceptions, the ascites samples with high chemokine concentrations worked more effective as chemoattractants as the samples with only low or moderate concentrations. The anti-CXCR3 antibody blocked the movement towards ascites and decreased the migration rate in all but one sample (Figure 30 and 31).

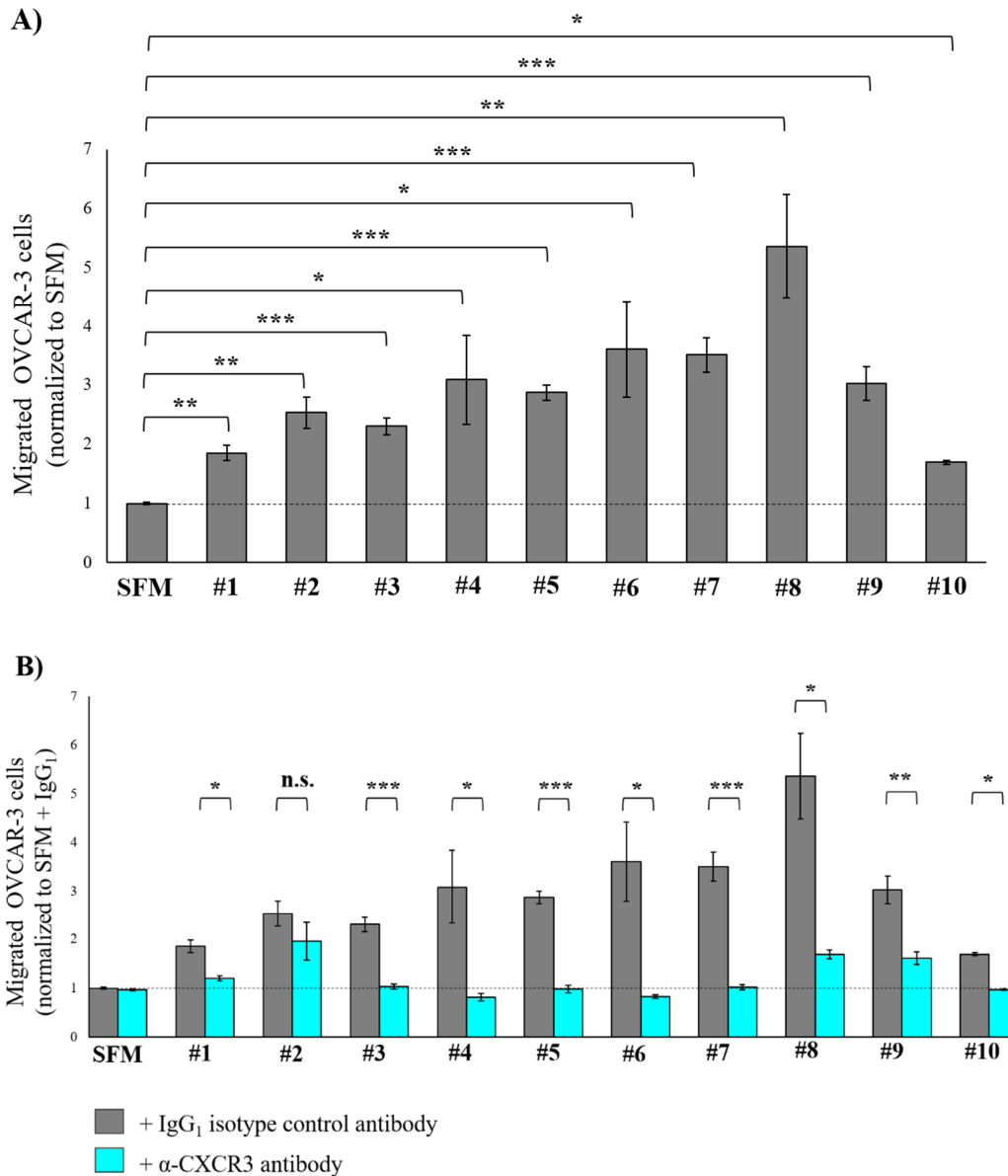


Figure 30: Migration of OVCAR-3 cells towards human ascites

A) OVCAR-3 cells migrated towards ten different ascites samples or serum-free medium as a control. **B)** Migration of OVCAR-3 cells treated with either α -CXCR3 (turquoise bars) or IgG₁ isotype control antibody (grey bars) towards ten different ascites samples or serum-free medium as a control. Statistical significance was calculated and defined as * $p \leq 0.05$, ** $p \leq 0.005$, or *** $p \leq 0.001$.

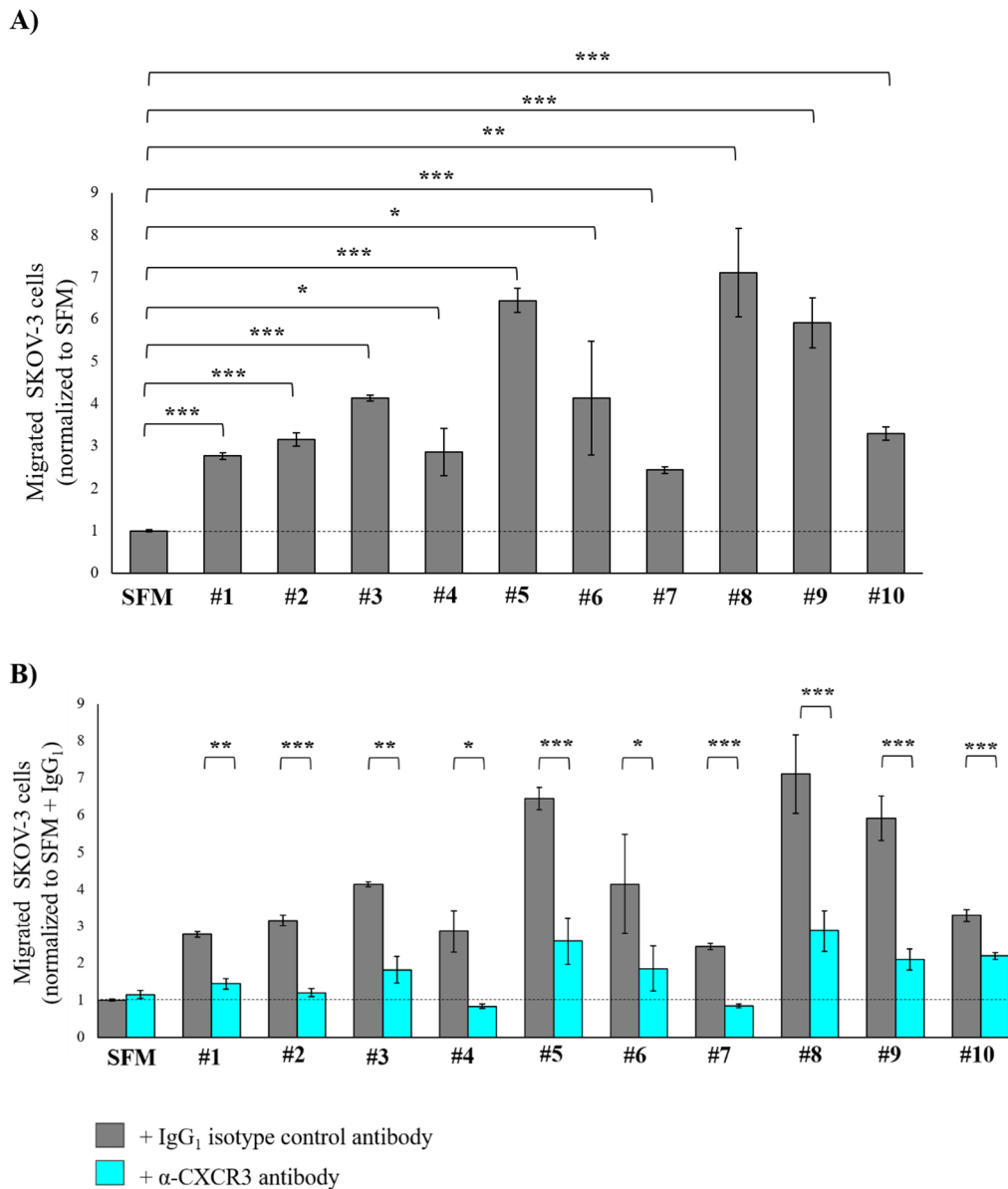


Figure 31: Migration of SKOV-3 cells towards human ascites

A) SKOV-3 cells migrated towards ten different ascites samples or serum-free medium as a control.

B) Migration of SKOV-3 cells treated with either α-CXCR3 (turquoise bars) or IgG₁ isotype control antibody (grey bars) towards ten different ascites samples or serum-free medium as a control. Statistical significance was calculated and defined as * $p \leq 0.05$, ** $p \leq 0.005$, or *** $p \leq 0.001$.

3.4. CXCR3 in primary epithelial ovarian cancer cells

Epithelial ovarian cancer (EOC) cells were isolated from ascites of patients with ovarian cancer as described in material and methods. By means of the protocol all successful isolated growing cells are tumor cells, the chance of a fibroblast contamination is very low and was excluded morphologically. The isolation process was successful in four out of six cases. One cell line, EOC #6, stopped growing after

several passages. The cells were examined by microscopy and were morphologically identified as tumor cells (Figure 32).

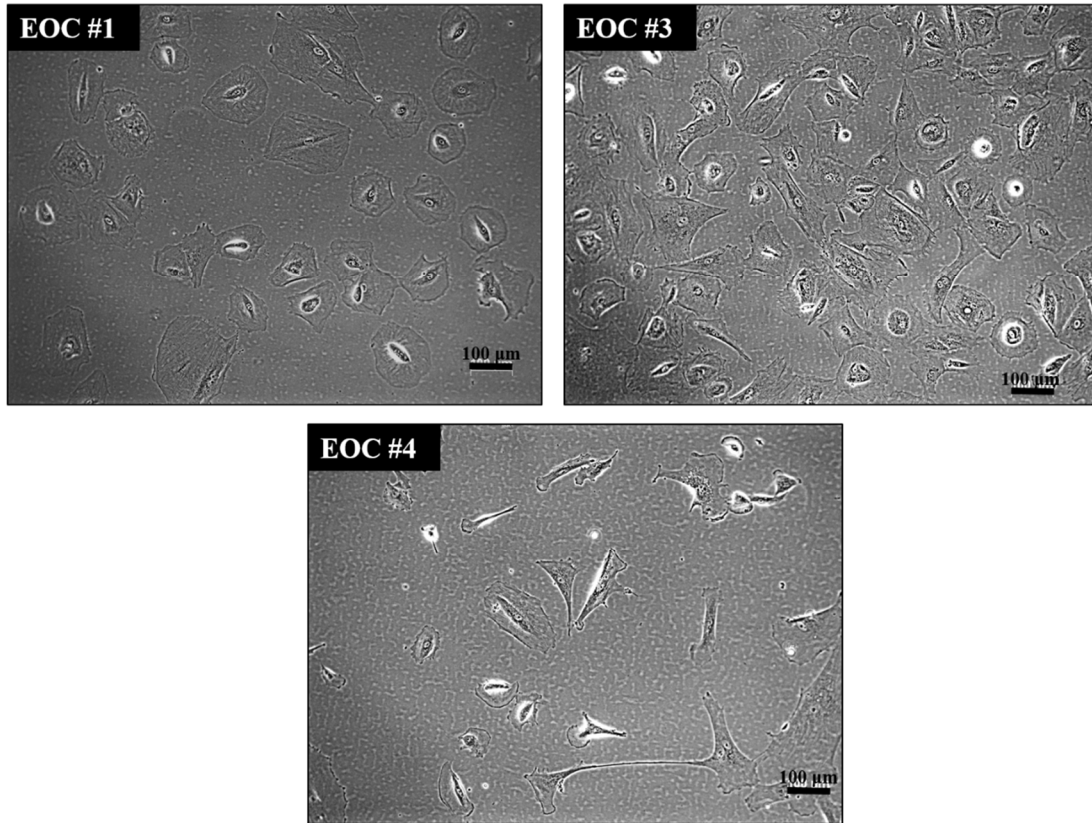


Figure 32: Primary epithelial ovarian cancer cells

Epithelial ovarian cancer cells were isolated from ascitic fluid from ovarian cancer patients. The isolation was successful in four out of six cases. EOC #6 stopped growing after several passages, so that it was not possible to generate an image of the living cells.

To analyze the migratory capacity of the EOC cells, the four different EOC cells were subjected to migration assays. As chemoattractant the stored ascitic fluid out of which the cells were isolated was used. For the assay, the cells were seeded in the upper chamber of Transwell® inserts, placed in 24-well assay plates® and treated with 1 µg/ml of either anti-CXCR3 antibody or IgG₁ isotype control antibody for 30 min. Subsequently the ascitic fluid was added to the lower chambers of the assay plate, or serum-free medium as a control. After four hours of migration, the insert membranes were washed, fixed and stained and migrated cells were counted. The number of migrated cells was normalized to that of EOC cells treated with IgG₁ isotype control which migrated towards serum-free medium, as this was the non-directed random baseline migration. Both EOC #1 and EOC #3 cells migrated towards ascites in a statistical significant manner compared to the baseline migration ($p=0.002$ for

EOC #1; $p=0.022$ for EOC #3). The use of the anti-CXCR3 antibody reduced the movement of EOC #3 cells and completely blocked EOC #1 cell migration ($p=0.028$ for EOC #1; $p=0.038$ for EOC #3). The cells EOC #4 and EOC #6 did not migrate towards ascites, so the antibody also had no impact on migration.

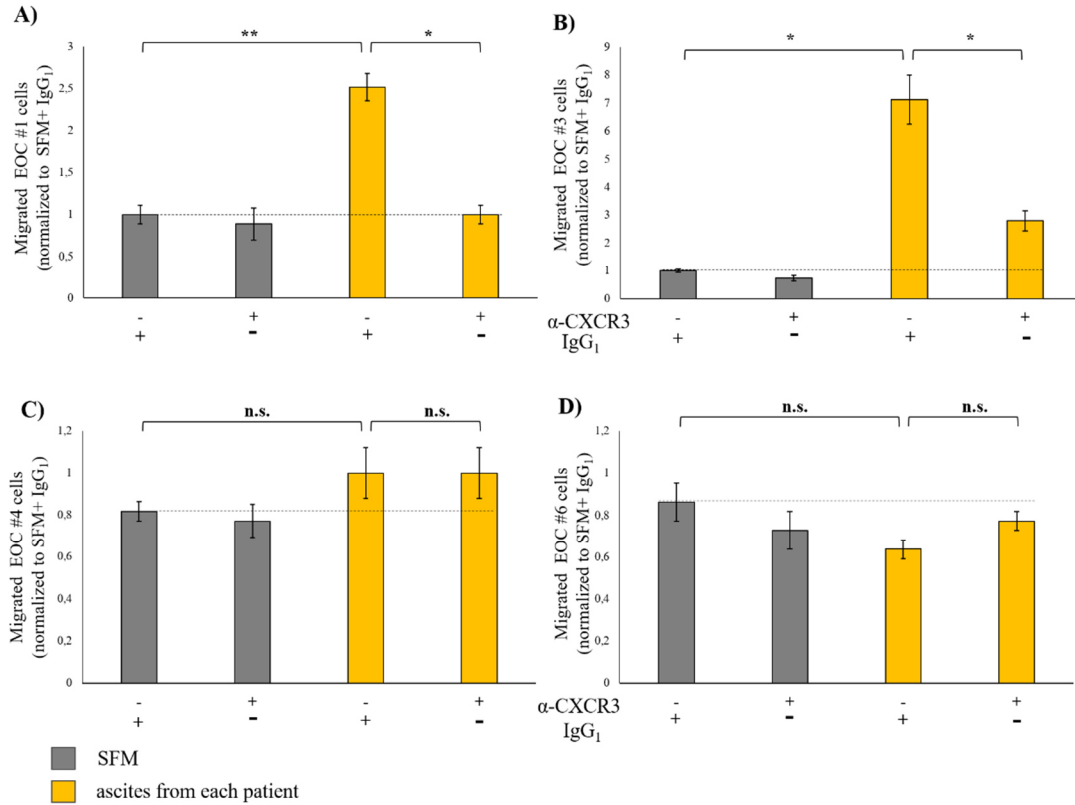


Figure 33: Migration of EOC cells towards ascites

Migration of **A)** EOC #1, **B)** EOC #3, **C)** EOC #4 and **D)** EOC #6 towards the ascitic fluid they were originally isolated from. Cells were either treated with α -CXCR3 (marked with '+') or with IgG₁ isotype control (marked with '+') and migrated towards serum-free medium (grey bars) as control or towards ascites from each patient (yellow bars). The number of migrated cells was normalized to the baseline migration observed from migration of control IgG₁ treated cells towards serum-free medium. Statistical significance was calculated and defined as * $p \leq 0.05$, ** $p \leq 0.005$, or *** $p \leq 0.001$.

4. Stable knockdown of CXCR3 in murine ovarian cancer cells

4.1. CXCR3 expression in ID8 cells

To investigate the behavior of ovarian cancer cells that lack CXCR3 expression a mCXCR3 knockdown in murine ovarian cancer cells was planned. Before generating a downregulated expression, the cell line had first to be analyzed if it expresses mCXCR3 natively. Therefore, ID8 wildtype murine ovarian cancer cells were seeded, left untreated and were lysed after they have reached a 70% confluence. The lysates

were applied under reducing conditions to a SDS-gel. After gel electrophoresis, the proteins were transferred to a PVDF membrane. Immunostaining with the polyclonal antibody directed against mCXCR3 revealed the expression of the murine receptor mCXCR3 in ID8 cells (Figure 34). As it is known for murine CXCR3, only one isoform of the receptor exists and is expressed and therefore, only one mCXCR3 band can be seen on the PVDF membrane. However, the polyclonal antibody is not as specific as a monoclonal antibody, revealing several presumably unspecific bands on the western blot membrane.

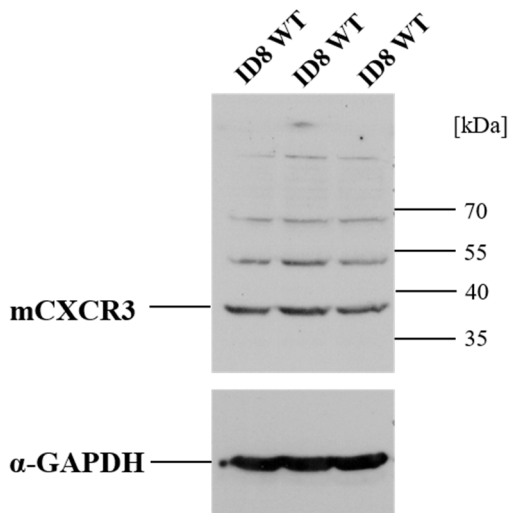


Figure 34: Protein expression of mCXCR3 in ID8 cells

Western blot with lysates from ID8 cells immunostained with α -CXCR3 antibody and α -GAPDH antibody as endogenous control.

To further confirm the expression of mCXCR3 in ID8 cells, the cells were immunostained with the anti-CXCR3 antibody (R&D) or with an isotype control, followed by an Alexa488 conjugate and analyzed by flow cytometry. For the FACS staining of the ID8 cells, the same anti-CXCR3 antibody was used as for the human ovarian cancer cells, because it also detects murine CXCR3. The FACS confirms that native wildtype ID8 cells express the receptor mCXCR3 (Figure 35).

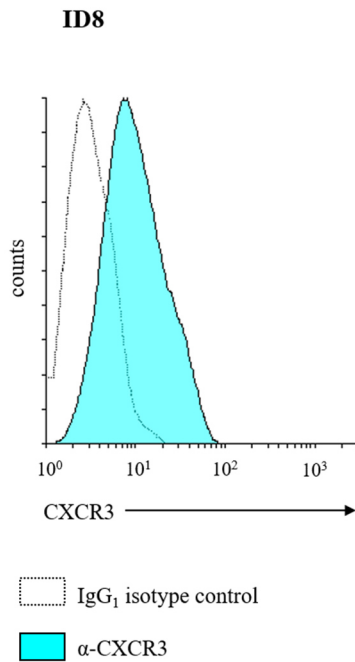


Figure 35: FACS analysis of wildtype ID8 cells

Expression of mCXCR3 in ID8 wildtype cells was measured by flow cytometry. Cells were immunostained with either α -CXCR3 antibody (turquoise) or with IgG₁ isotype control (white, dotted), both followed by an Alexa488 conjugate.

4.2. Generation of stable mCXCR3 knockdown cells

The murine ovarian cancer cell line ID8 was stably transfected with the eukaryotic expression plasmid pRS, harboring the shRNA matching the mCXCR3 open reading frame sequence. Two different shRNAs were used. As a control, cells were transfected with the pRS vector containing a scrambled shRNA. The pRS vector contains a resistance gene for puromycin. Therefore, stable transfected cell clones were selected by puromycin supplemented ID8 growth medium. Despite of their puromycin resistance, some cells express the mCXCR3 shRNA only weakly or not at all, leading to a heterogenous expression pattern of transfected cells. To achieve a successful knockdown, single cell clones were isolated in order to generate cells with no or low mCXCR3 expression. To investigate the mCXCR3 expression of the cell clones, a FACS analysis was performed, comparing knockdown cell clones (k.d.) and scrambled shRNA (scr) clones. Two cell clones showed a drastic decreased mCXCR3 expression compared to ID8 scrambled shRNA control clones, clone ID8-B1 and ID8-B4 (Figure 36).

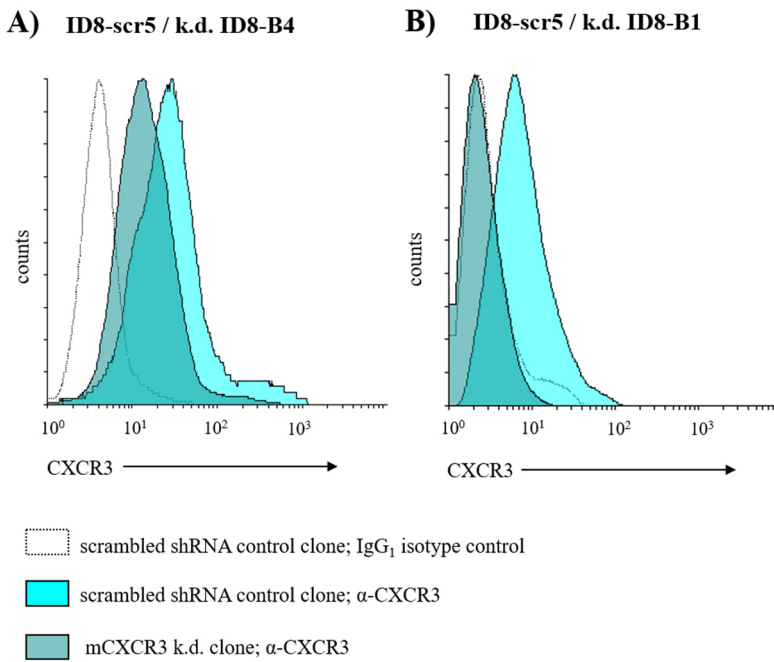


Figure 36: FACS analysis of transfected ID8 cells

Cells were immunostained with either anti-CXCR3 antibody or with IgG₁ isotype control, both followed by an Alexa488 conjugate. The overlay histograms compare mCXCR3 expression of scrambled shRNA clone #5 stained with either α-CXCR3 antibody (turquoise) or with isotype control (white, dotted) with a knockdown clone (blue). **A)** shows knockdown clone #B4, **B)** knockdown clone #B1, which curve nearly covers the curve of the scr5 isotype control.

4.3. Migratory capacity of mCXCR3 knockdown cells

The mCXCR3 knockdown cells were applied into migration assays to analyze their migratory capacity towards the murine chemokine ligand mCXCL10. The most successful knockdown clones ID8-B1 and ID8-B4 were used, as well as a scrambled shRNA control (ID8-scr5). The cells were seeded in the upper chamber of Transwell[®] inserts, placed in 24-well assay plates and mCXCL10 was added to the lower chambers of the assay plate, or 0.1% BSA/PBS as a control. After four hours of migration, the insert membranes were washed, fixed and stained and migrated cells were counted as described in Material and Methods. The number of migrated cells was normalized to that of cells which migrated towards 0.1% BSA/PBS, as this was regarded as the spontaneous baseline migration. Both mCXCR3 knockdown clones showed a statistically significant impaired migration towards mCXCL10 compared to the scrambled shRNA control cells ($p=0.006$ for B1; $p<0.001$ for B4) (Figure 37).

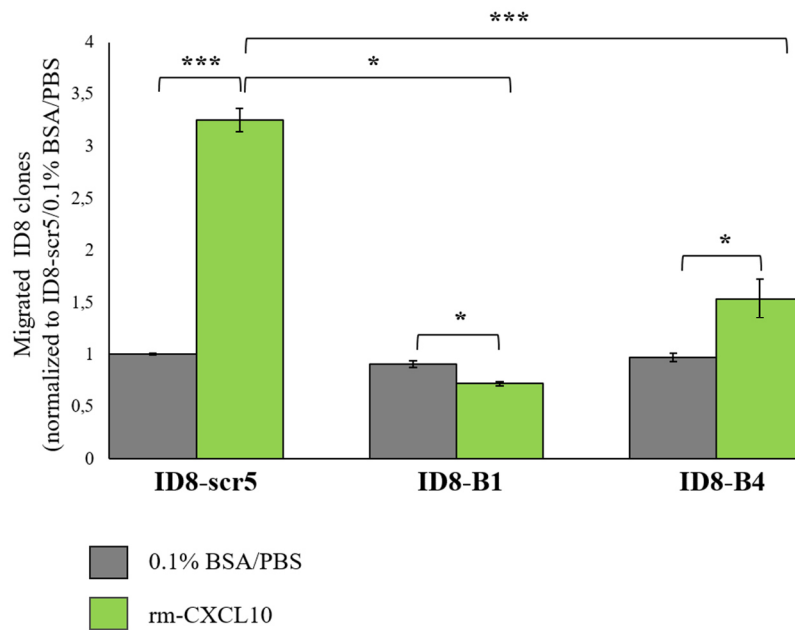


Figure 37: Migration of mCXCR3 knockdown cells towards mCXCL10

Migration of the mCXCR3 knockdown cells ID8-B1 and ID8-B4 and the scrambled shRNA control ID8-scr5 towards mCXCL10 (green bars) or towards 0.1% BSA/PBS (grey bars) as control. The number of migrated cells was normalized to the baseline migration observed from migration of ID8-scr5 cells towards 0.1% BSA/PBS. Statistical significance was calculated and defined as * $p \leq 0.05$, ** $p \leq 0.005$, or *** $p \leq 0.001$.

4.4. Proliferation of mCXCR3 knockdown cells

The impact of the mCXCR3 knockdown on ID8 cell proliferation was analyzed by manual counting. Therefore, the cells were seeded in triplicates in three 24-well plates for each time point. 24 h, 48 h and 72 h post-seeding the cells were detached with trypsin and counted manually in a Neubauer counting chamber using trypan blue solution. The two mCXCR3 knockdown clones ID8-B1 and ID8-B4 appeared to have a decreased proliferation rate compared to scrambled shRNA control cells and ID8 wildtype cells (Figure 38).

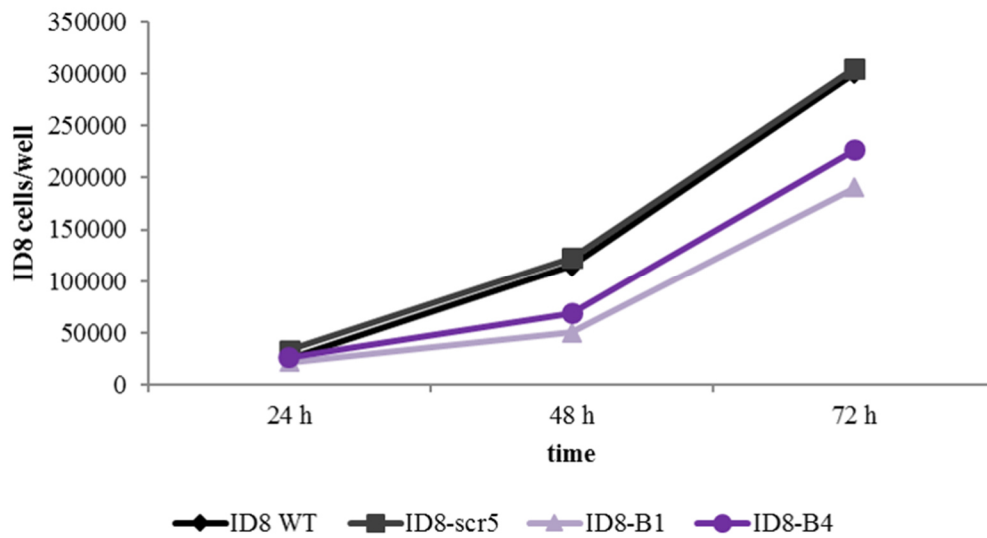


Figure 38: Proliferation of mCXCR3 knockdown cells

The mCXCR3 knockdown cells ID8-B1 (light purple line, triangles), ID8-B4 (purple line, circles), the scrambled shRNA control cells ID8-scr5 (grey line, rectangle) and ID8 wildtype cells (black line, diamonds) were seeded in cell culture plates and counted manually 24 h, 48 h and 72 h after seeding.

VII. DISCUSSION

1. CXCL9 and CXCL10 are potent anti-tumor mediators

Ovarian cancer is still a highly deadly and often a chemoresistant disease, therefore new therapeutic approaches are necessary. Recently, ovarian cancer was identified as an immunogenic tumor as the role of tumor-suppressive lymphocytic infiltration of tumors was elucidated. The amount and type of tumor infiltrating immune cells is dependent on the chemokine content of the tumor microenvironment. A high chemokine concentration at the tumor site is required to mediate a sufficient trafficking of immune effector cells into the tumor (Abastado, 2012). An accumulation of the chemokine ligands CXCL9 and CXCL10 in the tumor milieu is responsible for the recruitment of CXCR3⁺ effector T lymphocytes and NK cells with anti-tumor reactivity (Andersson et al., 2009; Wendel et al., 2008). The CXCR3 ligands are not only responsible for chemotactic migration, but also for expansion of CD4⁺ and CD8⁺ T lymphocytes, attraction of T helper cells type 1 and induction of their polarization (Groom et al., 2012; Hu et al., 2011). Thus the development of immune therapies implementing CXCR3 ligands that attract T, NK and NKT effector cells into tumors can serve as an effective anti-tumor strategy.

The current immunotherapies such as adoptive T cell transfer and anti-cancer vaccines are not very efficient or beneficial for the patients also because of the limited recruitment of tumor specific T cells to the tumor microenvironment. In a study by Bedognetti et al., a high expression of the chemokine ligands CXCL9, CXCL10, CXCL11 and CCL5 in pretreated metastatic melanoma tumors was associated with responsiveness to adoptive T cell transfer (Bedognetti et al., 2013). Another study showed that the blockage of the programmed cell death protein-1 (PD-1) pathway increased the expression of IFN- γ and CXCL10, resulting in increased numbers of transferred T cells at the tumor site and tumor regression in a melanoma and adenocarcinoma model (Peng et al., 2012). Thus, mechanisms that increase the intratumoral levels of CXCL9 and CXCL10 and by this enhance the recruitment of CXCR3⁺ effector NK and T cells to the tumor microenvironment have shown to promote effective anti-tumor responses. If the enhanced expression of chemokine ligands is not only responsible for an increased anti-tumor lymphocytic infiltration but

has further a direct impact on ovarian cancer patient survival was so far not yet determined.

In this thesis, the chemokine ligands CXCL9 and CXCL10 were identified for the first time as independent favorable prognostic markers in advanced high-grade serous ovarian cancer (HGSC). A high expression of CXCL9 and CXCL10 was each correlated with a significantly prolonged overall survival of 48 versus 22 months ($p<0.001$) for CXCL9 and 48 versus 27 months ($p<0.001$) for CXCL10. A high expression of CXCL10 was furthermore correlated with a longer progression-free survival reaching borderline significance ($p=0.056$). The combined overexpression of both chemokines was associated with an even better outcome compared to the overexpression of only one of the two chemokines (OS 52 vs. 29 months, $p<0.001$), suggesting additive effects. The worst prognosis had patients whose tumors expressed both chemokines at a low level with a median overall survival of only 19 months. The favorable prognostic effect of the chemokine overexpression was independent of each other and of other clinical parameters including postsurgical residual tumor mass and lymph node metastasis.

These results further suggest that the expression of CXCL9 and CXCL10 and their actions in recruiting tumor infiltrating lymphocytes may be an important tumorsuppressive mechanism in ovarian cancer. New tools to increase the chemokine ligand expression in the tumor microenvironment have to be identified and developed. A systemical administration of recombinant CXCL10 to mice bearing highly malignant mammary tumors showed a significant tumor growth inhibition and an increase of CD4⁺ T cell infiltration (Dorsey et al., 2002). A pharmacological approach to raise the intratumoral CXCR3 ligand expression and hence the intratumoral immune infiltration is to suppress endogenous prostaglandin E2 by cyclooxygenase inhibition through indomethacin or acetylsalicylic acid (Bronger et al., 2012). More studies and clinical trials involving direct patient applications are needed to further develop this chemokine-dependent anti-tumor strategy. However, it has to be considered, that an overexpression of CXCL9 and CXCL10 may not only attract more cytotoxic T cells, but also more T regulatory cells which are linked to pro-tumor effects. CXCR3⁺ T regulatory cells are found to be highly enriched in ovarian carcinomas, where they suppress proliferation and IFN- γ secretion of effector cells. CXCR3 ligands attract both effector T cells and regulatory T cells in the same ratio to tumor sites (Redjimi et

al., 2012). The pro-tumor effects of T regulatory cells can be compensated by a higher amount of CD8⁺ tumor infiltrating lymphocytes, as a high ratio of CD8⁺/CD4⁺ TILs was associated with a prolonged overall survival (Sato et al., 2005). Thus, future therapeutic options have the challenge to not only increase the quantity of tumor infiltrating immune cells, but also the quality and to establish a perfect balance of effector and regulatory lymphocytes. The results of this thesis suggest a tumor-suppressive net effect of CXCR3 ligands.

2. CXCR3 as therapeutic target

Since ovarian tumors proliferate rapidly, metastasize to the peritoneal cavity and are only temporarily sensitive to chemotherapy, ovarian cancer is still a highly deadly disease. Especially the control of formation of intraabdominal and distant metastases remains a major therapeutic challenge. During the initial tumorigenesis ovarian cancer cells undergo an epithelial-mesenchymal transition (EMT), lose their polarity and their cell-cell adhesion and become more invasive and migratory. In this process, a change in cadherin and integrin expression is involved, as well as an upregulation of several proteases (Kalluri et al., 2009; Lengyel, 2010). Once the cells are detached from the primary tumor, the ovarian cancer cells are thought to be passively carried by peritoneal fluid or ascites to the mesothelium of peritoneum and omentum, where they can actively attach and revert back to their epithelial cell type (Lengyel, 2010). Several studies demonstrated an involvement of CXCR3 in actin reorganization, protease expression, migration, invasion and cancer metastasis in mouse models of melanoma, colorectal cancer and breast cancer (Kawada et al., 2007; Kawada et al., 2004; Walser et al., 2006). A CXCR3 overexpression in human colorectal cancer and in breast cancer cells was furthermore associated with a poor prognosis for patients (Kawada et al., 2007; Ma et al., 2009). In this thesis, CXCR3 expressed by tumor cells was identified as independent negative prognostic factor in advanced high-grade serous ovarian cancer. A high expression of CXCR3 was correlated with a statistically significant shortened progression-free and overall survival (PFS 11 vs. 19 months, $p < 0.001$; OS 22 vs. 48 months, $p < 0.001$). This negative prognostic effect of the receptor overexpression on progression-free and overall survival was independent of other clinical parameters including postsurgical residual tumor mass and lymph node metastasis.

A study about basement-membrane type VII collagen (ColVII), a protein which loss increases the risk of skin cancer, demonstrated a promoting role of CXCL10-CXCR3 interaction in EMT and metastasis of invasive skin cancer cells (Martins et al., 2009). So it seems, that activation of tumor CXCR3 upregulates the epithelial-mesenchymal transition of cancer cells and expression of proteases, leading to a more invasive and aggressive phenotype and finally to cancer metastasis and to a poor patient outcome. This hypothesis is supported by the finding that upon stimulation with CXCL9 and thus activation of CXCR3 on ovarian cancer cells, several proteases including MMP-2 and MMP-3 were upregulated.

The poor outcome of the receptor overexpression in advanced high-grade serous ovarian carcinoma appears to be compensable by a high expression of the ligand CXCL9. Tumor receptor overexpression in combination with a low CXCL9 expression was associated with a worse outcome comparing with tumors that express either CXCL9^{high}/CXCR3^{high} or CXCL9^{low}/CXCR3^{low} (PFS 4 vs. 14 months, $p=0.002$; OS 19 vs. 29 months, $p=0.031$). An overexpression of CXCL9 with a coexisting low CXCR3 expression was correlated with a better overall survival comparing with tumors that express either CXCL9^{high}/CXCR3^{high} or CXCL9^{low}/CXCR3^{low} (58 vs. 29 months; $p<0.001$). So even in the presence of a lot tumor cell CXCR3, a high concentration of CXCL9 is still associated with an improved outcome. However, this was not true for CXCL10. The study mentioned above by Martins et al. indicated an interaction of the receptor CXCR3 and the ligand CXCL10 in EMT promotion, this could be the reason, why a high CXCL10 expression in advanced high-grade serous ovarian carcinoma could not compensate the poor outcome of CXCR3 overexpression, in contrast to the other CXCR3 ligand CXCL9. Tumor CXCR3 expression was furthermore shown to be promoted and up-regulated by exposure to high concentrations of CXCL10 secreted by breast cancer cells and not down-regulated and internalized, what would be the conventional regulatory mechanism for chemokine receptors (Goldberg-Bittman et al., 2004). In contrast, high CXCL9 concentrations were shown to have a rather repulsive than attracting effect on melanoma cells (Amatschek et al., 2011). Moreover, recently an “antagonistic” CXCL10 variant was identified, that is antagonistic to chemotaxis. It is generated by post-translational processing through cleaving a *Val-Pro* dipeptide from the N-terminus of CXCL10, a process catalyzed by dipeptidyl peptidases. This variant of CXCL10 still binds to the

CXCR3 receptor but fails to induce receptor-mediated signaling or internalization (Casrouge et al., 2011). A *de novo* sequence analysis identified the presence of the “antagonistic” variant of CXCL10 in high-grade serous ovarian cancers, but not in benign tumors and its expression was not correlated well with lymphocytic infiltration (Rainczuk et al., 2014). The fact that a high CXCL10 expression is associated with a prolonged overall and progression-free survival in high-grade serous ovarian cancer only when there is a concomitant low CXCR3 expression, could be explained by the possible interaction of CXCL10 and CXCR3 in EMT induction and metastasis promotion. Moreover, ovarian cancers that overexpress the receptor could preferentially secrete the “antagonistic” variant of CXCL10 that is incapable of recruiting immune cells to the tumor microenvironment as a mechanism of immune evasion.

Regarding the negative prognostic effect of the CXCR3 overexpression in advanced high-grade serous ovarian carcinomas, together with the possible interaction with CXCL10 in the induction of EMT, it was hypothesized, that CXCR3 is responsible for the homing of CXCR3⁺ cancer cells into organs with abundant chemokine ligand expression and that it is involved in the peritoneal spread of ovarian cancer cells. The immunohistochemical slides showed that the invasive tumor front expresses higher amounts of CXCR3. The analyzed ovarian cancer cell lines OVCAR-3 and SKOV-3 expressed functionally active CXCR3 as they were able to migrate towards the chemokine ligand CXCL9 in a CXCR3-dependent manner. Although the increase of migrated cells from baseline migration to migration towards the chemokine ligand was just about 1.2-fold, it was still statistically significant. According to the literature, CXCL9 is a less potent chemoattractant for CXCR3⁺ cells compared with the other ligands, as it was shown that stimulation of murine breast cancer cells with CXCL10 or CXCL11 stimulated calcium flux, whereas CXCL9 was less effective at inducing calcium mobilization (Walser et al., 2006). The use of the anti-CXCR3 antibody but not an IgG₁ isotype control antibody completely blocked the migration towards CXCL9, so that the migration of ovarian cancer cells towards CXCL9 seems to be CXCR3-dependent. The antibody treated cells migrated even less than the baseline migration. This could be due to chemotaxis-independent mechanisms upon chemokine receptor activation like a lower induction of the epithelial-mesenchymal transition upon CXCR3-blockage.

To intensify these results, a knockdown of mCXCR3 in the murine ovarian cancer cells ID8 was performed. These cells were no longer able to migrate towards mCXCL10. The ligand activation of the receptor seems to enhance the migratory capacity of cancer cells, but it did not increase cancer cell proliferation as a stimulation with either recombinant human CXCL9 or CXCL10 had no impact on the cell proliferation of OVCAR-3 and SKOV-3 cells. However, in a study by Lau et al. the chemokine ligand CXCL11 was shown to induce proliferation of ovarian cancer cells via CXCR3 (Lau et al., 2014). This contrast might be due to the different cell lines used or to divergent functions of the chemokine ligands.

Furthermore, ELISA-examined ascites samples of 102 patients with high-grade serous ovarian cancer revealed the presence of CXCL9 and CXCL10 in chemotactically active concentrations. Several ascites samples were able to attract OVCAR-3 and SKOV-3 cells in migration assays and this migration could be suppressed by the use of an anti-CXCR3 antibody. The studies by Kim et al. support these results by showing that epithelial ovarian cancer cells that express other chemokine receptors, namely CX₃CR1 and XCR1, actively migrate towards their ligands CX₃CL1 and XCL1, respectively, and towards ascites in a receptor-dependent manner. Both ligands are present in the ascitic fluid of patients with epithelial ovarian cancer. By silencing the receptors with siRNAs the migration towards either the chemokine ligands or ascitic fluid was drastically reduced and also the formation of colon, spleen and liver metastases was reduced *in vivo* (M. Kim et al., 2012a; M. Kim et al., 2012b).

Moreover, epithelial ovarian cancer cells directly isolated from ascites from patients with serous ovarian cancer were able to migrate towards ascites, and this migration could be again blocked by an anti-CXCR3 antibody. Others in the laboratory group confirmed a CXCR3 expression in all cells. By means of the isolation protocol it is a rare success to isolate and grow EOC cells from patients who are undergoing chemotherapy (Shepherd et al., 2006). Three patients received chemotherapy and this could be the reason why the isolation was possible only in four out of six cases, why only two out of four cell lines were migratory active and why one cell line even stopped growing after several passages. Nevertheless, as stated above, two epithelial ovarian cancer cell lines were able to migrate towards ascites in a CXCR3-dependent manner.

Although no correlation between chemokine ligand concentration in ascites, residual tumor and survival was found, the presence of CXCL9 and CXCL10 in ascitic fluid

seems to activate and thus attract CXCR3⁺ ovarian cancer cells to detach from the primary tumor and to metastasize into the peritoneal cavity. It can be hypothesized that tumor cells trigger their emigration by secreting cytokines like IFN- γ into the peritoneal fluid or in the blood, which may induce the expression of chemokines in chemotactically active concentrations. This in turn could prompt the peritoneal spread of CXCR3⁺ ovarian cancer cells.

For lymph node metastasis however, CXCR3 appears not to play a role, as this metastatic pathway is thought to be rather passive. Not all, but only about 56% of the analyzed metastatic lymph nodes were highly CXCR3 expressing metastases. In the survival analysis of high-grade serous ovarian cancers, the lymph node status was not an independent prognostic factor for both overall and progression-free survival. This covers with the discovery of master student Theresa Dawidek, who found out, that while only about one third of the analyzed primary ovarian tumors showed a high CXCR3 expression, all corresponding omentum and peritoneum metastases expressed high CXCR3 and only the lymph node metastases were balanced between low and high CXCR3 expression (Dawidek, 2014).

As a sum of these results, it is postulated that CXCR3 plays a role in the peritoneal metastasis of high-grade serous ovarian cancers, what makes CXCR3 a potential therapeutic target. A pharmacological antagonism of CXCR3 was already shown to inhibit lung metastasis in a murine model of breast cancer, while local tumors were not affected. The effect of this treatment was dependent on NK cells, so that the inhibitor concentration necessary to inhibit host immune-cell CXCR3 may be higher than the concentration required to inhibit tumor CXCR (Walser et al., 2006).

3. Conclusion

Additional to the standard therapy two mechanisms should be considered for future therapeutic options for ovarian cancer: enhancing the intratumoral CXCL9 and CXCL10 concentrations while suppressing the tumor cell CXCR3 function at the same time. An increased intratumoral chemokine concentration would cause an enhanced lymphocytic infiltration and could restrain CXCR3⁺ tumor cells to their primary site and thus hinder them from metastasizing. Moreover, the ligand abundancy would prevent the decoy receptor function of CXCR3 on tumor cells. Studies are needed to evaluate pharmacological mechanisms to increase the ligand concentration at tumor

sites or to invent vehicles for ligand delivery to the tumor microenvironment. However, the enhanced intratumoral ligand concentration could also increase the activation of CXCR3 on tumor cells and thus its pro-malignant functions. Therefore, a simultaneous suppression of tumor CXCR3 is necessary, as it could decrease the migration of ovarian cancer cells towards ascites and thus possibly the peritoneal spread. The difficulty in implementing the chemokine system in future therapies is to antagonize tumor CXCR3 without impacting the CXCR3 mediated lymphocytic tumor infiltration. Several investigations and studies are needed to bring the CXCR3 system closer to clinical application.

VIII. REFERENCES

- Abastado, J. P. (2012). The next challenge in cancer immunotherapy: controlling T-cell traffic to the tumor. *Cancer Res*, 72(9), 2159-2161.
- Allen, S. J., Crown, S. E., & Handel, T. M. (2007). Chemokine: receptor structure, interactions, and antagonism. *Annu Rev Immunol*, 25, 787-820.
- Amatschek, S., Lucas, R., Eger, A., Pflueger, M., Hundsberger, H., Knoll, C., Grosse-Kracht, S., Schuett, W., Koszik, F., Maurer, D., & Wiesner, C. (2011). CXCL9 induces chemotaxis, chemorepulsion and endothelial barrier disruption through CXCR3-mediated activation of melanoma cells. *Br J Cancer*, 104(3), 469-479.
- Andersson, A., Yang, S. C., Huang, M., Zhu, L., Kar, U. K., Batra, R. K., Elashoff, D., Strieter, R. M., Dubinett, S. M., & Sharma, S. (2009). IL-7 promotes CXCR3 ligand-dependent T cell antitumor reactivity in lung cancer. *J Immunol*, 182(11), 6951-6958.
- Bedognetti, D., Spivey, T. L., Zhao, Y., Uccellini, L., Tomei, S., Dudley, M. E., Ascierto, M. L., De Giorgi, V., Liu, Q., Delogu, L. G., Sommariva, M., Sertoli, M. R., Simon, R., Wang, E., Rosenberg, S. A., & Marincola, F. M. (2013). CXCR3/CCR5 pathways in metastatic melanoma patients treated with adoptive therapy and interleukin-2. *Br J Cancer*, 109(9), 2412-2423.
- Billottet, C., Quemener, C., & Bikfalvi, A. (2013). CXCR3, a double-edged sword in tumor progression and angiogenesis. *Biochim Biophys Acta*, 1836(2), 287-295.
- Bolton, K. L., Chenevix-Trench, G., Goh, C., Sadetzki, S., Ramus, S. J., Karlan, B. Y., Lambrechts, D., Despierre, E., Barrowdale, D., McGuffog, L., Healey, S., Easton, D. F., Sinilnikova, O., Benitez, J., Garcia, M. J., Neuhausen, S., Gail, M. H., Hartge, P., Peock, S., Frost, D., Evans, D. G., Eeles, R., Godwin, A. K., Daly, M. B., Kwong, A., Ma, E. S., Lazaro, C., Blanco, I., Montagna, M., D'Andrea, E., Nicoletto, M. O., Johnatty, S. E., Kjaer, S. K., Jensen, A., Hogdall, E., Goode, E. L., Fridley, B. L., Loud, J. T., Greene, M. H., Mai, P. L., Chetrit, A., Lubin, F., Hirsh-Yechezkel, G., Glendon, G., Andrulis, I. L., Toland, A. E., Senter, L., Gore, M. E., Gourley, C., Michie, C. O., Song, H., Tyrer, J., Whittemore, A. S., McGuire, V., Sieh, W., Kristoffersson, U., Olsson, H., Borg, A., Levine, D. A., Steele, L., Beattie, M. S., Chan, S., Nussbaum, R. L., Moysich, K. B., Gross, J., Cass, I., Walsh, C., Li, A. J., Leuchter, R., Gordon, O., Garcia-Closas, M., Gayther, S. A., Chanock, S. J., Antoniou, A. C., Pharoah, P. D., Embrace, kConFab, I., & Cancer Genome Atlas Research, N. (2012). Association between BRCA1 and BRCA2 mutations and survival in women with invasive epithelial ovarian cancer. *JAMA*, 307(4), 382-390.
- Bronger, H., Kraeft, S., Schwarz-Boeger, U., Cerny, C., Stockel, A., Avril, S., Kiechle, M., & Schmitt, M. (2012). Modulation of CXCR3 ligand secretion by prostaglandin E2 and cyclooxygenase inhibitors in human breast cancer. *Breast Cancer Res*, 14(1), R30.

- Burger, R. A., Sill, M. W., Monk, B. J., Greer, B. E., & Sorosky, J. I. (2007). Phase II trial of bevacizumab in persistent or recurrent epithelial ovarian cancer or primary peritoneal cancer: a Gynecologic Oncology Group Study. *J Clin Oncol*, *25*(33), 5165-5171.
- Burges, A., Ataseven, B., Lutz, L., Rack, B., Seck, K., Pölcher, M., Schmalfeldt, B., & Späthe, K. (2014). Systemische Primärtherapie einschließlich molekularbiologischer Therapieansätze. In B. Schmalfeldt (Ed.), *Manual Maligne Ovarialtumoren* (10 ed., pp. 52-62). München: W. Zuckschwerdt Verlag.
- Cambien, B., Karimjee, B. F., Richard-Fiardo, P., Bziouech, H., Barthel, R., Millet, M. A., Martini, V., Birnbaum, D., Scoazec, J. Y., Abello, J., Al Saati, T., Johnson, M. G., Sullivan, T. J., Medina, J. C., Collins, T. L., Schmid-Alliana, A., & Schmid-Antomarchi, H. (2009). Organ-specific inhibition of metastatic colon carcinoma by CXCR3 antagonism. *Br J Cancer*, *100*(11), 1755-1764.
- Campanella, G. S., Colvin, R. A., & Luster, A. D. (2010). CXCL10 can inhibit endothelial cell proliferation independently of CXCR3. *PLoS One*, *5*(9), e12700.
- Cancer Genome Atlas Research, N. (2011). Integrated genomic analyses of ovarian carcinoma. *Nature*, *474*(7353), 609-615.
- Casrouge, A., Decalf, J., Ahloulay, M., Lababidi, C., Mansour, H., Vallet-Pichard, A., Mallet, V., Mottez, E., Mapes, J., Fontanet, A., Pol, S., & Albert, M. L. (2011). Evidence for an antagonist form of the chemokine CXCL10 in patients chronically infected with HCV. *J Clin Invest*, *121*(1), 308-317.
- Cerny, C., Bronger, H., Davoodi, M., Sharma, S., Zhu, L., Obana, S., Sharma, J., Ebrahimi, R., St John, M., Lee, J. M., Salgia, R., Strieter, R. M., Dubinett, S. M., & Sharma, S. (2014). The Role of CXCR3/Ligand Axis in Cancer. *International trends in immunity*, *3*(2), 19-25.
- Chen, D. S., & Mellman, I. (2013). Oncology meets immunology: the cancer-immunity cycle. *Immunity*, *39*(1), 1-10.
- Colvin, R. A., Campanella, G. S., Sun, J., & Luster, A. D. (2004). Intracellular domains of CXCR3 that mediate CXCL9, CXCL10, and CXCL11 function. *J Biol Chem*, *279*(29), 30219-30227.
- Dagan-Berger, M., Feniger-Barish, R., Avniel, S., Wald, H., Galun, E., Grabovsky, V., Alon, R., Nagler, A., Ben-Baruch, A., & Peled, A. (2006). Role of CXCR3 carboxyl terminus and third intracellular loop in receptor-mediated migration, adhesion and internalization in response to CXCL11. *Blood*, *107*(10), 3821-3831.
- Datta, D., Flaxenburg, J. A., Laxmanan, S., Geehan, C., Grimm, M., Waaga-Gasser, A. M., Briscoe, D. M., & Pal, S. (2006). Ras-induced modulation of CXCL10 and its receptor splice variant CXCR3-B in MDA-MB-435 and MCF-7 cells: relevance for the development of human breast cancer. *Cancer Res*, *66*(19), 9509-9518.
- Dawidek, T. (2014). *Das CXCR3-Chemokinsystem und seine immunmodulatorische Rolle im Ovarialkarzinom*. (Master Thesis), Technische Universität München,

München.

Despierre, E., Lambrechts, D., Neven, P., Amant, F., Lambrechts, S., & Vergote, I. (2010). The molecular genetic basis of ovarian cancer and its roadmap towards a better treatment. *Gynecol Oncol*, *117*(2), 358-365.

Dorsey, R., Kundu, N., Yang, Q., Tannenbaum, C. S., Sun, H., Hamilton, T. A., & Fulton, A. M. (2002). Immunotherapy with interleukin-10 depends on the CXC chemokines inducible protein-10 and monokine induced by IFN-gamma. *Cancer Res*, *62*(9), 2606-2610.

Ehlert, J. E., Addison, C. A., Burdick, M. D., Kunkel, S. L., & Strieter, R. M. (2004). Identification and partial characterization of a variant of human CXCR3 generated by posttranscriptional exon skipping. *J Immunol*, *173*(10), 6234-6240.

Engl, T., Relja, B., Blumenberg, C., Muller, I., Ringel, E. M., Beecken, W. D., Jonas, D., & Blaheta, R. A. (2006). Prostate tumor CXC-chemokine profile correlates with cell adhesion to endothelium and extracellular matrix. *Life Sci*, *78*(16), 1784-1793.

Farber, J. M. (1990). A macrophage mRNA selectively induced by gamma-interferon encodes a member of the platelet factor 4 family of cytokines. *Proc Natl Acad Sci U S A*, *87*(14), 5238-5242.

Ferguson, S. S., Downey, W. E., 3rd, Colapietro, A. M., Barak, L. S., Menard, L., & Caron, M. G. (1996). Role of beta-arrestin in mediating agonist-promoted G protein-coupled receptor internalization. *Science*, *271*(5247), 363-366.

Furuya, M., Suyama, T., Usui, H., Kasuya, Y., Nishiyama, M., Tanaka, N., Ishiwata, I., Nagai, Y., Shozu, M., & Kimura, S. (2007). Up-regulation of CXC chemokines and their receptors: implications for proinflammatory microenvironments of ovarian carcinomas and endometriosis. *Hum Pathol*, *38*(11), 1676-1687.

Furuya, M., Yoneyama, T., Miyagi, E., Tanaka, R., Nagahama, K., Miyagi, Y., Nagashima, Y., Hirahara, F., Inayama, Y., & Aoki, I. (2011). Differential expression patterns of CXCR3 variants and corresponding CXC chemokines in clear cell ovarian cancers and endometriosis. *Gynecol Oncol*, *122*(3), 648-655.

Garcia-Lopez, M. A., Sanchez-Madrid, F., Rodriguez-Frade, J. M., Mellado, M., Acevedo, A., Garcia, M. I., Albar, J. P., Martinez, C., & Marazuela, M. (2001). CXCR3 chemokine receptor distribution in normal and inflamed tissues: expression on activated lymphocytes, endothelial cells, and dendritic cells. *Lab Invest*, *81*(3), 409-418.

Goldberg-Bittman, L., Neumark, E., Sagi-Assif, O., Azenshtein, E., Meshel, T., Witz, I. P., & Ben-Baruch, A. (2004). The expression of the chemokine receptor CXCR3 and its ligand, CXCL10, in human breast adenocarcinoma cell lines. *Immunol Lett*, *92*(1-2), 171-178.

Gorbachev, A. V., Kobayashi, H., Kudo, D., Tannenbaum, C. S., Finke, J. H., Shu, S., Farber, J. M., & Fairchild, R. L. (2007). CXC chemokine ligand 9/monokine induced by IFN-gamma production by tumor cells is critical for T cell-mediated suppression

- of cutaneous tumors. *J Immunol*, 178(4), 2278-2286.
- Groom, J. R., Richmond, J., Murooka, T. T., Sorensen, E. W., Sung, J. H., Bankert, K., von Andrian, U. H., Moon, J. J., Mempel, T. R., & Luster, A. D. (2012). CXCR3 chemokine receptor-ligand interactions in the lymph node optimize CD4⁺ T helper 1 cell differentiation. *Immunity*, 37(6), 1091-1103.
- Hermanek, P., & Wittekind, C. (1994). Residual tumor (R) classification and prognosis. *Semin Surg Oncol*, 10(1), 12-20.
- Holschneider, C. H., & Berek, J. S. (2000). Ovarian cancer: epidemiology, biology, and prognostic factors. *Semin Surg Oncol*, 19(1), 3-10.
- Hu, J. K., Kagari, T., Clingan, J. M., & Matloubian, M. (2011). Expression of chemokine receptor CXCR3 on T cells affects the balance between effector and memory CD8 T-cell generation. *Proc Natl Acad Sci U S A*, 108(21), E118-127.
- Jayson, G. C., Kohn, E. C., Kitchener, H. C., & Ledermann, J. A. (2014). Ovarian cancer. *Lancet*, 384(9951), 1376-1388.
- Jelovac, D., & Armstrong, D. K. (2011). Recent progress in the diagnosis and treatment of ovarian cancer. *CA Cancer J Clin*, 61(3), 183-203.
- Jiang, S., Pan, A. W., Lin, T. Y., Zhang, H., Malfatti, M., Turteltaub, K., Henderson, P. T., & Pan, C. X. (2015). Paclitaxel Enhances Carboplatin-DNA Adduct Formation and Cytotoxicity. *Chem Res Toxicol*, 28(12), 2250-2252.
- Kalluri, R., & Weinberg, R. A. (2009). The basics of epithelial-mesenchymal transition. *J Clin Invest*, 119(6), 1420-1428.
- Kandalaf, L. E., Powell, D. J., Jr., Singh, N., & Coukos, G. (2011). Immunotherapy for ovarian cancer: what's next? *J Clin Oncol*, 29(7), 925-933.
- Karin, N., & Wildbaum, G. (2015). The Role of Chemokines in Shaping the Balance Between CD4(+) T Cell Subsets and Its Therapeutic Implications in Autoimmune and Cancer Diseases. *Front Immunol*, 6, 609.
- Kawada, K., Hosogi, H., Sonoshita, M., Sakashita, H., Manabe, T., Shimahara, Y., Sakai, Y., Takabayashi, A., Oshima, M., & Taketo, M. M. (2007). Chemokine receptor CXCR3 promotes colon cancer metastasis to lymph nodes. *Oncogene*, 26(32), 4679-4688.
- Kawada, K., Sonoshita, M., Sakashita, H., Takabayashi, A., Yamaoka, Y., Manabe, T., Inaba, K., Minato, N., Oshima, M., & Taketo, M. M. (2004). Pivotal role of CXCR3 in melanoma cell metastasis to lymph nodes. *Cancer Res*, 64(11), 4010-4017.
- Kawada, K., & Taketo, M. M. (2011). Significance and mechanism of lymph node metastasis in cancer progression. *Cancer Res*, 71(4), 1214-1218.
- Kiechle, M., Meindl, A., & Anthuber, C. (2014). Hereditäres Ovarialkarzinom. In B. Schmalfeldt (Ed.), *Manual Maligne Ovarialtumoren* (10 ed., pp. 29-36). München: W. Zuckschwerdt Verlag.

- Kim, C. H., Nagata, K., & Butcher, E. C. (2003). Dendritic cells support sequential reprogramming of chemoattractant receptor profiles during naive to effector T cell differentiation. *J Immunol*, *171*(1), 152-158.
- Kim, M., Rooper, L., Xie, J., Kajdacsy-Balla, A. A., & Barbolina, M. V. (2012a). Fractalkine receptor CX(3)CR1 is expressed in epithelial ovarian carcinoma cells and required for motility and adhesion to peritoneal mesothelial cells. *Mol Cancer Res*, *10*(1), 11-24.
- Kim, M., Rooper, L., Xie, J., Rayahin, J., Burdette, J. E., Kajdacsy-Balla, A. A., & Barbolina, M. V. (2012b). The lymphotactin receptor is expressed in epithelial ovarian carcinoma and contributes to cell migration and proliferation. *Mol Cancer Res*, *10*(11), 1419-1429.
- Kondo, T., Ito, F., Nakazawa, H., Horita, S., Osaka, Y., & Toma, H. (2004). High expression of chemokine gene as a favorable prognostic factor in renal cell carcinoma. *J Urol*, *171*(6 Pt 1), 2171-2175.
- Kosary, C. L. (1994). FIGO stage, histology, histologic grade, age and race as prognostic factors in determining survival for cancers of the female gynecological system: an analysis of 1973-87 SEER cases of cancers of the endometrium, cervix, ovary, vulva, and vagina. *Semin Surg Oncol*, *10*(1), 31-46.
- Krebs in Deutschland 2011/2012*. (2015). (10 ed.). Berlin: Robert Koch Institut und die Gesellschaft der epidemiologischen Krebsregister in Deutschland e. V.
- Kurman, R. J., & Shih Ie, M. (2010). The origin and pathogenesis of epithelial ovarian cancer: a proposed unifying theory. *Am J Surg Pathol*, *34*(3), 433-443.
- Lacotte, S., Brun, S., Muller, S., & Dumortier, H. (2009). CXCR3, inflammation, and autoimmune diseases. *Ann N Y Acad Sci*, *1173*, 310-317.
- Lasagni, L., Francalanci, M., Annunziato, F., Lazzeri, E., Giannini, S., Cosmi, L., Sagrinati, C., Mazzinghi, B., Orlando, C., Maggi, E., Marra, F., Romagnani, S., Serio, M., & Romagnani, P. (2003). An alternatively spliced variant of CXCR3 mediates the inhibition of endothelial cell growth induced by IP-10, Mig, and I-TAC, and acts as functional receptor for platelet factor 4. *J Exp Med*, *197*(11), 1537-1549.
- Lau, T. S., Chung, T. K., Cheung, T. H., Chan, L. K., Cheung, L. W., Yim, S. F., Siu, N. S., Lo, K. W., Yu, M. M., Kulbe, H., Balkwill, F. R., & Kwong, J. (2014). Cancer cell-derived lymphotoxin mediates reciprocal tumour-stromal interactions in human ovarian cancer by inducing CXCL11 in fibroblasts. *J Pathol*, *232*(1), 43-56.
- Lee, J. H., Kim, H. N., Kim, K. O., Jin, W. J., Lee, S., Kim, H. H., Ha, H., & Lee, Z. H. (2012). CXCL10 promotes osteolytic bone metastasis by enhancing cancer outgrowth and osteoclastogenesis. *Cancer Res*, *72*(13), 3175-3186.
- Leibovich-Rivkin, T., Lebel-Haziv, Y., Lerrer, S., Weitzenfeld, P., & Ben-Baruch, A. (2013). The versatile world of inflammatory chemokines in cancer. In M. R. Shurin, V. Umansky, & A. Malyguine (Eds.), *The tumor immunoenvironment* (pp. 135-175). New York: Springer Science+Business Media.

- Lengyel, E. (2010). Ovarian cancer development and metastasis. *Am J Pathol*, *177*(3), 1053-1064.
- Levanon, K., Crum, C., & Drapkin, R. (2008). New insights into the pathogenesis of serous ovarian cancer and its clinical impact. *J Clin Oncol*, *26*(32), 5284-5293.
- Li, Y., Reader, J. C., Ma, X., Kundu, N., Kochel, T., & Fulton, A. M. (2015). Divergent roles of CXCR3 isoforms in promoting cancer stem-like cell survival and metastasis. *Breast Cancer Res Treat*, *149*(2), 403-415.
- Liu, C., Luo, D., Reynolds, B. A., Meher, G., Katritzky, A. R., Lu, B., Gerard, C. J., Bhadha, C. P., & Harrison, J. K. (2011). Chemokine receptor CXCR3 promotes growth of glioma. *Carcinogenesis*, *32*(2), 129-137.
- Loetscher, M., Gerber, B., Loetscher, P., Jones, S. A., Piali, L., Clark-Lewis, I., Baggiolini, M., & Moser, B. (1996). Chemokine receptor specific for IP10 and mig: structure, function, and expression in activated T-lymphocytes. *J Exp Med*, *184*(3), 963-969.
- Luster, A. D., & Ravetch, J. V. (1987). Biochemical characterization of a gamma interferon-inducible cytokine (IP-10). *J Exp Med*, *166*(4), 1084-1097.
- Ma, X., Norsworthy, K., Kundu, N., Rodgers, W. H., Gimotty, P. A., Goloubeva, O., Lipsky, M., Li, Y., Holt, D., & Fulton, A. (2009). CXCR3 expression is associated with poor survival in breast cancer and promotes metastasis in a murine model. *Mol Cancer Ther*, *8*(3), 490-498.
- Malpica, A., Deavers, M. T., Lu, K., Bodurka, D. C., Atkinson, E. N., Gershenson, D. M., & Silva, E. G. (2004). Grading ovarian serous carcinoma using a two-tier system. *Am J Surg Pathol*, *28*(4), 496-504.
- Martins, V. L., Vyas, J. J., Chen, M., Purdie, K., Mein, C. A., South, A. P., Storey, A., McGrath, J. A., & O'Toole, E. A. (2009). Increased invasive behaviour in cutaneous squamous cell carcinoma with loss of basement-membrane type VII collagen. *J Cell Sci*, *122*(Pt 11), 1788-1799.
- Mayr, D., Dettmar, P., Dorn, J., Schmalzried, H., & Schmoeckel, E. (2014). Histologische Klassifikation maligner und potenziell maligner Ovarialtumoren, Stadieneinteilung und Prognosefaktoren. In B. Schmalfeldt (Ed.), *Manual Maligne Ovarialtumoren* (pp. 20-28). München: W. Zuckschwerdt Verlag.
- Moore, C. B., Guthrie, E. H., Huang, M. T., & Taxman, D. J. (2010). Short hairpin RNA (shRNA): design, delivery, and assessment of gene knockdown. *Methods Mol Biol*, *629*, 141-158.
- Mulligan, A. M., Raitman, I., Feeley, L., Pinnaduwege, D., Nguyen, L. T., O'Malley, F. P., Ohashi, P. S., & Andrulis, I. L. (2013). Tumoral lymphocytic infiltration and expression of the chemokine CXCL10 in breast cancers from the Ontario Familial Breast Cancer Registry. *Clin Cancer Res*, *19*(2), 336-346.
- Murakami, T., Kawada, K., Iwamoto, M., Akagami, M., Hida, K., Nakanishi, Y.,

- Kanda, K., Kawada, M., Seno, H., Taketo, M. M., & Sakai, Y. (2013). The role of CXCR3 and CXCR4 in colorectal cancer metastasis. *Int J Cancer*, *132*(2), 276-287.
- Murphy, P. M., Baggiolini, M., Charo, I. F., Hebert, C. A., Horuk, R., Matsushima, K., Miller, L. H., Oppenheim, J. J., & Power, C. A. (2000). International union of pharmacology. XXII. Nomenclature for chemokine receptors. *Pharmacol Rev*, *52*(1), 145-176.
- Park, M. K., Amichay, D., Love, P., Wick, E., Liao, F., Grinberg, A., Rabin, R. L., Zhang, H. H., Gebeyehu, S., Wright, T. M., Iwasaki, A., Weng, Y., DeMartino, J. A., Elkins, K. L., & Farber, J. M. (2002). The CXC chemokine murine monokine induced by IFN-gamma (CXC chemokine ligand 9) is made by APCs, targets lymphocytes including activated B cells, and supports antibody responses to a bacterial pathogen in vivo. *J Immunol*, *169*(3), 1433-1443.
- Peng, W., Liu, C., Xu, C., Lou, Y., Chen, J., Yang, Y., Yagita, H., Overwijk, W. W., Lizee, G., Radvanyi, L., & Hwu, P. (2012). PD-1 blockade enhances T-cell migration to tumors by elevating IFN-gamma inducible chemokines. *Cancer Res*, *72*(20), 5209-5218.
- Petro, M., Kish, D., Guryanova, O. A., Ilyinskaya, G., Kondratova, A., Fairchild, R. L., & Gorbachev, A. V. (2013). Cutaneous tumors cease CXCL9/Mig production as a result of IFN-gamma-mediated immunoediting. *J Immunol*, *190*(2), 832-841.
- Pradelli, E., Karimdjee-Soilihi, B., Michiels, J. F., Ricci, J. E., Millet, M. A., Vandenbos, F., Sullivan, T. J., Collins, T. L., Johnson, M. G., Medina, J. C., Kleinerman, E. S., Schmid-Alliana, A., & Schmid-Antomarchi, H. (2009). Antagonism of chemokine receptor CXCR3 inhibits osteosarcoma metastasis to lungs. *Int J Cancer*, *125*(11), 2586-2594.
- Qin, S., Rottman, J. B., Myers, P., Kassam, N., Weinblatt, M., Loetscher, M., Koch, A. E., Moser, B., & Mackay, C. R. (1998). The chemokine receptors CXCR3 and CCR5 mark subsets of T cells associated with certain inflammatory reactions. *J Clin Invest*, *101*(4), 746-754.
- Rainczuk, A., Rao, J. R., Gathercole, J. L., Fairweather, N. J., Chu, S., Masadah, R., Jobling, T. W., Deb-Choudhury, S., Dyer, J., & Stephens, A. N. (2014). Evidence for the antagonistic form of CXC-motif chemokine CXCL10 in serous epithelial ovarian tumours. *Int J Cancer*, *134*(3), 530-541.
- Redjimi, N., Raffin, C., Raimbaud, I., Pignon, P., Matsuzaki, J., Odunsi, K., Valmori, D., & Ayyoub, M. (2012). CXCR3+ T regulatory cells selectively accumulate in human ovarian carcinomas to limit type I immunity. *Cancer Res*, *72*(17), 4351-4360.
- Roby, K. F., Taylor, C. C., Sweetwood, J. P., Cheng, Y., Pace, J. L., Tawfik, O., Persons, D. L., Smith, P. G., & Terranova, P. F. (2000). Development of a syngeneic mouse model for events related to ovarian cancer. *Carcinogenesis*, *21*(4), 585-591.
- Rossi, D., & Zlotnik, A. (2000). The biology of chemokines and their receptors. *Annu Rev Immunol*, *18*, 217-242.

- Rotondi, M., Chiovato, L., Romagnani, S., Serio, M., & Romagnani, P. (2007). Role of chemokines in endocrine autoimmune diseases. *Endocr Rev*, 28(5), 492-520.
- Rottman, M., Dorn, J., Schubert-Fritschle, G., & Engel, J. (2014). Epidemiologie. In B. Schmalfeldt (Ed.), *Manual Maligne Ovarialtumoren* (10. ed., pp. 1-10). München: W. Zuckschwerdt Verlag.
- Sato, E., Olson, S. H., Ahn, J., Bundy, B., Nishikawa, H., Qian, F., Jungbluth, A. A., Frosina, D., Gnjjatic, S., Ambrosone, C., Kepner, J., Odunsi, T., Ritter, G., Lele, S., Chen, Y. T., Ohtani, H., Old, L. J., & Odunsi, K. (2005). Intraepithelial CD8+ tumor-infiltrating lymphocytes and a high CD8+/regulatory T cell ratio are associated with favorable prognosis in ovarian cancer. *Proc Natl Acad Sci U S A*, 102(51), 18538-18543.
- Schmalfeldt, B., Anthuber, C., Ataseven, B., Bauerfeind, I., Burges, A., Höß, C., Kern, C., Kolben, M., Pölcher, M., Rehbock, J., & Schwoerer, M. (2014a). Operative Primärtherapie. In B. Schmalfeldt (Ed.), *Manual Maligne Ovarialtumoren* (10 ed., pp. 37-51). München: W. Zuckschwerdt Verlag.
- Schmalfeldt, B., Beer, D., Burges, A., Anthuber, C., & Schelling, M. (2014b). Früherkennung und Diagnostik. In B. Schmalfeldt (Ed.), *Manual Maligne Ovarialtumoren* (10 ed., pp. 11-19). München: W. Zuckschwerdt Verlag.
- Shen, D., & Cao, X. (2015). Potential role of CXCR3 in proliferation and invasion of prostate cancer cells. *Int J Clin Exp Pathol*, 8(7), 8091-8098.
- Shepherd, T. G., Thériault, B. L., Campbell, E. J., & Nachtigal, M. W. (2006). Primary culture of ovarian surface epithelial cells and ascites-derived ovarian cancer cells from patients. *Nature Protocols*, 1(6), 2643-2649.
- Siegel, R. L., Miller, K. D., & Jemal, A. (2015). Cancer statistics, 2015. *CA Cancer J Clin*, 65(1), 5-29.
- Specht, K., Harbeck, N., Smida, J., Annecke, K., Reich, U., Naehrig, J., Langer, R., Mages, J., Busch, R., Kruse, E., Klein-Hitpass, L., Schmitt, M., Kiechle, M., & Hoefler, H. (2009). Expression profiling identifies genes that predict recurrence of breast cancer after adjuvant CMF-based chemotherapy. *Breast Cancer Res Treat*, 118(1), 45-56.
- Strieter, R. M., Belperio, J. A., Phillips, R. J., & Keane, M. P. (2004). CXC chemokines in angiogenesis of cancer. *Semin Cancer Biol*, 14(3), 195-200.
- Strieter, R. M., Polverini, P. J., Kunkel, S. L., Arenberg, D. A., Burdick, M. D., Kasper, J., Dzuiba, J., Van Damme, J., Walz, A., Marriott, D., & et al. (1995). The functional role of the ELR motif in CXC chemokine-mediated angiogenesis. *J Biol Chem*, 270(45), 27348-27357.
- Sundar, S., Neal, R. D., & Kehoe, S. (2015). Diagnosis of ovarian cancer. *BMJ*, 351, h4443.
- Tan, D. S., Agarwal, R., & Kaye, S. B. (2006). Mechanisms of transcoelomic

- metastasis in ovarian cancer. *Lancet Oncol*, 7(11), 925-934.
- Taub, D. D. (2000). Modified microchemotaxis assays. *Methods Mol Biol*, 138, 105-112.
- Thompson, B. D., Jin, Y., Wu, K. H., Colvin, R. A., Luster, A. D., Birnbaumer, L., & Wu, M. X. (2007). Inhibition of G alpha i2 activation by G alpha i3 in CXCR3-mediated signaling. *J Biol Chem*, 282(13), 9547-9555.
- Tinelli, A., Malvasi, A., Leo, G., Vergara, D., Pisano, M., Ciccarese, M., Chiuri, V. E., & Lorusso, V. (2010). Hereditary ovarian cancers: from BRCA mutations to clinical management. A modern appraisal. *Cancer Metastasis Rev*, 29(2), 339-350.
- Tingulstad, S., Skjeldestad, F. E., Halvorsen, T. B., & Hagen, B. (2003). Survival and prognostic factors in patients with ovarian cancer. *Obstet Gynecol*, 101(5 Pt 1), 885-891.
- Tothill, R. W., Tinker, A. V., George, J., Brown, R., Fox, S. B., Lade, S., Johnson, D. S., Trivett, M. K., Etemadmoghadam, D., Locandro, B., Traficante, N., Fereday, S., Hung, J. A., Chiew, Y. E., Haviv, I., Australian Ovarian Cancer Study, G., Gertig, D., DeFazio, A., & Bowtell, D. D. (2008). Novel molecular subtypes of serous and endometrioid ovarian cancer linked to clinical outcome. *Clin Cancer Res*, 14(16), 5198-5208.
- Trotta, T., Costantini, S., & Colonna, G. (2009). Modelling of the membrane receptor CXCR3 and its complexes with CXCL9, CXCL10 and CXCL11 chemokines: putative target for new drug design. *Mol Immunol*, 47(2-3), 332-339.
- Vandercappellen, J., Van Damme, J., & Struyf, S. (2008). The role of CXC chemokines and their receptors in cancer. *Cancer Lett*, 267(2), 226-244.
- Vang, R., Shih Ie, M., & Kurman, R. J. (2009). Ovarian low-grade and high-grade serous carcinoma: pathogenesis, clinicopathologic and molecular biologic features, and diagnostic problems. *Adv Anat Pathol*, 16(5), 267-282.
- Vanguri, P., & Farber, J. M. (1990). Identification of CRG-2. An interferon-inducible mRNA predicted to encode a murine monokine. *J Biol Chem*, 265(25), 15049-15057.
- Walser, T. C., Ma, X., Kundu, N., Dorsey, R., Goloubeva, O., & Fulton, A. M. (2007). Immune-mediated modulation of breast cancer growth and metastasis by the chemokine Mig (CXCL9) in a murine model. *J Immunother*, 30(5), 490-498.
- Walser, T. C., Rifat, S., Ma, X., Kundu, N., Ward, C., Goloubeva, O., Johnson, M. G., Medina, J. C., Collins, T. L., & Fulton, A. M. (2006). Antagonism of CXCR3 inhibits lung metastasis in a murine model of metastatic breast cancer. *Cancer Res*, 66(15), 7701-7707.
- Wendel, M., Galani, I. E., Suri-Payer, E., & Cerwenka, A. (2008). Natural killer cell accumulation in tumors is dependent on IFN-gamma and CXCR3 ligands. *Cancer Res*, 68(20), 8437-8445.
- Wittekind, C., Asamura, H., & Sobin, L. (2015). *TNM-Atlas: Ein illustrierter*

Leitfaden zur TNM/pTNM-Klassifikation maligner Tumoren (C. Wittekind Ed. 6. ed.). Weinheim: Wiley-VCH Verlag GmbH & Co. KGaA.

Wu, Z., Han, X., Yan, J., Pan, Y., Gong, J., Di, J., Cheng, Z., Jin, Z., Wang, Z., Zheng, Q., & Wang, Y. (2012). The prognostic significance of chemokine receptor CXCR3 expression in colorectal carcinoma. *Biomed Pharmacother*, 66(5), 373-377.

Xanthou, G., Williams, T. J., & Pease, J. E. (2003). Molecular characterization of the chemokine receptor CXCR3: evidence for the involvement of distinct extracellular domains in a multi-step model of ligand binding and receptor activation. *Eur J Immunol*, 33(10), 2927-2936.

Yang, X., Chu, Y., Wang, Y., Zhang, R., & Xiong, S. (2006). Targeted in vivo expression of IFN-gamma-inducible protein 10 induces specific antitumor activity. *J Leukoc Biol*, 80(6), 1434-1444.

Ye, J., Ma, C., Wang, F., Hsueh, E. C., Toth, K., Huang, Y., Mo, W., Liu, S., Han, B., Varvares, M. A., Hoft, D. F., & Peng, G. (2013). Specific recruitment of gammadelta regulatory T cells in human breast cancer. *Cancer Res*, 73(20), 6137-6148.

Zhang, L., Conejo-Garcia, J. R., Katsaros, D., Gimotty, P. A., Massobrio, M., Regnani, G., Makrigiannakis, A., Gray, H., Schlienger, K., Liebman, M. N., Rubin, S. C., & Coukos, G. (2003). Intratumoral T cells, recurrence, and survival in epithelial ovarian cancer. *N Engl J Med*, 348(3), 203-213.

IX. ACKNOWLEDGEMENTS

First and foremost, I especially want to thank my supervisor Dr. Holger Bronger for mentoring my project, for all his ideas, the encouraging discussions and advices and his outstanding support and guidance throughout this project. It was a pleasure to be a member of his research team. Thank you for making all this possible!

I am very grateful to Prof. Dr. Manfred Schmitt for giving me the opportunity to work in his department, for his supervision of my project and his generous support. I also want to thank him for giving me the chance to travel to several international conferences including Spiers, South Africa and Tiers, Italy.

I would like to thank Prof. Dr. Michael Groll for supervising and promoting this thesis at the Department of Chemistry, Technische Universität München.

Huge thanks go to all my former and present colleagues for creating this friendly and supportive atmosphere at work including team events and trips and several festivities. Particularly I want to thank Alexandra Stöckel for introducing me to the lab and for her constant help, Daniela Hellmann for teaching me the immunohistochemical techniques, Elisabeth Schüren, Anke Benge and Sabine Creutzburg for helping me with cell culture, western blot or general lab issues and Rosalinde Bräuer, Sandra Baur, Daniela Hellmann, Daniela Zech and Joachim Hornung for their enormous work providing me with the immunohistochemical slides. I want to thank Daniela as well for the work with the EOC cells and Joachim for sharing his FACS knowledge and experience with me.

My special thanks go to Anne Karge for her ongoing friendship and for introducing me to the lab and to the wonderful world of western blots, as well as for all the fun we had in- and outside of the lab together with Dominique Sauter, Julia Hingerl, Julia Miller and Anna Kellner.

Another special thanks go to Theresa Dawidek not only for supporting my project with her metastasis research, but also for the great time we spent together.

I especially want to thank my colleagues Daniela Zech and Tobias Dreyer for their friendship, their support and help during countless discussions and for generating such

an enjoyable atmosphere at work. We had a great time in- and outside of the lab together with Jil Jelsma, Joachim Hornung, Raphael Biel and Thúy An Phạm.

I want to acknowledge the people with whom I was fortunate to cooperate with and who I met during this thesis: Dr. Stefanie Avril who evaluated the immunohistochemical stainings. Prof. Dr. Viktor Magdolen who let me be part of the protease world and who gave me the opportunity to take part at the international conference in Brisbane, Australia. Prof. Dr. Ute Reuning who shared her knowledge and gave good advices. Gwen Zwingenberger who introduced me to the migration assay techniques. Prof. Dr. Sherven Sharma who gave me the chance to be part of his lab at UCLA, Los Angeles, USA to review about CXCR3.

A very special thanks goes to my friends and my family for their love, support and help during all this time. I thank Evelyn a lot for proofreading this thesis.

Finally, I thank Steve so much for his unlimited love, support, confidence, patience and encouragement. I would not be where I am today without you.